1 OF 2

20 5

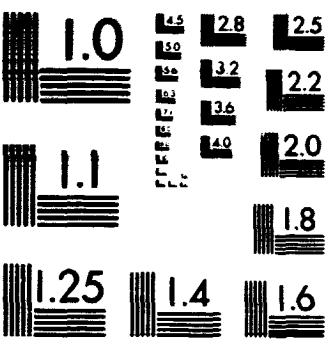

MICROCOPY RESOLUTION TEST CHART
NATIONAL BUREAU OF STANDARDS-1963-A

NASA CR-151968

Walden

(NASA-CR-151968) EVALUATION OF TECHNIQUES FOR REMOVAL OF SPACECRAFT CONTAMINANTS FROM ACTIVATED CARBON Final Report (Abcor, Inc., Wilmington, Mass.) 108 p HC A06/MF A01 CSCL 22B G3/18

N77-20159

Unclas
24655

Final Report

EVALUATION OF TECHNIQUES FOR REMOVAL OF SPACECRAFT CONTAMINANTS FROM ACTIVATED CARBON

Contract No. NAS2-8742

Submitted to:

National Aeronautics and Space Administration
Ames Research Center
Moffett Field, California 94035

Submitted by:

Kenneth J. McNulty
Robert L. Goldsmith
Gordon A. Goldsmith
Peter R. Hoover
Jerry Nwankwo
Amos Turk

The Walden Division of Abcor, Inc.
850 Main Street, Wilmington, Massachusetts 01887

March 1977

toward a better environment . . .

NASA CR-151968

Walden

Final Report

EVALUATION OF TECHNIQUES FOR REMOVAL OF SPACECRAFT CONTAMINANTS FROM ACTIVATED CARBON

Contract No. NAS2-8742

Submitted to:

National Aeronautics and Space Administration
Ames Research Center
Moffett Field, California 94035

Submitted by:

Kenneth J. McNulty
Robert L. Goldsmith
Gordon A. Goldsmith
Peter R. Hoover
Jerry Nwankwo
Amos Turk

The Walden Division of Abcor, Inc.
850 Main Street, Wilmington, Massachusetts 01887

March 1977

toward a better environment . . .

TABLE OF CONTENTS

TABLE OF CONTENTS

LIST OF FIGURES

LIST OF FIGURES (continued)

LIST OF TABLES

SECTION 1

SUMMARY

Adsorption on activated carbon is the primary technique proposed for the removal of trace organic contaminants from spacecraft atmospheres. In order to minimize the total equivalent weight of the contaminant control system, a regenerable carbon bed is proposed for the removal of weakly adsorbed contaminants. The objective of this program was to evaluate alternative techniques for the regeneration of carbon contaminated with various spacecraft contaminants. A two-phase program was conducted to acheive this objective.

During Phase I four different modes of regeneration were evaluated:

-- thermal desorption via vacuum,
-- thermal desorption via nitrogen purge,
-- in-situ catalytic oxidation of adsorbed contaminants, and
-- in-situ non-catalytic oxidation of adsorbed contaminants.

These modes of regeneration were evaluated using three different types of tests: TGA (thermal gravimetric analysis) tests, DSC (differential scanning colorimetry) tests, and carbon column tests. Three different contaminants, diisobutyl ketone, caprylic acid, and acrolein were used in Phase I tests.

DSC tests were conducted with carbons containing catalyst loadings of 0%, 0.3%, 0.8%, and 1.5% by weight. As the catalyst loading increased, the catalytic oxidation of the contaminant (DIBK) occurred at lower temperatures. The 0.8% loading gave the greatest temperature separation between oxidation of contaminant and oxidation of the carbon particle. At the higher catalyst loading (1.5%) the carbon particle became pyrophoric upon oxidation of the contaminant. From these tests the preferred catalyst loading is 0.8%

Single-cycle TGA and DSC tests were conducted with each of the selected contaminants. These tests defined the temperatures at which desorption and oxidation of the contaminants occurred and the temperatures at which oxidation of the carbon particle became appreciable. The results were used to select regeneration conditions for multiple-cycle tests.

Multiple-cycle carbon column tests were conducted with DIBK at selected regeneration conditions. For regeneration by thermal desorption (both vacuum and nitrogen purge) a heel of undesorbed contaminant built up over ten cycles to a loading of 0.02 g/g carbon but remained constant at that level during all subsequent cycles. For regeneration by both non-catalytic and catalytic oxidation, the working capacity decreased as the number of cycles increased. The loss in working capacity was the combined result of carbon oxidation and contaminant heel build-up, with the latter effect predominating. Based on the results of these tests at the selected regeneration conditions, it was concluded that thermal desorption (using either vacuum or nitrogen purge) is simpler, more reliable, safer, and easier to control than oxidative regeneration.

During Phase II, tests were conducted in carbon columns designed to model the performance of the proposed prototype regenerable carbon bed. Three types of tests were conducted:

-- single-cycle, single-contaminant tests,
-- multiple-cycle, single-contaminant tests, and
-- multiple-cycle, multiple-contaminant tests.

Single-cycle, single-contaminant tests were conducted with acetone and Freon 12 to determine the desorption dynamics and the extent of desorption as a function of regeneration conditions for both vacuum and nitrogen-purge thermal desorption. Based on the results of these tests preferred regeneration conditions were selected.

Multiple-cycle tests were conducted with a single-contaminant (acetone) in order to determine the rate at which the working capacity of the carbon decreased. As in Phase I tests, the working capacity of the carbon rapidly reached a steady value with very little subsequent decline.

Most of the Phase II effort was focused on conducting repetitive adsorption-desorption tests with a multi-contaminant mixture containing the 21 primary spacecraft contaminants projected to be controlled by the regenerable carbon bed. The contaminant feed concentrations during adsorption were adjusted to levels projected for typical spacecraft operation. These tests indicated a gradual loss in working capacity. At the regeneration conditions investigated, the working capacity decreased to about 75% of the initial working capacity after 13 repetitive cycles and appeared to be decreasing linearly.

Based on the multiple-cycle, multi-contaminant tests, it is concluded that, at the conditions investigated, nitrogen-purge thermal desorption is preferred to vacuum thermal desorption. The desorption temperatures (105°C) and times (76 minutes) were the same for both modes of regeneration. The vacuum-regenerated column exhibited the disadvantage of poor removal efficiencies for weakly adsorbed contaminants when the adsorption was conducted with columns regenerated to less than 85% of the initial working capacity. In addition the decrease in working capacity with cycle number was somewhat greater for the vacuum-regenerated column. Furthermore, it is anticipated that the implementation of a nitrogen-purge system (or an air-purge system) will involve fewer development problems than the implementation of a self-contained vacuum system for regeneration without the dumping of contaminants into space.

SECTION 2
INTRODUCTION

The removal of trace contaminants from the atmospheres of manned spacecraft is essential for the maintenance of safe working conditions, particularly for missions of extended duration. Contaminants are continuously generated by such processes as biological functions, materials off-gassing, equipment leaks, and scientific experiments. A wide variety of contaminants (approximately 150) have been identified in spacecraft, simulator, and material off-gassing tests. The contaminant control system must be capable of removing contaminants with very diverse physical and chemical properties.

The Lockheed Missile and Space Company (LMSC) has made a detailed study of various systems for contaminant control[1,2,3,4]. A simplified flow schematic of the selected system is shown in Figure 1. Air from the cabin passes through a high-flow fixed (i.e., nonregenerable) bed of activated carbon for the removal of contaminants having a high production rate. The flow rate through the fixed bed (1133 ℓ/min = 40 CFM) is required to maintain the steady state concentration of pyruvic acid below its maximum allowable concentration. A carbon weight of 15.5 kg (34 lb) is required for the control of pyruvic acid generated during a 6-man, 180-day mission. In addition to pyruvic acid, the fixed bed controls all contaminants adsorbed more strongly than pyruvic acid and a number of contaminants adsorbed more weakly than pyruvic acid but generated at a lower rate.

Because some contaminants are weakly adsorbed on activated carbon, they would require an extraordinarily large quantity of carbon for removal by a fixed bed. These contaminants are removed by passing a portion of the effluent from the fixed bed through a low-flow control loop consisting of a regenerable carbon bed, a pre-sorber, a catalytic oxidizer, and a post-sorber. The flow rate through this control loop (120 ℓ/min = 4.25 CFM) is fixed by the requirement of maintaining the steady state concentration of methyl alcohol below its maximum allowable

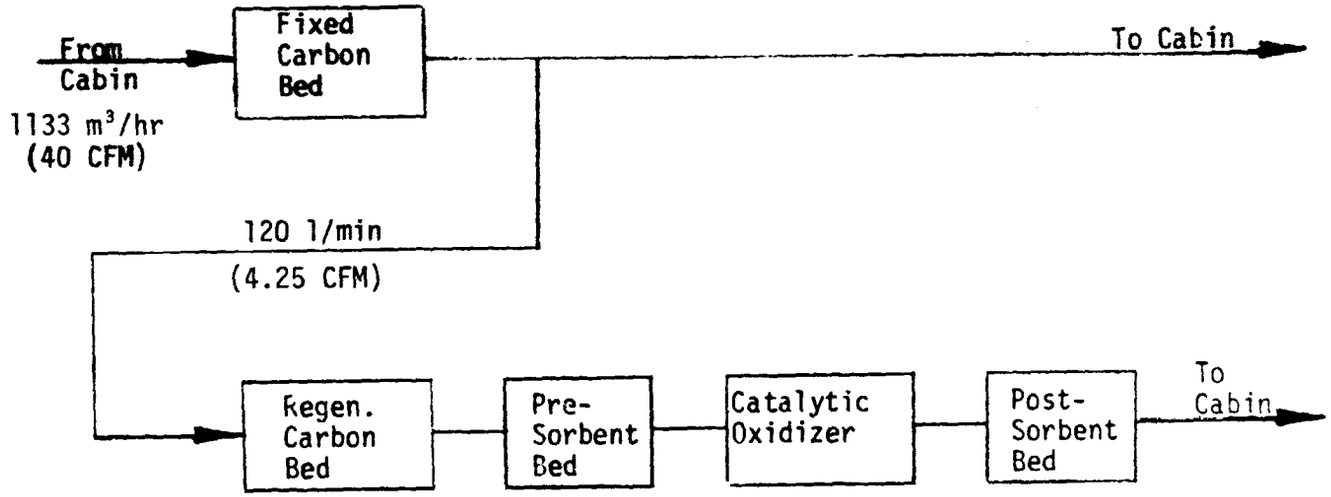

Figure 1. Selected contaminant control system for 12-man 180-day mission

concentration. The regenerable carbon bed contains 5.8 kg (12.7 lbs.) of activated carbon and is regenerated daily. This bed controls the bulk of the contaminants which break through the fixed bed prior to the end of the 180-day mission. The pre-sorber removes certain acid gases, such as HCl, HF, NO_2, and SO_2, by LiOH absorption. These gases rapidly break through the regenerable carbon bed and, if not removed, could poison the catalyst in the catalytic oxidizer. The catalytic oxidizer removes hydrogen, carbon monoxide, and very weakly adsorbed organics, such as methane, ethane, ethylene, etc. The post-sorber removes toxic oxidation products such as HCl, HF, Cl_2, $COCl_2$, NO_2 and SO_2 which result from the oxidation of very weakly adsorbed organics which break through the regenerable bed.

The primary function of the regenerable bed is to protect the catalyst (1/2% Pd on alumina) in the catalytic oxidizer from poisoning by compounds containing halogens, nitrogen, and sulfur. The regenerable bed removes almost all of the potential poisons in addition to many other compounds which could be controlled by the catalytic oxidizer without threat of catalyst deactivation. The selected mode of carbon bed regeneration is vacuum thermal desorption in which the heated carbon bed is vented to space. Out of a total cycle time of 24 hours, regeneration requires 3.33 hours and is carried out at a mean carbon temperature of 422°K (300°F).

Research related to possible improvements in the operation of the regenerable carbon bed has been conducted by the Walden Research Division of Abcor, Inc. During a previous program[5] research efforts were directed toward evaluating the possibility of using a catalyst-impregnated carbon for in-situ regeneration by catalytic oxidation of adsorbed contaminants. It was postulated that, during regeneration, adsorbed contaminants could migrate over the carbon surface and be oxidized at active catalyst sites to CO_2, H_2O, and other oxidation products. It was hoped that the development of such a catalytic carbon would lead to a reduction in the power requirements for regeneration and would eliminate the controversial practice of "dumping" contaminants

into space where they could interfere with various instrumental measurements. This previous research program was successful in demonstrating that the catalyst (platinum) did promote oxidation of certain contaminants, but the temperature at which oxidation occurred was higher than anticipated. In addition it was learned that most of the same contaminants were oxidized without the catalyst at approximately the same temperature.

The overall objective of the present research program is to compare alternative modes of carbon bed regeneration. The regeneration modes selected for evaluation are:

-- thermal desorption via vacuum,
-- thermal desorption via nitrogen purge,
-- in-situ catalytic oxidation of adsorbed contaminants, and
-- in-situ non-catalytic oxidation of adsorbed contaminants.

Each of these regeneration techniques can be used without dumping contaminants into space: For oxidative regeneration the contaminants are oxidized in-situ. For thermal desorption the desorbed contaminants must either be compressed to atmospheric pressure (vacuum pump) or removed from the bed by a low-flow nitrogen purge stream. For both of the thermal desorption techniques, additional treatment is required for storage or disposal of the concentrated contaminants. This would require the development of additional components such as, for example, a non-catalytic thermal oxidation unit for oxidation of the concentrated contaminants.

This report follows the program organization and execution by dividing the work into two Phases:

Phase I - Evaluation of Alternative Regeneration Techniques, and
Phase II - Demonstration of Selected Regeneration Techniques.

The experimental procedures, results, and conclusions are discussed separately for each Phase.

SECTION 3

PHASE I: EVALUATION OF ALTERNATIVE REGENERATION TECHNIQUES

I. EXPERIMENTAL APPARATUS AND PROCEDURES

During Phase I three types of tests were conducted to evaluate the four modes of carbon regeneration: thermal gravimetric analysis (TGA), differential scanning calorimetry (DSC), and carbon column tests.

A. TGA APPARATUS

The TGA apparatus is shown schematically in Figures 2 and 3 for the adsorption mode and regeneration mode, respectively. For adsorption, a dried stream of nitrogen was split into a purge stream and a carrier stream. The purge stream was passed through the control end of the balance and out through the exit to avoid accumulation of contaminant in the balance. The carrier stream was sparged through a constant-temperature saturator and passed through the inner tube of the concentric furnace tube. The carrier gas passed over the carbon sample on the sample pan, was redirected by the platinum baffles, and passed out through the exit with the purge gas. The sample was held at a constant temperature during adsorption by a furnace surrounding the furnace tube.

During regeneration (Figure 3) a controlled flow of compressed air was passed through an activated carbon bed, a calcium sulfate bed, and a molecular sieve bed for organic and moisture removal. The air passed over the sample and out to the collection and analysis components. The furnace was programmed to heat the sample at a given rate, typically 15°C/min, and the sample weight was plotted against sample temperature as measured by the thermocouple placed next to the carbon on the sample pan. Several carbon particles were used for the sample giving a typical weight of 40 mg.

A hypothetical TGA trace during which oxidation occurs is shown by the solid curve of Figure 4. The weight decreases smoothly at first until the temperature reaches about 250°C. Then the highly exothermic oxidation reaction causes a disproportionate temperature increase in the sample as the weight of adsorbed contaminant decreases to zero. Since the oxidation reaction is complete the sample temperature cools back to the furnace tem-

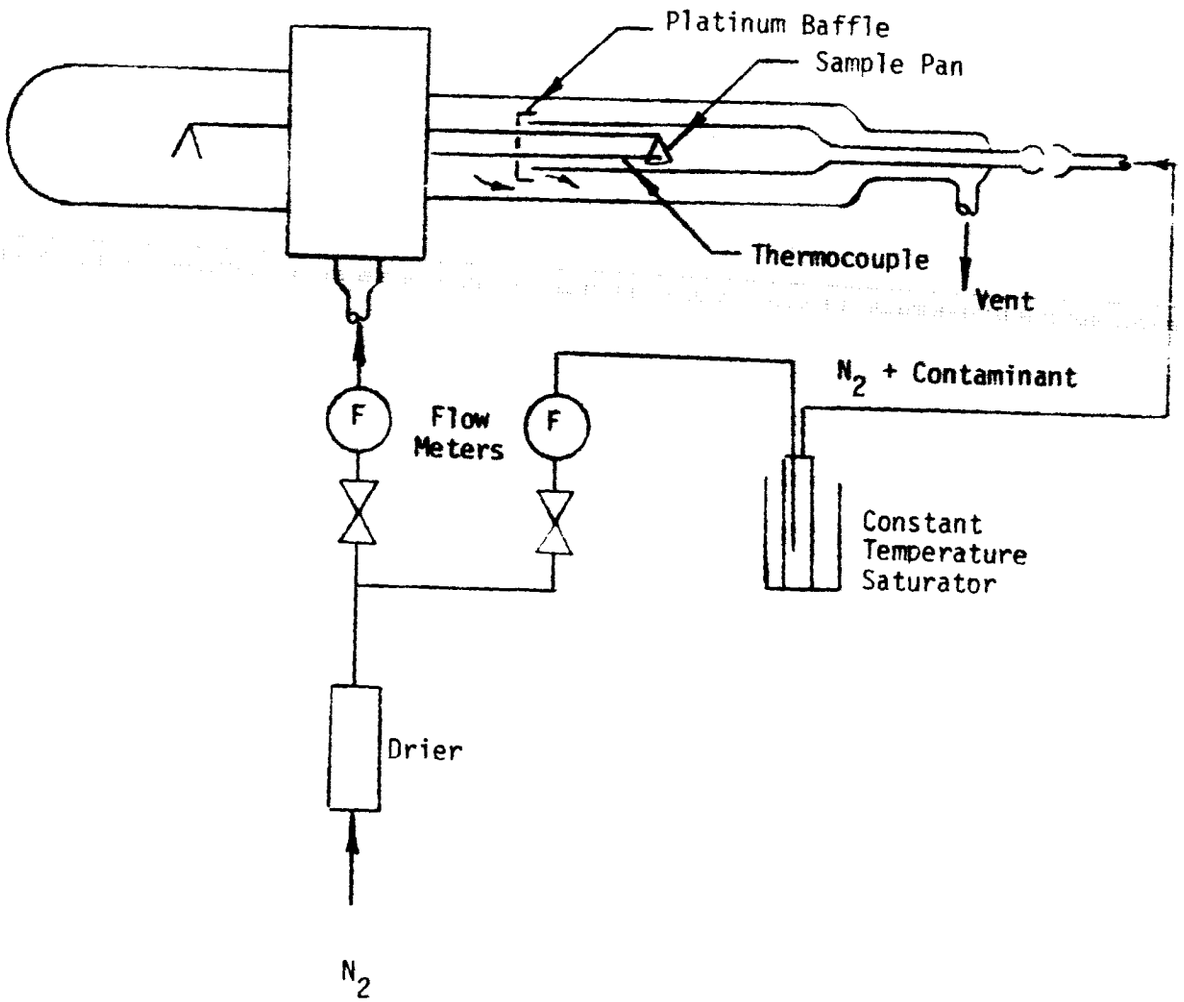

FIGURE 2: TGA APPARATUS: ADSORPTION MODE

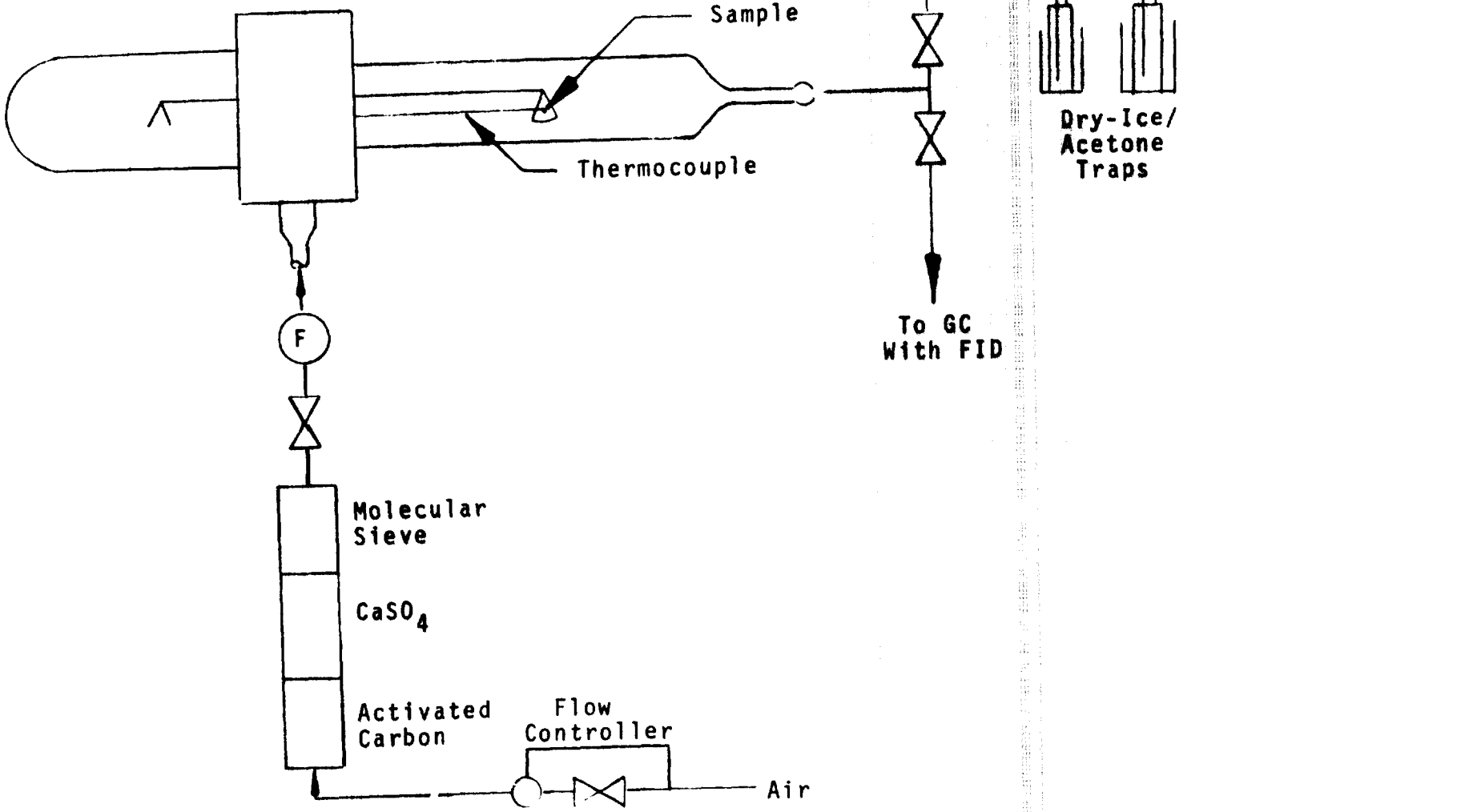

FIGURE 3: TGA APPARATUS: OXIDATION MODE

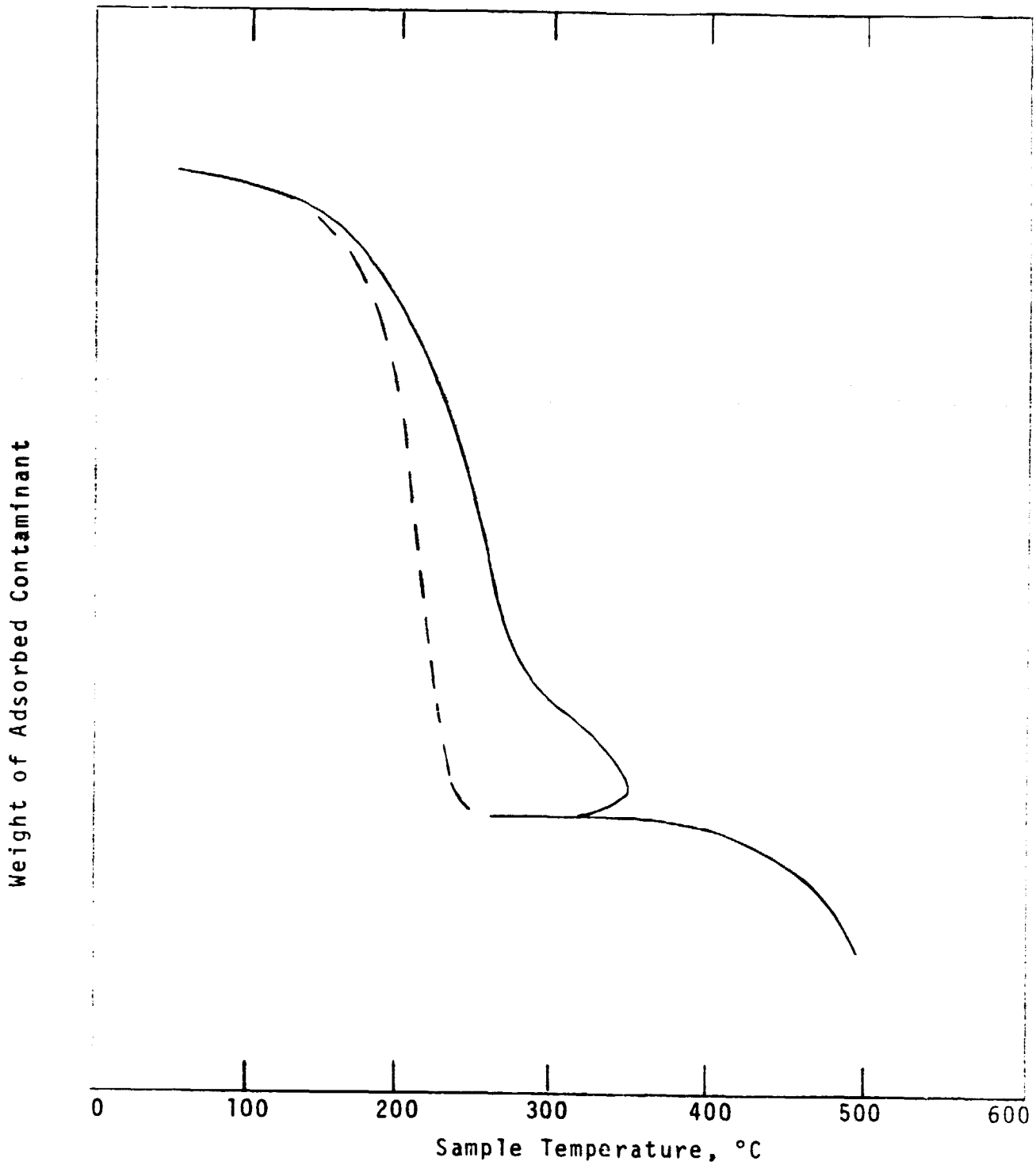

FIGURE 4: TYPICAL TGA TRACE

perature (250°C), and the sample weight remains constant at 0 mg until about 375°C where the carbon begins to oxidize. If the heat of reaction were removed, the TGA trace would follow the dashed line of Figure 4.

B. DSC APPARATUS

A cross-section of the DSC apparatus is shown schematically in Figure 5. A contaminated carbon particle was placed in the sample pan and a flow of 300 cc/min of purified air was passed over the sample via inlet and outlet ports to the gas space over the sample. A thermocouple was attached to the sample pan with reference junction attached to the reference pan. The thermocouple measures the temperature difference between sample and reference. This difference results when an exothermic or endothermic process occurs within the sample. This ΔT is plotted against the cell temperature which was uniformly increased by a programmed heat input, typically at a rate of 10 to 15°C/min.

A hypothetical DSC trace is shown in Figure 6. The negative peak at low temperature indicates an endothermic process, i.e., thermal desorption of contaminant. The positive peak at higher temperature indicates an exothermic oxidation reaction. The final exothermic rise in the DSC trace indicates oxidation of carbon as can be seen by comparison to the curve for no contaminant adsorbed.

C. APPARATUS FOR CARBON COLUMN TESTS

The flow schematic for adsorption tests with carbon columns is shown in Figure 7. A low pressure regulator (PR) used to regulate the supply presure of laboratory compressed air. The air was treated by passing it through a cartridge filter containing activated carbon, a long column of activated carbon, and a Balston Grade B filter which removed essentially all particulates. The compressed air flow was split into two streams: a carrier and a diluent. The carrier stream was sparged through an impinger containing the contaminant at an elevated temperature. This air/contaminant mixture was cooled to room temperature in the cooling coil. Excess contaminant condensed resulting in a contaminant-saturated air stream at room temperature. Conta-

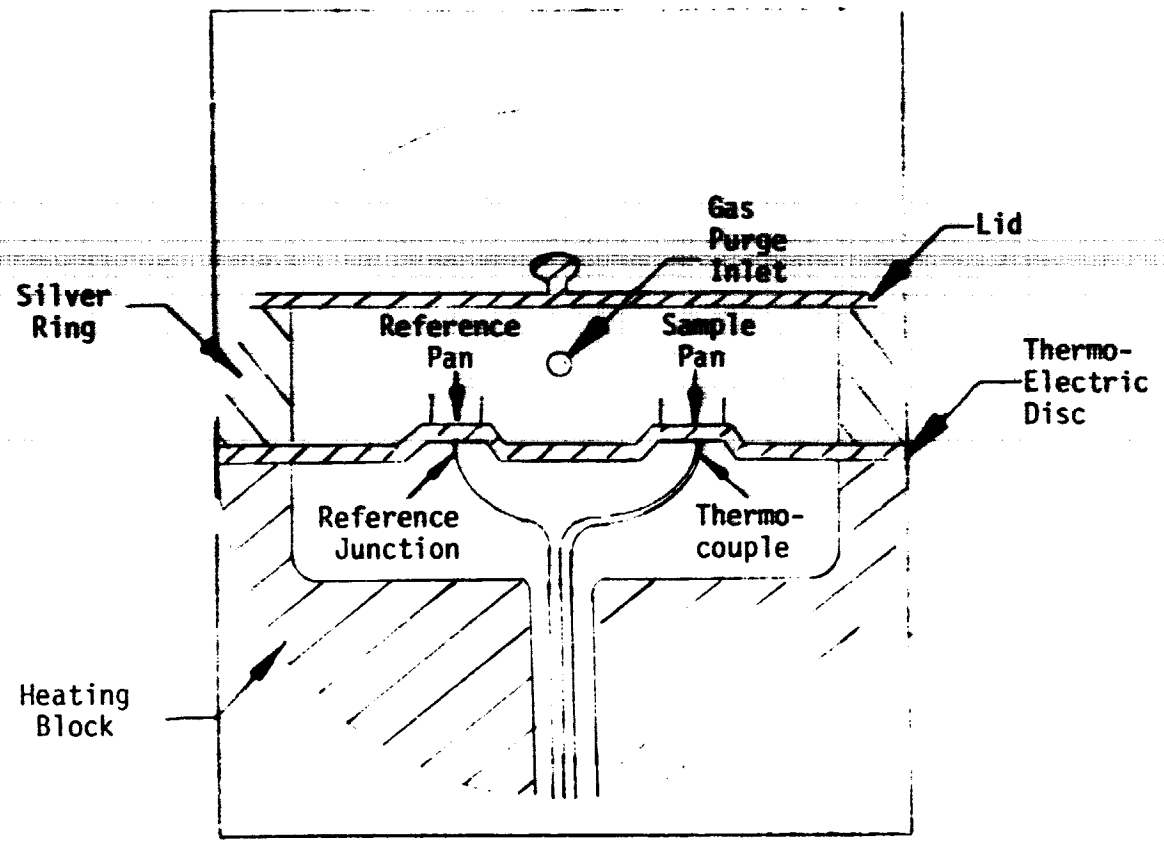

FIGURE 5: CROSS SECTION OF DSC CELL

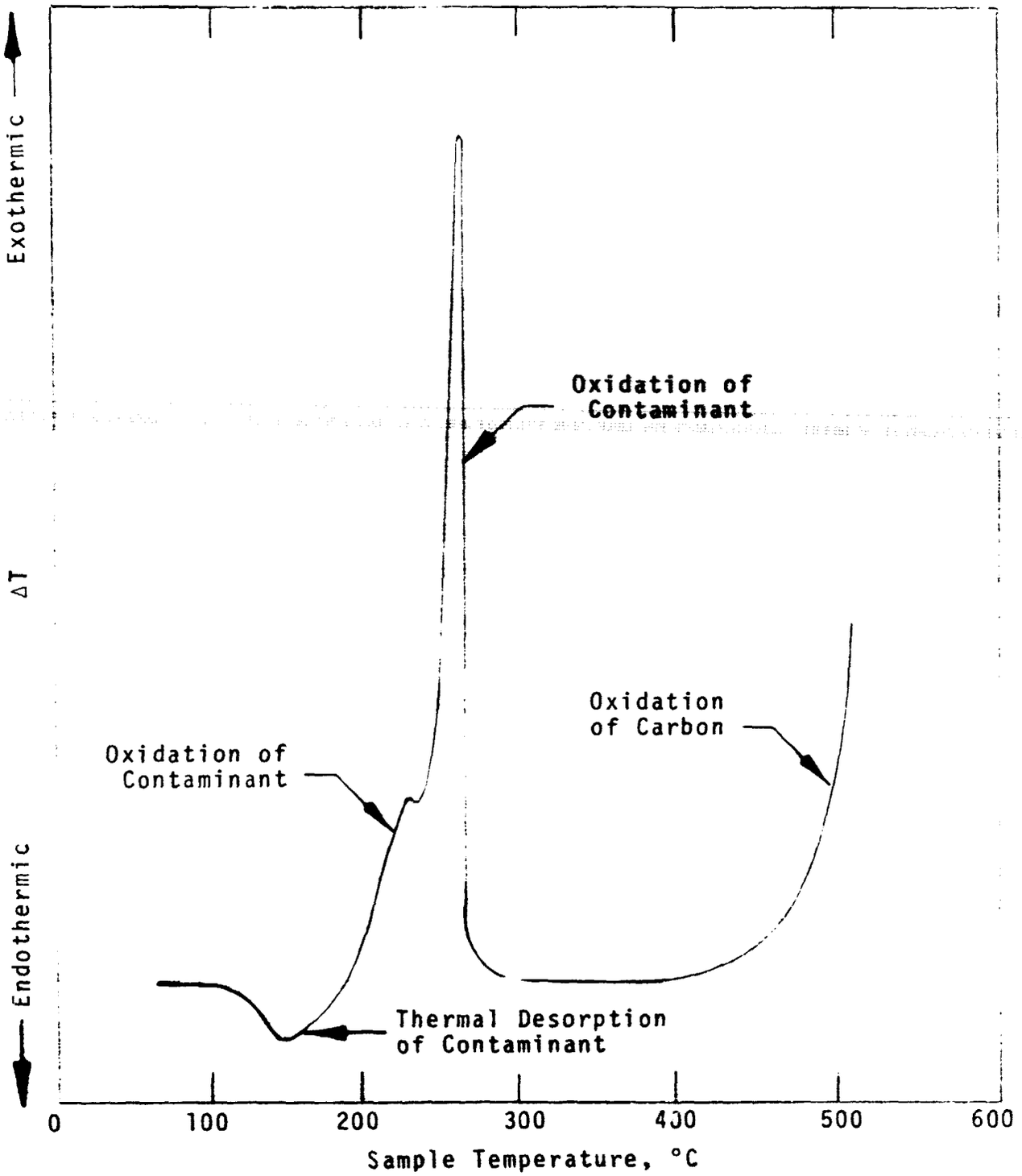

FIGURE 6: HYPOTHETICAL DSC TRACE

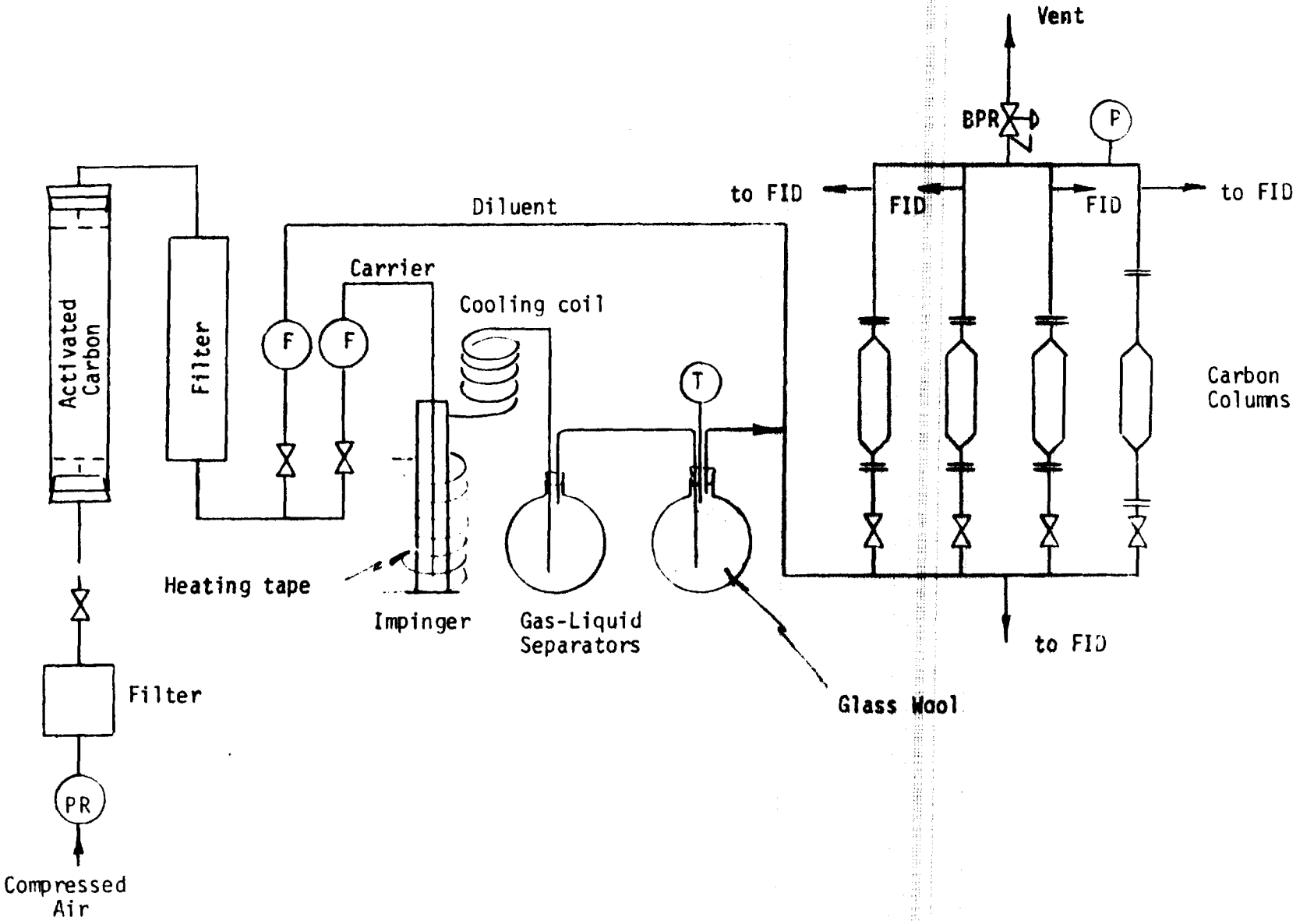

FIGURE 7: FLOW SCHEMATIC FOR ADSORPTION

minant droplets were separated from the air stream in two flasks, the second packed with glass wool.

The saturated stream was diluted by a factor of about 5 to 1 in order to prevent gross condensation within the pores of the carbon. Equal flows of the contaminated air stream were passed through each of four carbon columns. The effluent streams are combined and passed through a back pressure regulator (BPR) to vent. The back pressure regulator provided a slight positive pressure to force any selected stream through a capillary flow restriction to the flame ionization detector (FID). The stream selected for analysis was attached to the FID by flexible tubing while the other sample ports were blocked off. Each column was removed and weighed before and after adsorption.

The flow schematic for regeneration is shown in Figure 8. From left to right the columns were regenerated by nitrogen-sweep thermal desorption, non-catalytic oxidation, catalytic oxidation, and vacuum thermal desorption. Each column was wrapped with a heating tape, and thermocouples (TC) were inserted to measure the carbon bed temperature at the bottom and top of the bed. The external wall temperature was also measured at the center of the column.

Purified compressed nitrogen was used as the sweep gas in the first column and as a coolant in the second and third columns. Filtered and carbon-purified compressed air (see Figure 7) was used for oxidative regeneration. The flow rates were controlled by needle valves and measured with rotameters. Heating tapes were used to pre-heat the gas streams to the ignition point of the reaction.

For vacuum thermal desorption a rotary vacuum pump was used to evacuate the column. The pump and column were separated by a cold trap.

The details of the column design are shown in Figure 9. The columns were constructed of glass with standard taper joints at top and bottom for demounting. The carbon bed was supported by a stainless steel screen placed over the support rods shown in Figure 9. The L/D of the bed was approxi-

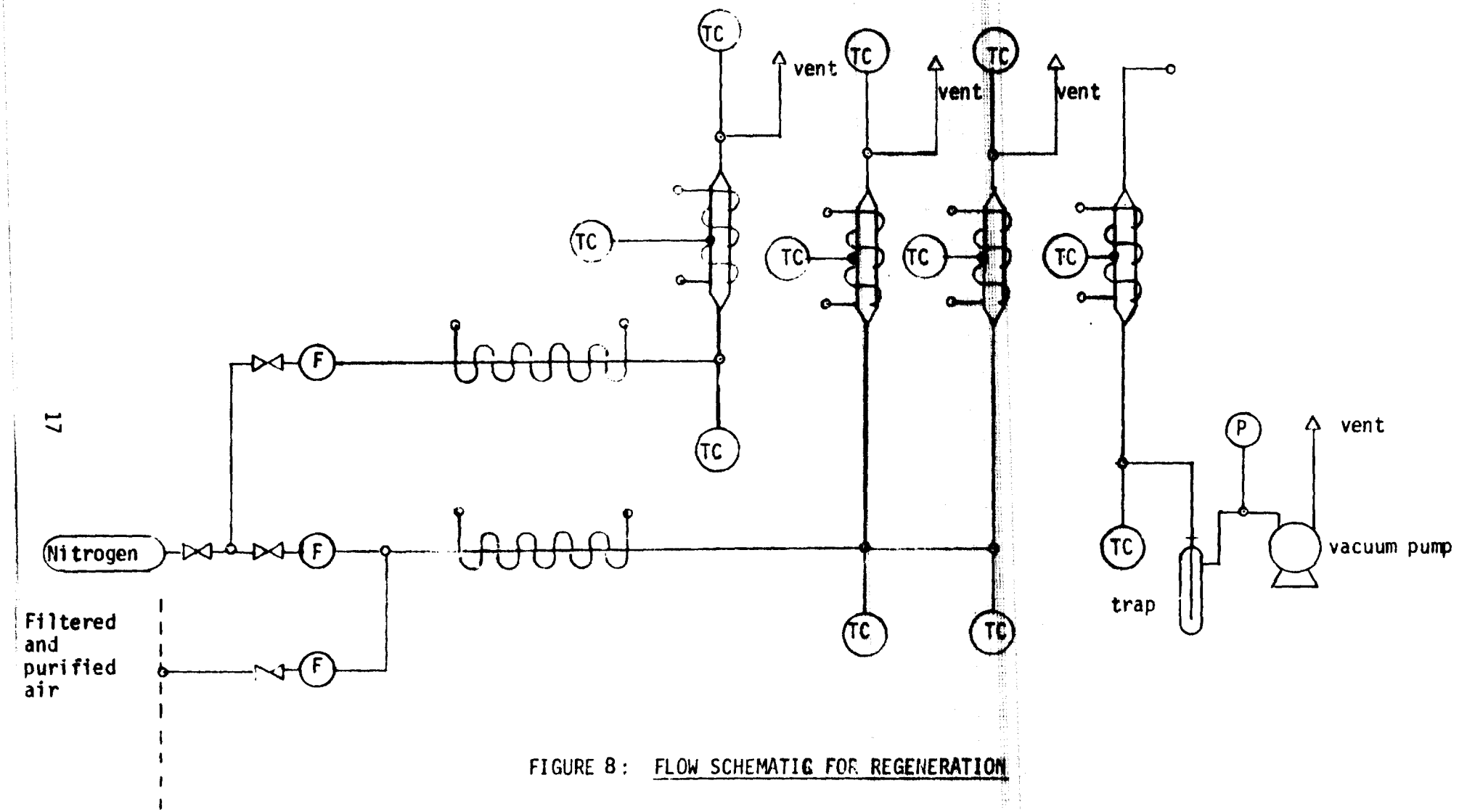

FIGURE 8: FLOW SCHEMATIC FOR REGENERATION

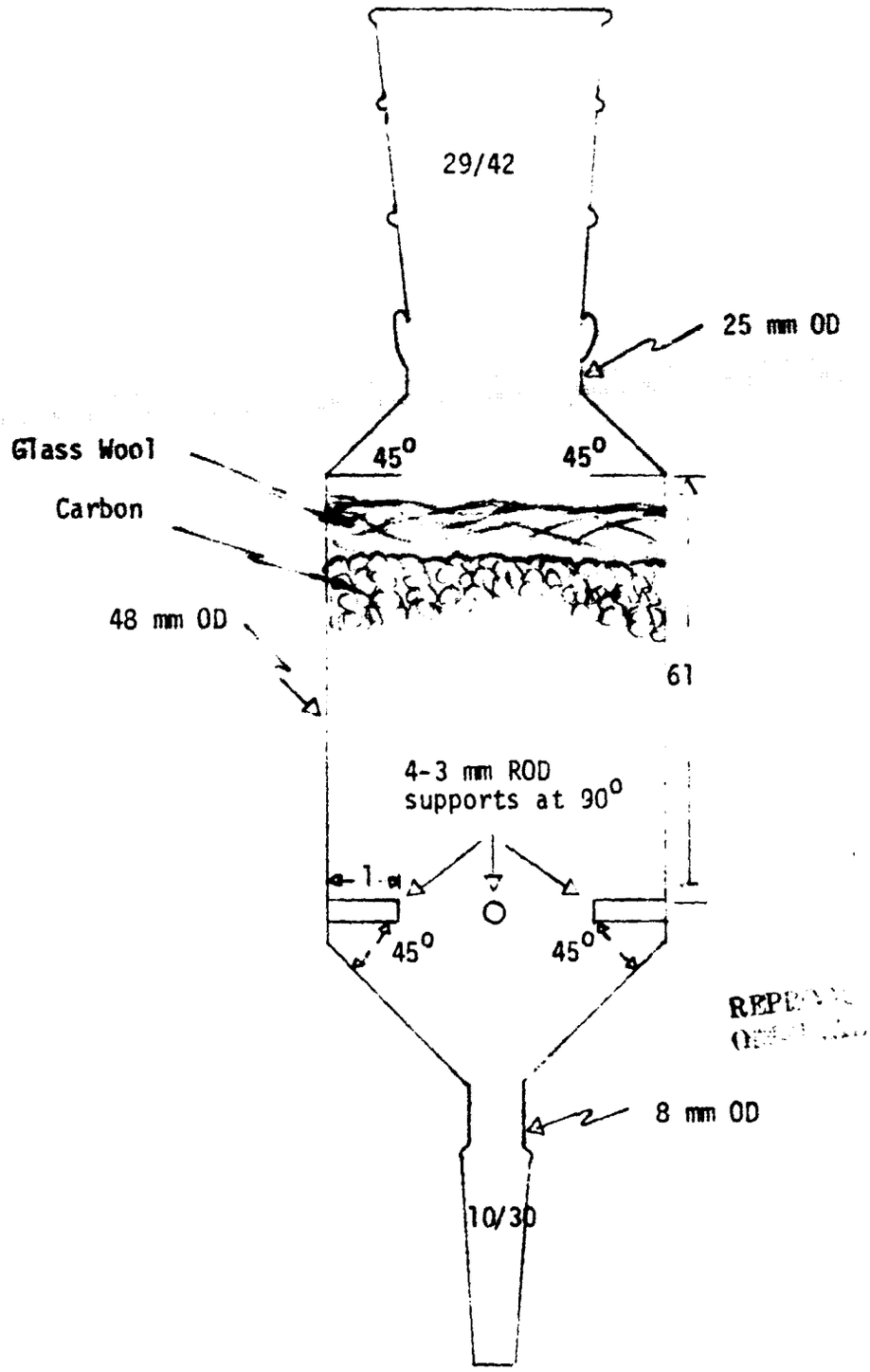

FIGURE 9: DETAILS OF CARBON COLUMN

mately 1.0. The bed was covered with a layer of glass wool to prevent loss of carbon fines. Because of the high temperatures used for regeneration, stopcock grease was not used on the ground joints.

For vacuum thermal desorption, the column design was similar to that shown in Figure 9. The column dimensions were the same, but the end connections were glass-to-metal seals with stainless steel compression fittings. This assembly was leak tight and could be heated to 450°C. However, it was more expensive and the interior was less accessible than with the other columns.

D. CARBONS AND CONTAMINANTS

The carbon used in all tests was Pittsburgh BPL 6 x 16 (Calgon Corp.). This carbon was selected because of its high kindling temperature. The catalytic carbons were prepared by Matthey-Bishop, Inc. A catalyst of "noble metal" composition was deposited on the activated carbon (Pittsburgh BPL 6 x 16) by a "non-vapor-phase" impregnation procedure.

Tests were conducted with these different contaminants: diisobutyl ketone (DIBK), caprylic acid, and acrolein. These same contaminants were investigated in the previous program[4] and were selected as potential spacecraft contaminants which could not be completely removed from the carbon by thermal desorption alone[1]. These contaminants should provide a critical test of the capabilities of oxidative regeneration.

II. RESULTS AND DISCUSSION

A. OPTIMIZATION OF CATALYTIC CARBON WITH RESPECT TO CATALYST LOADING

Three different catalyst loadings were investigated to determine the optimum loading for catalytic oxidation of adsorbed contaminants. The DSC curves for oxidation of DIBK on carbons impregnated with 0%, 0.3%, 0.8%, and 1.5% catalyst are shown in Figure 10. Because of differences in sample size, contaminant loading, and y-axis sensitivity, the peak heights are not directly comparable. The curves have been displaced vertically to avoid excessive overlap.

For the curve for non-catalytic carbon (0% catalyst), three peaks are observed for oxidation of DIBK: A, C_1, and C_2. Peak A is attributed to oxidation of weakly adsorbed contaminant; while peaks C_1 and C_2 are attributed to oxidation of strongly adsorbed contaminant. Peak D is the result of oxidation of carbon, as was confirmed by conducting a separate test without the contaminant.

For the carbon containing 0.3 wt % catalyst, peaks A and C occur at the same temperature as for non-catalytic carbon and are attributed to oxidation on the carbon support of weakly adsorbed and strongly adsorbed contaminant, respectively. Peak B then corresponds to oxidation of DIBK on the deposited catalyst. Peak D again corresponds to oxidation of carbon.

For the carbon containing 0.8% catalyst, the two peaks (B_1 and B_2) observed for oxidation of contaminant occur at a significantly lower temperature than any of the peaks observed for lower catalyst loadings. Therefore, it is inferred that both of these peaks result from oxidation of contaminant on the catalyst, and the higher catalyst loading produces a higher catalytic activity. Peaks B_1 and B_2 may correspond to catalytic oxidation of weakly and strongly adsorbed contaminant, respectively. Peak D again corresponds to oxidation of the carbon support. The fine structure observed for peak D at catalyst loadings of 0.8% and 0.3% indicates that the carbon oxidizes in stages; the mechanism by which this occurs is

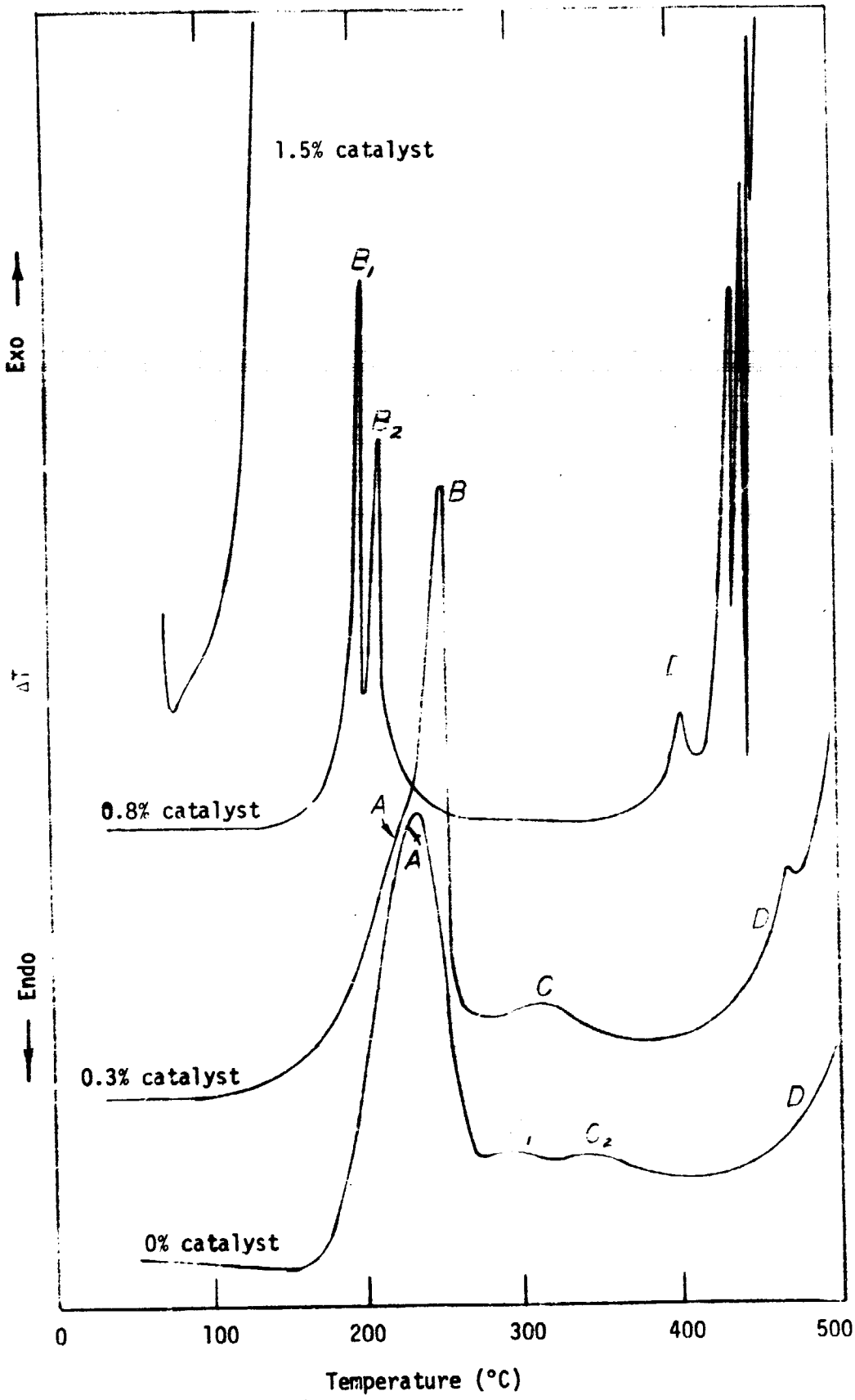

Figure 10: Comparison of DSC traces for carbons containing various loadings

not understood.

When the catalyst loading was increased to 1.5 wt %, the contaminated carbon became pyrophoric at about 125°C. At the conditions of this test the rate of heat release due to oxidation was greater than could be transferred to the surroundings, and no separation was obtained between the oxidation temperature of the contaminant and the carbon. It is apparent that the 1.5% catalytic carbon is very active and may be applicable to oxidation of adsorbed contaminants at much lower contaminant loadings. Alternatively it has the potential of being used as a simple oxidation catalyst for which the feed to the reactor would be heated to ~125°C (based on the result for DIBK).

The peak temperatures for regeneration of the various carbons investigated are given in Table 1. The greatest temperature separation between the strongly adsorbed contaminant peak and the start of carbon oxidation was obtained for the 0.8% catalyst loading. Therefore, based on the conditions and contaminant investigated, the optimum catalyst loading is about 0.8 wt %.

It is of interest to compare the activities of the catalytic carbon used in this program and that used in the previous program[4]. The catalytic carbon used in this program was prepared by Matthey Bishop, Inc. using a "non-vapor phase" procedure to deposit a "noble metal" catalyst in the carbon support (BPL 6x16). The catalytic carbon used in the previous program was prepared in-house using a solution impregnation procedure to deposit a platinum metal catalyst on the same carbon support.

DSC traces are compared in Figure 11 for oxidation of DIBK on catalytic carbon prepared by Matthey Bishop (solid line) and Walden Research[4] (dashed line). The catalyst loading was approximately 0.3 wt % for both carbons. For both curves the heating rate was 15°C/min, but, because of differences in sample size, contaminant loading, and y-axis sensitivity, the size of the peaks cannot be directly compared. It has been demonstrated that peaks A and C result from oxidation of DIBK on the carbon support, and peak D results from oxidation of the carbon itself.

Table 1

PEAK TEMPERATURES FOR REGENERATION OF VARIOUS CARBONS CONTAMINATED WITH DIBK

Carbon	Contaminant Peak Temps. (°C)	Start of Carbon Peak (°C)	Minimum Peak Separation (°C)
0.0% catalyst	235, 295, 350	410	60
0.3% catalyst	230, 255, 315	375	60
0.8% catalyst	205, 215	350	135
1.5% catalyst	~125	~125	0

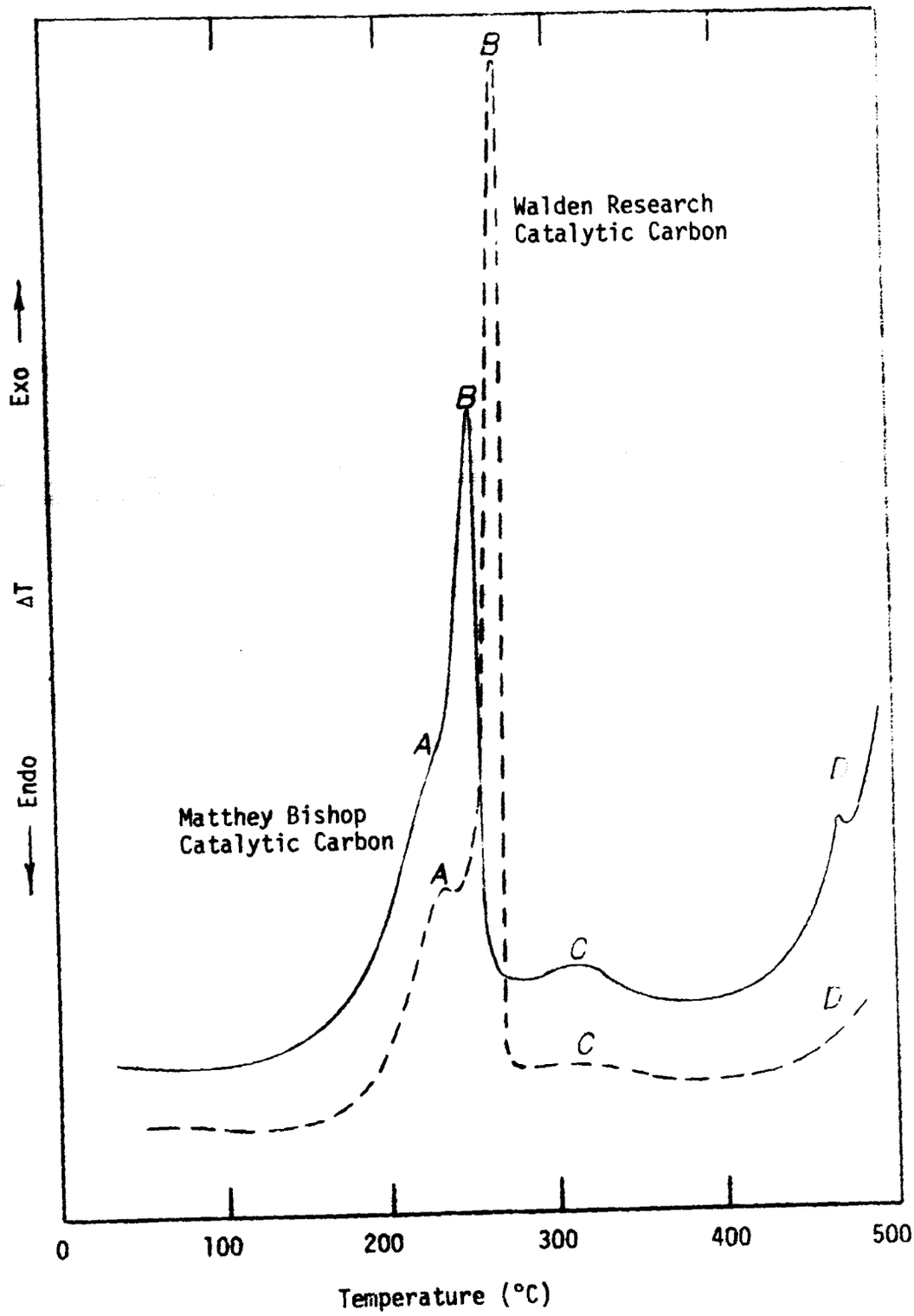

Figure 11: Comparison of DSC traces for catalytic carbon prepared in-house and prepared by Matthey Bishop. Catalyst Loading = 0.3 wt %

Peak B is the only peak resulting from oxidation of DIBK on the catalyst. As expected peaks A and C occur at the same temperature in the two DSC traces. However oxidation on the deposited catalyst occurs at a slightly lower temperature (15 to 20°C lower) for the Matthey Bishop catalytic carbon. This slight advantage is off-set by the fact that the carbon support also begins to oxidize at a lower temperature (peak D). Thus, in terms of the temperature separation between the oxidation of contaminant and the oxidation of carbon, the catalytic carbons are very similar. It is concluded that the "noble metal" catalyst and non-vapor-phase" impregnation procedure used by Matthey Bishop is not significantly superior to the platinum catalyst and the liquid-phase impregnation procedure used in the previous program.

B. COMPARISON OF REGENERATION MODES USING DSC AND TGA

Two types of DSC/TGA tests were conducted to compare alternative regeneration modes: 1) single-cycle tests with three contaminants (caprylic acid, DIBK, and acrolein), and 2) multiple -cycle tests with one contaminant (DIBK) and two different cut-off temperatures.

1. Single-Cycle Tests

TGA traces are shown in Figure 12 for various modes of regeneration of carbon contaminated with caprylic acid. The catalytic carbon contained 0.3 wt % catalyst. As the temperature was increased above ambient, there was relatively little weight loss until a temperature of about 200°C was reached. Above 200°C contaminant was removed more rapidly by oxidation than by thermal desorption alone. As a result, at a temperature of 325°C, which is below the ignition point of the carbon, the amounts of contaminant remaining were:

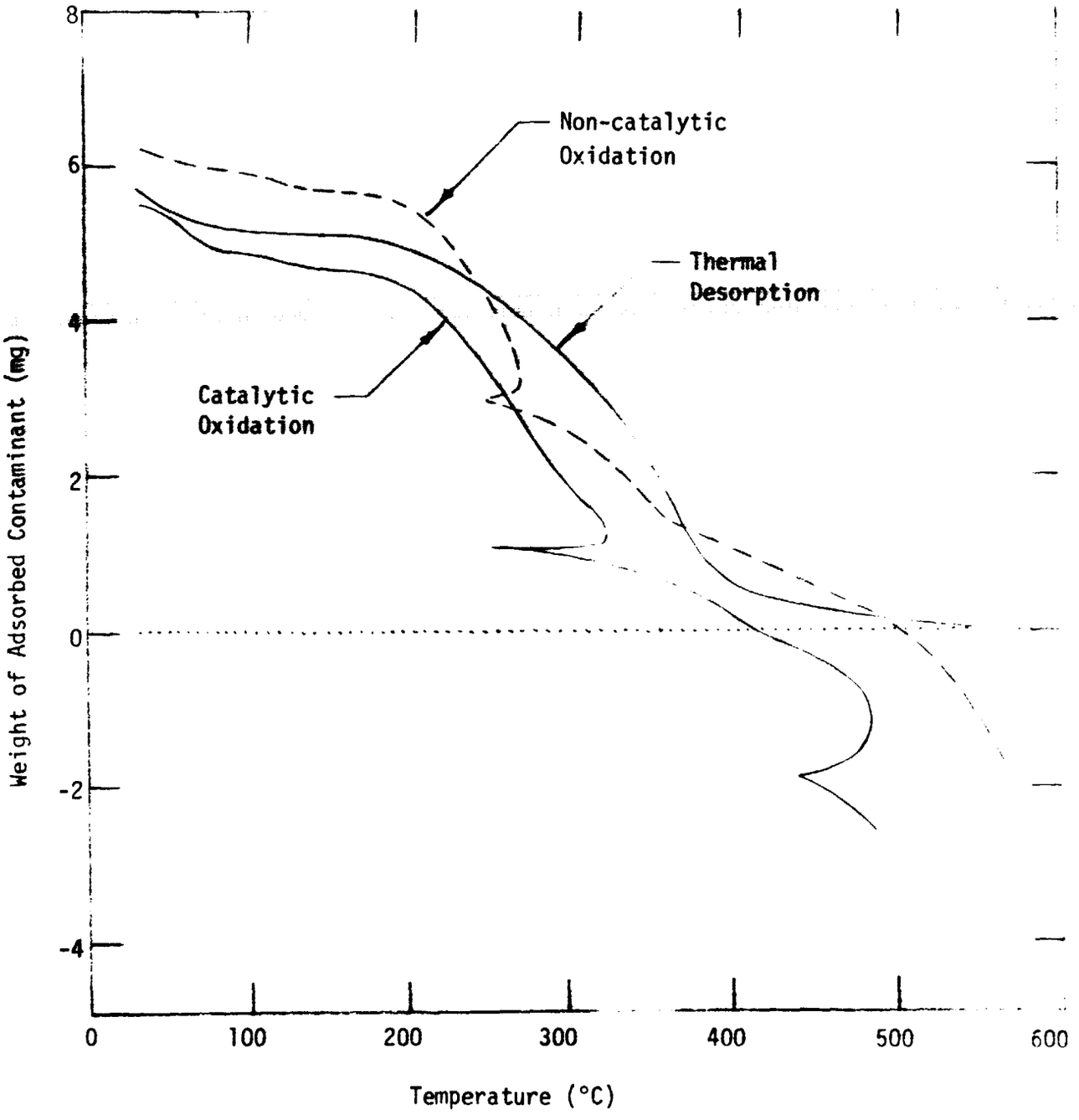

Figure 12: Comparison of TGA traces for three modes of carbon regeneration

Regneration Mode	Contaminant Remaining (mg)
Thermal Desorption	2.65
Non-catalytic Oxidation	2.00
Catalytic Oxidation	0.80

It is clear that if the regeneration were conducted by programmed heating to 325°C at a rate of 15°C/min, catalytic oxidation would be the preferred mode of regeneration. However, higher temperatures (or longer times) are required to remove the 0.80 mg of residual contaminant, and at higher temperatures (e.g. 400°C) the advantage of catalytic oxidation over thermal desorption is marginal. At a temperature of 400°C it is likely that the low contaminant weight observed for the catalytic carbon is due, in part, to oxidation of the carbon. In the temperature range between 360°C and 500°C, thermal desorption gives a lower residual than non-catalytic oxidation, and only when the carbon begins to oxidize at about 500°C does the weight for non-catalytic oxidative regeneration fall below that for thermal desorption. On the basis of these TGA results catalytic oxidation would seem to be the preferred mode of regeneration if the maximum regeneration temperature were limited to ~325°C. For regeneration at higher temperatures, thermal desorption would be preferred.

Similar curves were obtained for carbons contaminated with DIBK and acrolein. For acrolein thermal desorption occurred readily, and essentially all of the contaminant was removed at temperatures below 250°C. The DSC traces show an oxidation peak at 200°C for the catalytic carbon but no exothermic peaks for the non-catalytic carbon. Thus the catalyst does promote oxidation of acrolein. However, the TGA traces for the three modes of regeneration (thermal desorption, oxidation, and catalytic oxidation) were essentially identical. Therefore, no significant advantage is indicated for the use of catalytic carbon even though the catalyst promotes oxidation of acrolein.

For DIBK the results are more difficult to interpret because

moisture and pre-adsorbed contaminants were not removed from the carbon prior to the start of each run. Therefore it is difficult to accurately determine the point in the TGA traces at which the adsorbed contaminant weight reaches zero. The test procedure was revised following the single-cycle tests with DIBK to include a pre-treatment step of heating the carbon in nitrogen to the final desorption temperature. Since the multiple-cycle tests were conducted with DIBK, single-cycle tests with this contaminant were not repeated.

2. Multiple-Cycle Tests

Multiple-cycle tests were conducted with carbons contaminated with DIBK to compare the relative build-up of contaminant residual for the various modes of regeneration. Two types of carbon, catalytic (0.3% catalyst) and non-catalytic, were investigated. Each carbon was regenerated by both thermal desorption (in nitogen) and oxidation (in air). Two different terminal temperatures (350°C and 400°C) were investigated, and four repetitive TGA tests were conducted at each set of conditions. This required a total of 32 TGA tests.

Table 2 summarizes the test conditions and results. The final column gives the amount of contaminant remaining after programmed heating at a rate of 15°C/min to the indicated temperature. In all cases the initial contaminant loading was about 0.1 g DIBK/g carbon. At a regeneration temperature of 350°C, residual contaminant loadings of 0.063, 0.033, and 0.021 g/g carbon were obtained for thermal desorption, non-catalytic oxidation, and catalytic oxidation, respectively. At a regeneration temperature of 400°C, residual contaminant loadings of 0.044, 0.016, and 0.000 g/g carbon were obtained for thermal desorption, non-catalytic oxidation, and catalytic oxidation, respectively. Therefore, at both temperatures the lowest contaminant residuals were obtained by catalytic oxidation; the highest residuals, by thermal desorption.

Table 2.

RESIDUAL CONTAMINANT LOADINGS FOR MULTIPLE-CYCLE REGENERATIONS

Type of Carbon	Regeneration Atmosphere	Terminal Program Temperature (°C)	Cycle Number	Cumulative Residual Contaminant Loading (g/g carbon)
Catalytic	Nitrogen	350	1	.050
			2	.059
			3	.066
			4	.071
		400	1	.028
			2	.046
			3	.052
			4	.058
	Air	350	1	.011
			2	.019
			3	.019
			4	.021
		400	1	.007
			2	.007
			3	.006
			4	.000
Non-catalytic	Nitrogen	350	1	.049
			2	.058
			3	.062
			4	.063
		400	1	.027
			2	.031
			3	.041
			4	.044
	Air	350	1	.020
			2	.028
			3	.030
			4	.033
		400	1	.013
			2	.013
			3	.016
			4	.016

While the residual contaminant loading after regeneration (or contaminant "heel") is important in comparing various regeneration modes, the most meaningful measure of regenerability is the "working capacity" of the carbon. The working capacity of the carbon is defined as the weight of contaminant removed in a given regeneration cycle per unit weight of virgin carbon. Losses in working capacity can occur both by carbon oxidation and by heel build-up. Unfortunately, only the extent of heel build-up was determined during the repetitive-cycle TGA tests. Thus the loss in working capacity cannot be determined unless the extent of carbon oxidation can be determined from independent measurements or can be shown to be negligible.

DSC and TGA traces were obtained for catalytic and non-catalytic carbon prior to the adsorption of contaminant. These traces should indicate the temperature at which oxidation of carbon becomes important. Curves for non-catalytic carbon are shown in Figure 13. Both of the DSC curves show exothermic behavior above a temperature of 300°C. One TGA trace shows no loss of carbon until about 450°C; while the other TGA trace shows a gradual loss of weight with carbon oxidation occurring at much lower temperatures.

Corresponding curves for catalytic carbon (0.3% catalyst) are shown in Figure 14. The DSC curves show gradual evolution of heat starting at about 200°C and becoming appreciable between 350 and 400°C. The TGA curves show a gradual weight loss (after desorption of mositure) starting at about 200°C and becoming appreciable around 400°C.

These curves indicate the possibility of carbon oxidation for both catalytic and non-catalytic carbon, in the range of 350°C to 400°C. Therefore, the low residual loadings measured for oxidative regeneration may be due, in part, to oxidation of carbon.

The data of Table 2 indicate that the amount of residual contaminant picked up per cycle decreases as the number of cycles increase. That is, it appears that the residual contaminant loading (or heel) would level off if a sufficient number of cycles were conducted. The decrease in the apparent residual loading for the catalytic carbon regenerated in air at 400°C can be

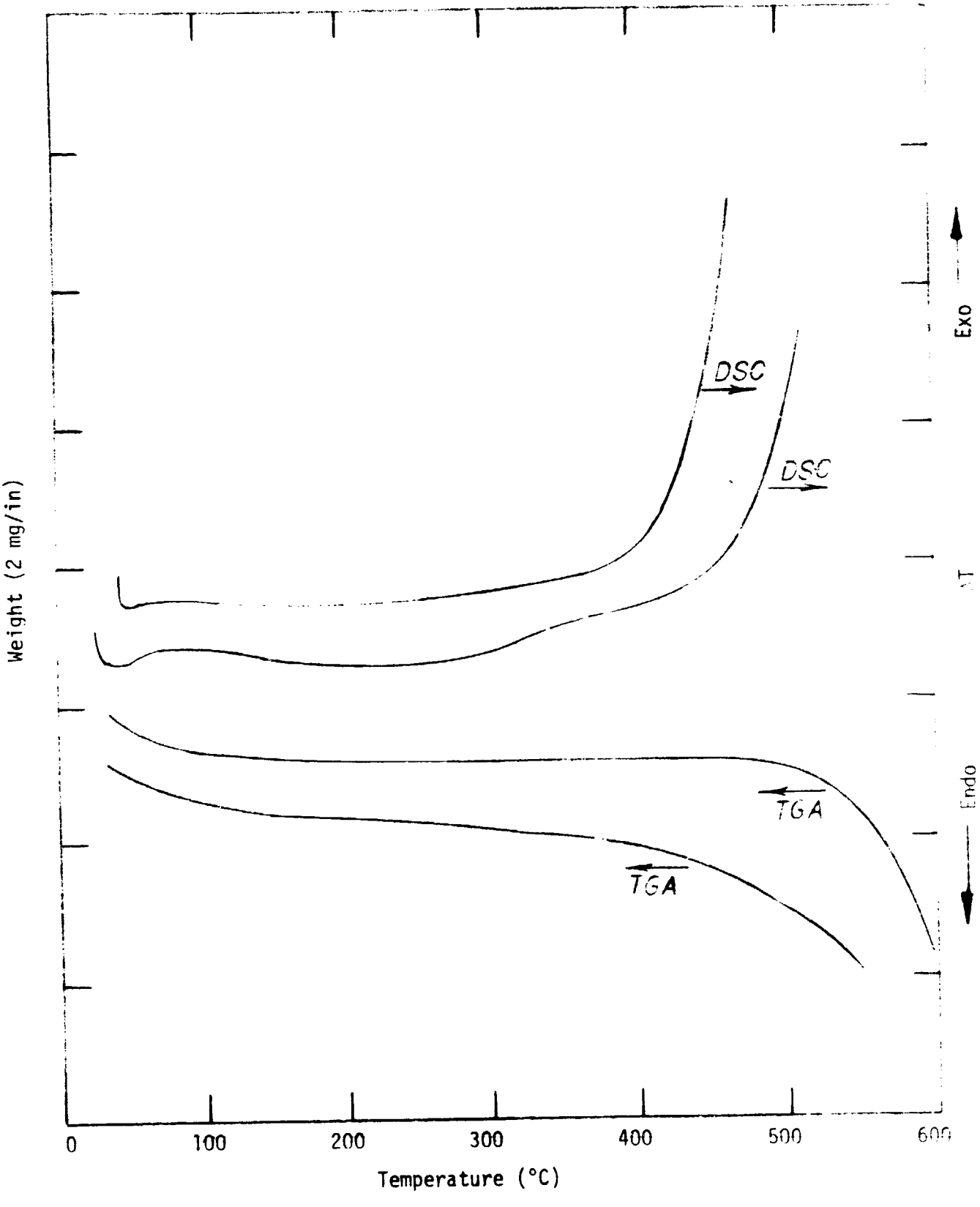

Figure 13: DSC and TGA traces for uncontaminated non-catalytic carbon heated in air

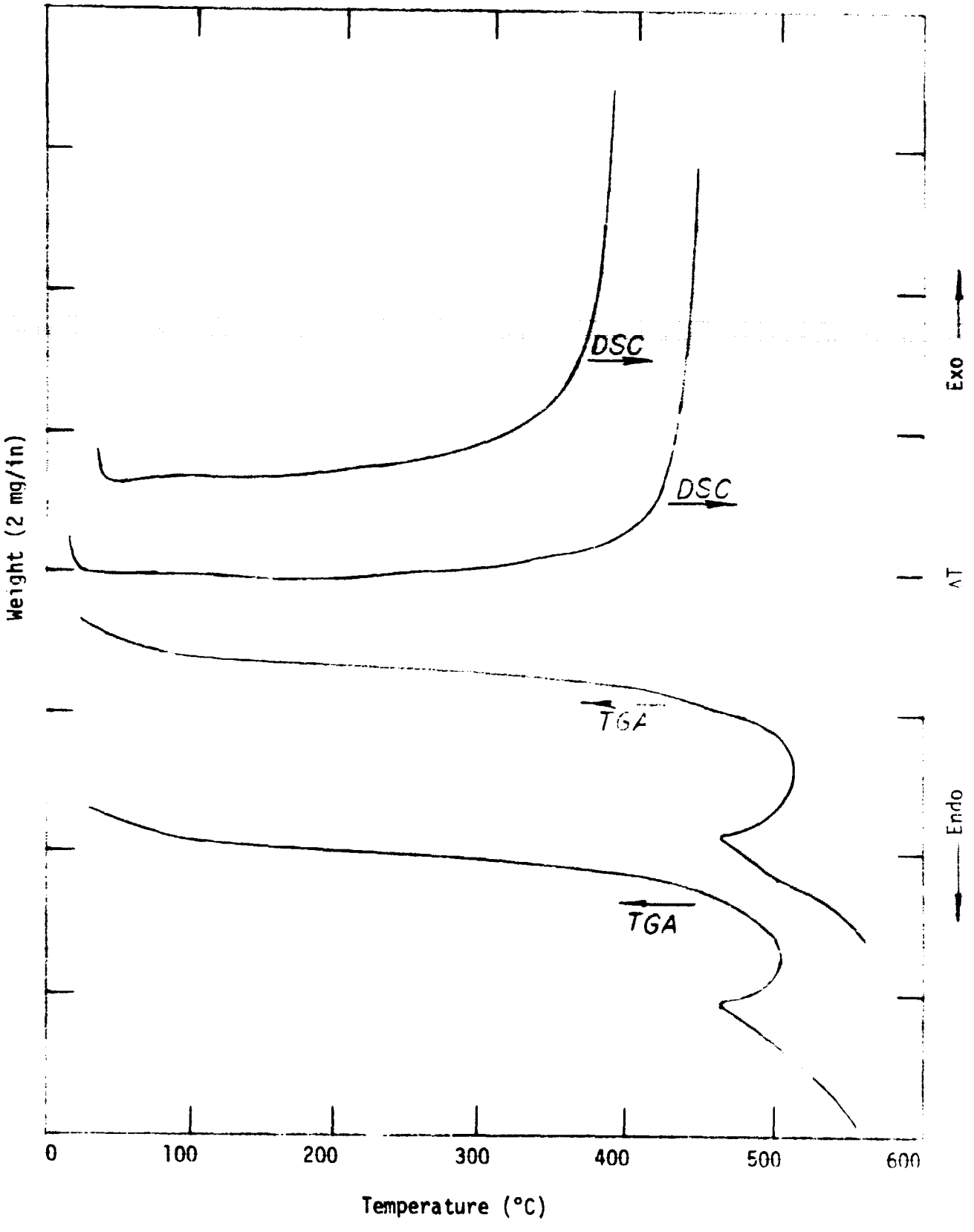

Figure 14: DSC and TGA traces for uncontaminated catalytic carbon (0.3% catalyst) heated in air

explained by postulating that while the contaminant loading levels off, the weight loss by carbon oxidation does not, and the latter eventually out-weighs the former. If this is true, loss of working capacity by carbon oxidation would be a more serious limitation to long term regenerability than an equivalent loss in working capacity by strongly adsorbed contaminants.

C. COMPARISON OF REGENERATION MODES USING CARBON COLUMNS

While TGA and DSC are of value in demonstrating differences in the various modes of regeneration, they are of limited value in projecting performance of an actual carbon bed. Their major limitation is that very small quantities of carbon (< 50 mg) are used, and dissipation of heat to the surroundings is much more rapid than in a packed bed. Carbon column tests were conducted to compare the alternative modes of regeneration under more realistic conditions.

1. Selection of Operating Conditions

Of the three contaminants (acrolein, caprylic acid, and DIBK) considered in this program, DIBK was selected for the carbon column tests. From the TGA and DSC curves, acrolein appeared to be readily removed by thermal desorption alone and would not provide a critical test for oxidative regeneration. Caprylic acid is inconvenient to work with because its vapor pressure is very low: to achieve a reasonably short adsorption cycle, the saturator and carbon columns would have to be maintained at an elevated temperature.

In comparing the various modes of regeneration, it is essential to know the working capacity of the carbon as a function of the number of adsorption-regeneration cycles. The easiest and most reliable method of determining the working capacity is to saturate the carbon column with the contaminant and determine the weight loss during regeneration of the column. The requirement of achieving saturation in a reasonably short time (24 hours) resulted in an unrealistically high contaminant concentration in the feed stream to the carbon columns. The feed concentration of DIBK was typically 2000 mg/

compared to a maximum allowable concentration (MAC) of 29 mg/m^3. Based on the potential plot for Pittsburgh BPL carbon[1], the predicted contaminant loading for the experimental tests is 0.35 g DIBK/g carbon. This is somewhat higher than the predicted loading of 0.25 g DIBK/g carbon for DIBK at its MAC in the feed stream. It is believed that the higher contaminant loading used in the experimental tests had no significant effect on the relative performance of the various regeneration modes.

Tests were conducted on two sets of columns; each set contained four columns regenerated by the four different techniques. The adsorption portion of the cycle required approximately 24 hours for complete bed saturation at the test conditions. While one set of columns was undergoing adsorption, the other set was being regenerated. Thus a complete adsorption/regeneration cycle required two days, and from the two sets of columns, two independent sets of data were obtained.

Since regeneration required more careful operator attention than adorption, the regeneration portion of the cycle was limited to a seven hour period during normal working hours. Based on the DSC curves of Figure 10 it was decided that the maximum temperature during oxidative regeneration should be kept below 350°C in order to prevent oxidation of carbon. Thus the oxidative columns were initially maintained at 300°C allowing a 50°C excursion for dissipation of the heat of reaction. The regeneration temperature for the 0.8% catalytic carbon was later reduced to 225°C to reduce carbon losses.

In order to allow a valid comparison between thermal desorption and oxidation, the thermal desorption columns were maintained at 350°C giving the same maximum regeneration temperature as for oxidative regeneration. For nitrogen-purge desorption the flow rate of nitrogen was arbitrarily set at 350 s.cc/min. Over the seven hour regeneration period, this is equivalent to about 2400 bed volumes of nitrogen. For vacuum desorption the vacuum system was capable of achieving pressures below 133 N/m^2 (1 torr).

When the contaminant loading is high much of the adsorbed

contaminant can be removed by thermal desorption. The potential advantage of oxidative regeneration is that it may be capable of removing very strongly adsorbed residual contaminant which cannot be removed by thermal desorption alone. Because of the high contaminant loading used in the experiemntal tests, the bulk of adsorbed contaminant was removed by nitrogen-purge thermal desorption prior to oxidation. The procedure consisted of heating the carbon column to 350°C for two hours in a notrogen flow of 350 s. cc/min. The column was then weighed to determine the amount of contaminant remaining, and the amount of oxygen required for oxidation was calculated. The oxidation was then carried out at 300°C (later decreased for the 0.8% catalytic carbon) over the remaining 5 hours of the regeneration period.

The amount of oxygen required to completely oxidize the contaminant remaining after thermal desorption was determined from the following generalized reaction.

$$(CH_2)_n + \frac{3}{2} nO_2 \longrightarrow nCO_2 + nH_2O$$

The stoichiometric amount of oxygen is 2,400 s. cc/g of organic. The required air flow rate over the 5 hour oxidation period was determined from the weight of residual contaminant and the stoichiometric factor. An actual flow rate 20% in excess of stoichiometric was used. The air flow was calculated on the basis of either the cumulative residual or the single-cycle residual, whichever was greater.

The heat of combustion for hydrocarbons is typically 46.5 MJ/kg (20,000 Btu/lb). This heat must be removed in order to prevent overheating of the carbon bed and run-away oxidation of the carbon. A coolant stream of nitrogen heated to 300°C was passed through the columns to make sure the heat of reaction was removed. For an allowable ΔT of 50°C for the nitrogen stream, i.e., 300°C to 350°C, the required nitrogen flow is 684,000 s. cc/g of organic. This flow was distributed evenly over the 5 hour regeneration period.

2. Results of Multiple-Cycle Tests

Contaminant loadings after adsorption and after regeneration are given as a function of cycle number in Table 3 for Set A and in Table 4 for Set B. The results are plotted in Figures 15 - 22.

During the early cycles for each test, insufficient time was allowed during the adsorption portion of the cycle for the entire carbon bed to reach saturation. After the adsorption time was increased (from 16 to 24 hours) the uptake was, in most cases, very reproducible. For Set A the saturation capacity of the virgin carbon was 0.340 g/g carbon (Figures 16, 18, and 20). Both of these values are very close to the value predicted from the potential plot (0.35 g/g carbon).

As shown by the adsorption data of Figure 21 and 22, a reproducible equilibrium uptake was not observed for the catalytic carbons. Separate adsorption tests were conducted with virgin samples of 0.3% and 0.8% catalytic carbon. The adsorptive capacities were 0.336 and 0.334 g/g carbon for the 0.3% and 0.8% catalytic carbons, respectively. These values are quite close to those for non-catalytic carbon. The catalytic carbons reached complete saturation after about 48 hours of adsorption. After 24 hours, the loading was about 99% of the final equilibrium loading. The reason for the scatter in the adsorption points for the catalytic carbons is not apparent.

The most consistent results were obtained for nitrogen-purge thermal desorption (Figures 15 and 16). In both Sets A and B, the "heel" of the undesorbed contaminant built up to about .02 g DIBK/g carbon over the first ten adsorption/regeneration cycles and remained constant over the remaining cycles. The equilibrium uptake remained constant throughout the tests, after sufficient time was allowed for adsorption, indicating no loss in carbon surface area. The only loss in working capacity results from the heel of undesorbed contaminant. (The working capacity is the difference between the loading after adsorption and after regeneration.) If the heel remains constant in subsequent cycles, the projected loss in working capacity is only about 6% for the nitrogen-purge thermal desorption of DIBK. This can easily be compensated for by increasing the design weight of the carbon bed by 6%.

TABLE 3

CONTAMINANT LOADINGS FOR REPETITIVE-CYCLE COLUMN TESTS (SET A)

Cycle Number	Column #1[a] (Thermal Des. - N_2 Purge) After Adsorption* (g/g carbon)	Column #1[a] (Thermal Des. - N_2 Purge) After Regeneration* (g/g carbon)	Column #2[b] (Oxidation - non-catalytic) After Adsorption* (g/g)	Column #2[b] (Oxidation - non-catalytic) After Regeneration* (g/g)	Column #3[c] (Oxidation - catalytic) After Adsorption* (g/g)	Column #3[c] (Oxidation - catalytic) After Regeneration* (g/g)	Column #4[d] (Thermal Des. - Vacuum) After Adsorption* (g/g)	Column #4[d] (Thermal Des. - Vacuum) After Regeneration* (g/g)
1	0.228	2.49×10^{-3}	0.172	2.79×10^{-3}	0.201	8.36×10^{-3}	0.303	3.90×10^{-3}
2	0.251	5.40×10^{-3}	0.155	3.09×10^{-3}	0.250	1.55×10^{-2}	0.344	3.55×10^{-3}
3	0.278	3.70×10^{-3}	0.252	2.37×10^{-3}	0.255	-1.21×10^{-2}	---	-------
4	0.230	7.08×10^{-3}	0.185	5.63×10^{-3}	0.232	1.94×10^{-3}	---	-------
5	0.181	1.06×10^{-2}	0.144	7.72×10^{-3}	0.168	-------	0.289	-------
6	0.245	-------	0.188	-------	0.198	-------	0.277	-------
7	0.284	1.31×10^{-2}	0.257	5.05×10^{-3}	0.238	8.02×10^{-3}	0.318	1.47×10^{-3}
8	0.322	1.40×10^{-2}	0.292	2.35×10^{-3}	0.266	-2.96×10^{-2}	0.313	3.68×10^{-3}
9	0.334	1.54×10^{-2}	0.325	6.92×10^{-4}	0.267	2.91×10^{-3}	0.329	2.01×10^{-2}
10	0.328	1.87×10^{-2}	0.282	3.23×10^{-3}	0.247	6.23×10^{-3}	0.324	1.51×10^{-2}
11	0.334	1.72×10^{-2}	0.324	2.46×10^{-3}	0.254	8.39×10^{-3}	0.328	2.25×10^{-2}
12	0.331	1.47×10^{-2}	0.320	5.42×10^{-4}	0.254	-2.84×10^{-2}	0.326	1.49×10^{-2}
13	0.341	2.06×10^{-2}	0.316	1.25×10^{-2}	0.283	3.62×10^{-2}	0.337	6.16×10^{-3}
14	0.332	2.04×10^{-2}	0.321	4.47×10^{-3}	0.269	3.83×10^{-2}	0.327	2.56×10^{-2}
15	0.333	2.17×10^{-2}	0.316	4.61×10^{-3}	0.271	3.31×10^{-2}	0.329	1.92×10^{-2}
16	---	2.08×10^{-2}	---	6.24×10^{-3}	---	1.72×10^{-2}	---	3.01×10^{-2}
17	0.334	2.17×10^{-2}	0.316	8.16×10^{-3}	0.257	2.17×10^{-2}	0.337	1.30×10^{-2}

* All loadings are reported as grams of contaminant per gram of virgin carbon.

[a] Weight of virgin carbon (i.e. weight of uncontaminated carbon on first cycle) = 29.8234 g

[b] Weight of virgin carbon = 33.2385 g

[c] Weight of virgin carbon = 34.8885 g; Catalyst loading = 0.3 wt%.

[d] Weight of virgin carbon = 31.4635 g for cycles 1 and 2; = 27.9361 g for remaining cycles

TABLE 4

CONTAMINANT LOADINGS FOR REPETITIVE-CYCLE COLUMN TESTS (SET B)

Cycle Number	Column #5[a] (Thermal Des. - N_2 Purge) After * Adsorption (g/g carbon)	After * Regeneration (g/g carbon)	Column #6[b] (Oxidation - non-catalytic) After * Adsorption (g/g carbon)	After * Regeneration (g/g carbon)	Column #7[c] (Oxidation - catalytic) After * Adsorption (g/g carbon)	After * Regeneration (g/g carbon)	Column #8[d] (Thermal Des. - Vacuum) After * Adsorption (g/g carbon)	After * Regeneration (g/g carbon)
1	0.298	-------	0.298	-------	0.305	-------	0.291	-------
2	0.311	1.89×10^{-3}	0.257	4.11×10^{-3}	0.246	1.06×10^{-2}	0.315	-------
3	0.234	8.84×10^{-3}	0.210	1.09×10^{-2}	0.223	1.04×10^{-2}	0.316	9.87×10^{-3}
4	0.336	8.74×10^{-3}	0.333	1.32×10^{-2}	0.304	6.62×10^{-3}	0.337	2.78×10^{-4}
5	0.337	1.20×10^{-2}	0.337	1.81×10^{-2}	0.298	-1.48×10^{-2}	0.339	-------
6	0.335	1.10×10^{-2}	0.337	1.73×10^{-2}	0.269	-4.27×10^{-3}	---	2.20×10^{-2}
7	0.339	1.41×10^{-2}	0.341	2.21×10^{-2}	0.258	1.28×10^{-3}	0.342	2.27×10^{-2}
8	0.310	1.55×10^{-2}	0.292	1.62×10^{-2}	0.247	7.51×10^{-3}	0.340	2.79×10^{-2}
9	0.339	1.50×10^{-2}	0.308	1.98×10^{-2}	0.284	2.05×10^{-2}	0.341	2.94×10^{-2}
10	0.337	1.84×10^{-2}	0.334	4.18×10^{-3}	0.277	1.34×10^{-2}	0.339	1.91×10^{-2}
11	0.338	1.78×10^{-2}	0.327	5.44×10^{-3}	0.255	-2.97×10^{-2}	0.340	2.12×10^{-2}
12	0.339	1.84×10^{-2}	0.325	3.70×10^{-3}	0.242	5.69×10^{-3}	0.342	3.00×10^{-2}
13	0.342	1.70×10^{-2}	0.325	5.44×10^{-3}	0.243	1.30×10^{-2}	0.345	4.88×10^{-2}
14	0.340	1.89×10^{-2}	0.324	9.24×10^{-3}	0.242	1.65×10^{-2}	0.344	3.64×10^{-2}
15	0.339	2.17×10^{-2}	0.320	6.37×10^{-3}	0.242	2.14×10^{-2}	0.342	3.09×10^{-2}

* All loadings are reported as grams of contaminant per gram of virgin carbon.

[a] Weight of virgin carbon = 34.3209 g

[b] Weight of virgin carbon = 36.0176 g

[c] Weight of virgin carbon = 36.3509 g; Catalyst loading = 0.8 wt %.

[d] Weight of virgin carbon = 30.8991 g

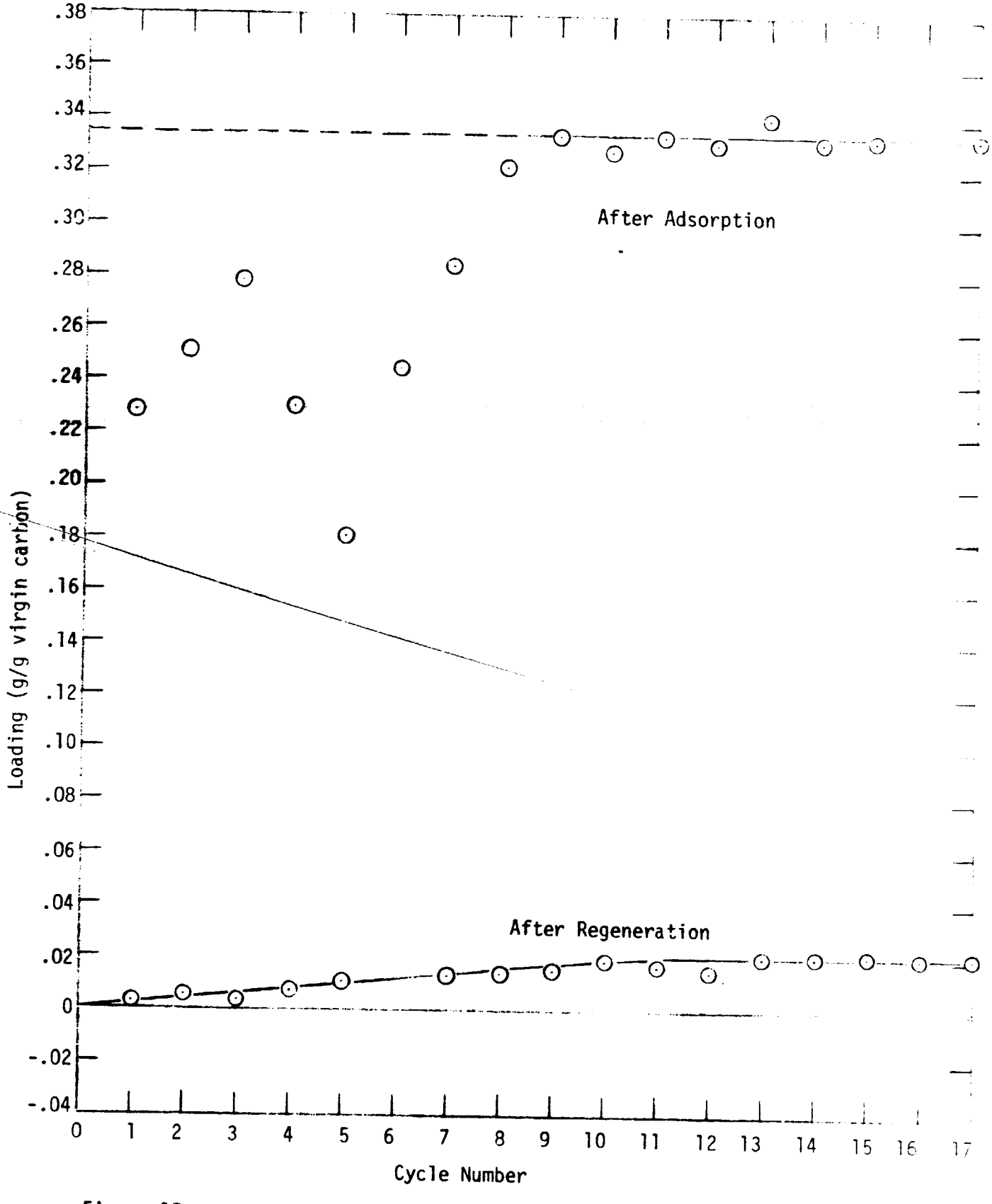

Figure 15: Loading of DIBK vs. cycle number for regeneration by nitrogen-purge thermal desorption (set A)

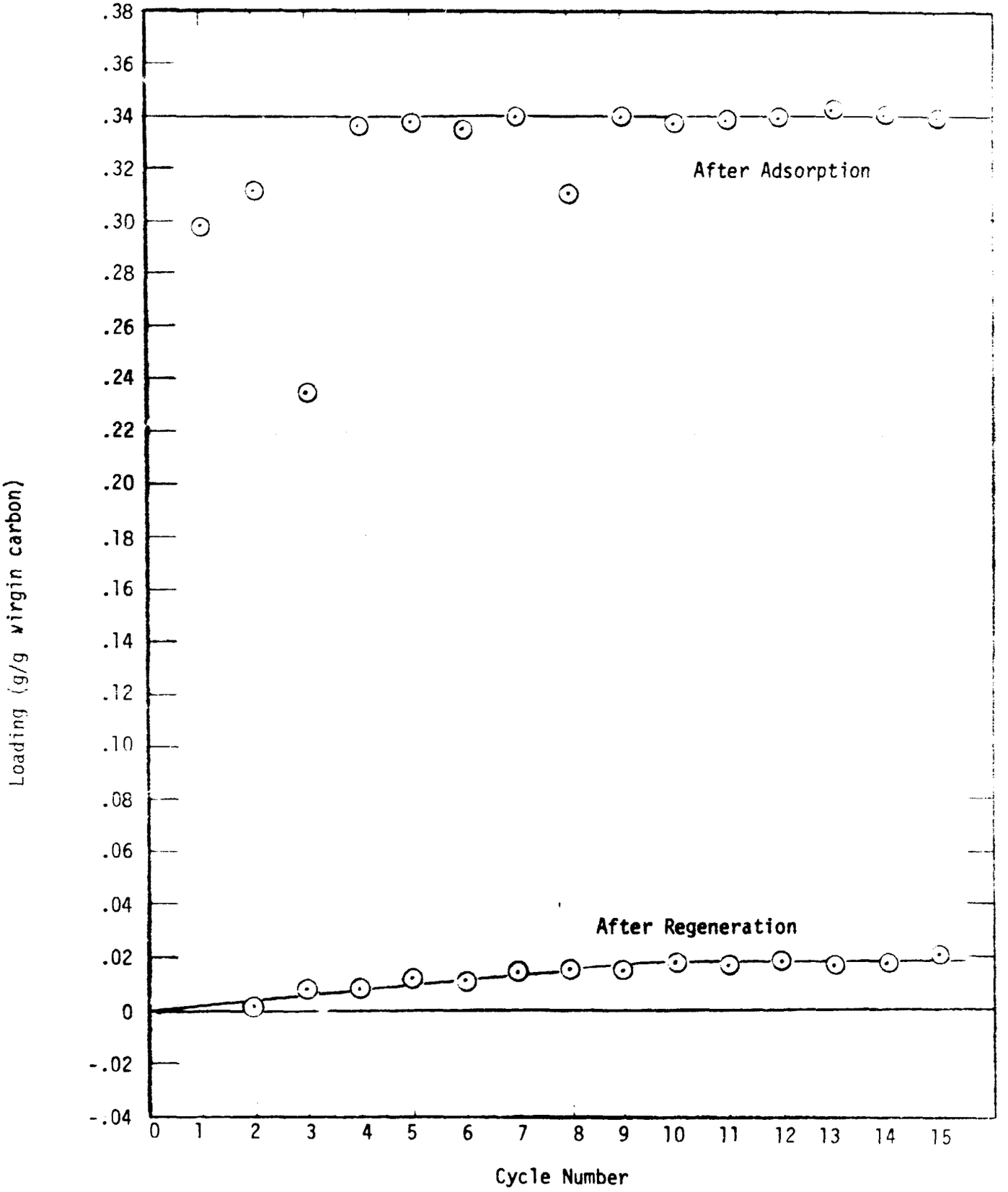

Figure 16: Loading of DIBK vs. cycle number for regeneration by nitrogen purge thermal desorption (Set B)

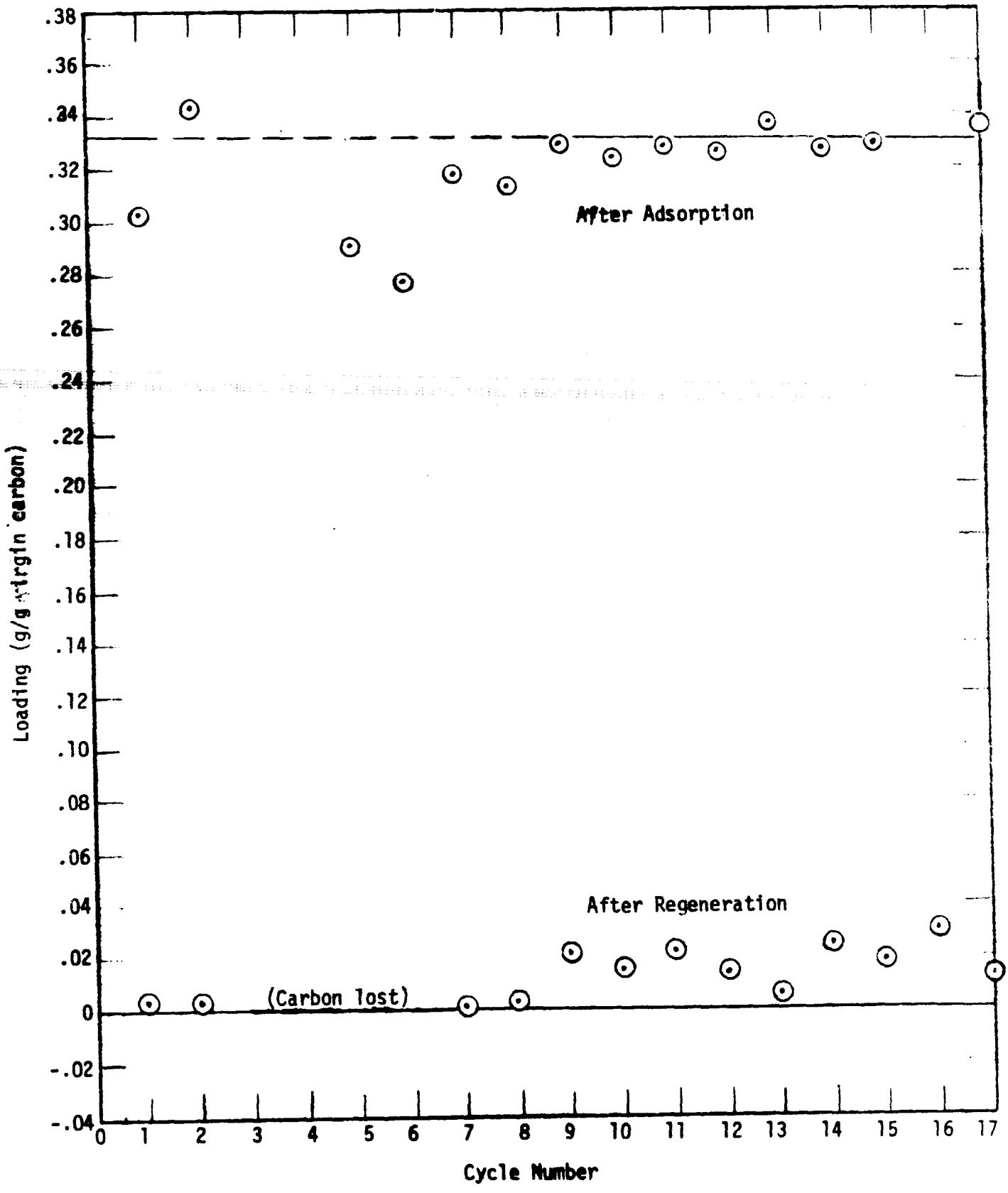

Figure 17: Loading of DIBK vs. cycle number for regeneration by vacuum thermal desorption (Set A).

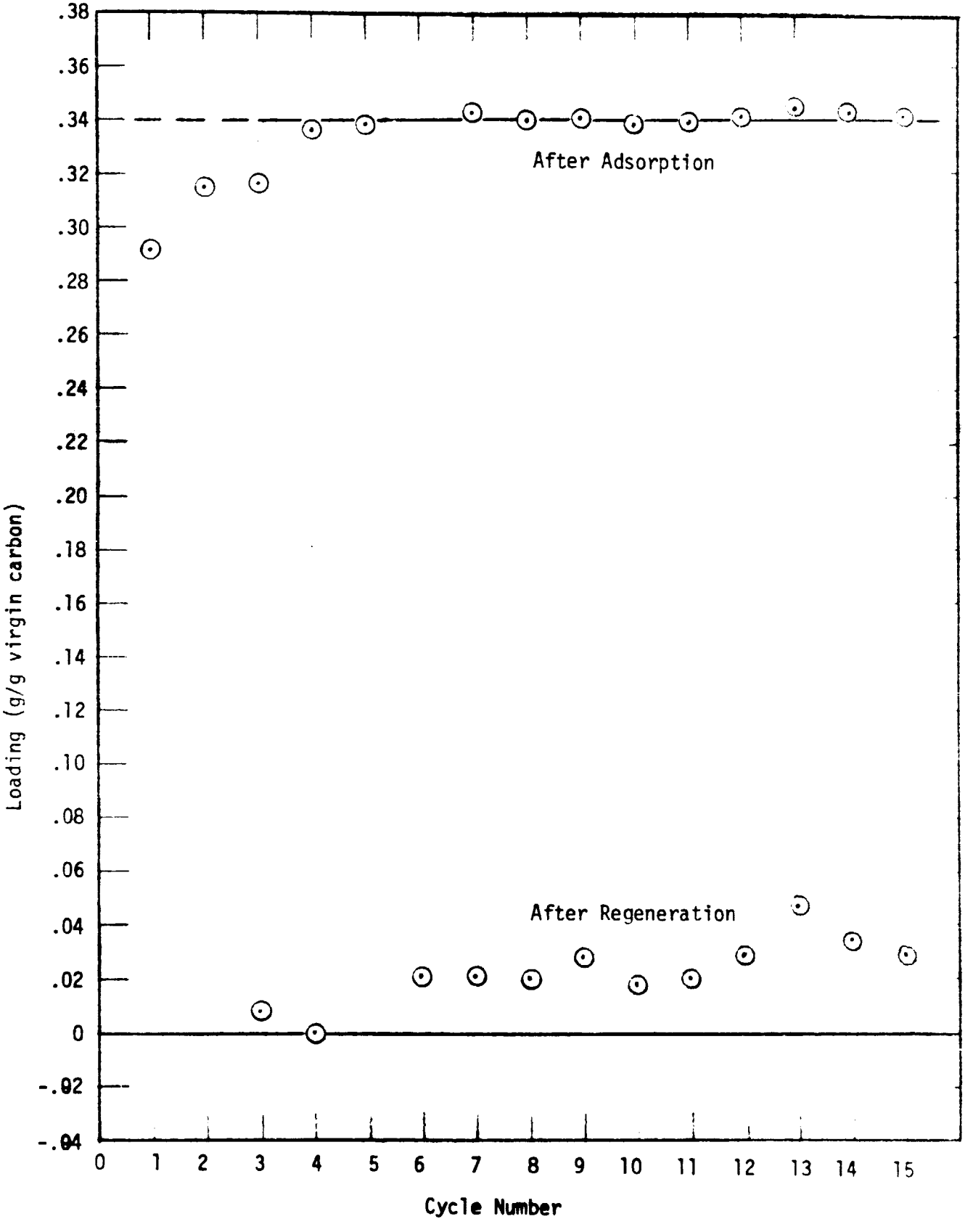

Figure 18. Loading of DIBK vs. cycle number for regeneration by vacuum thermal desorption (Set B).

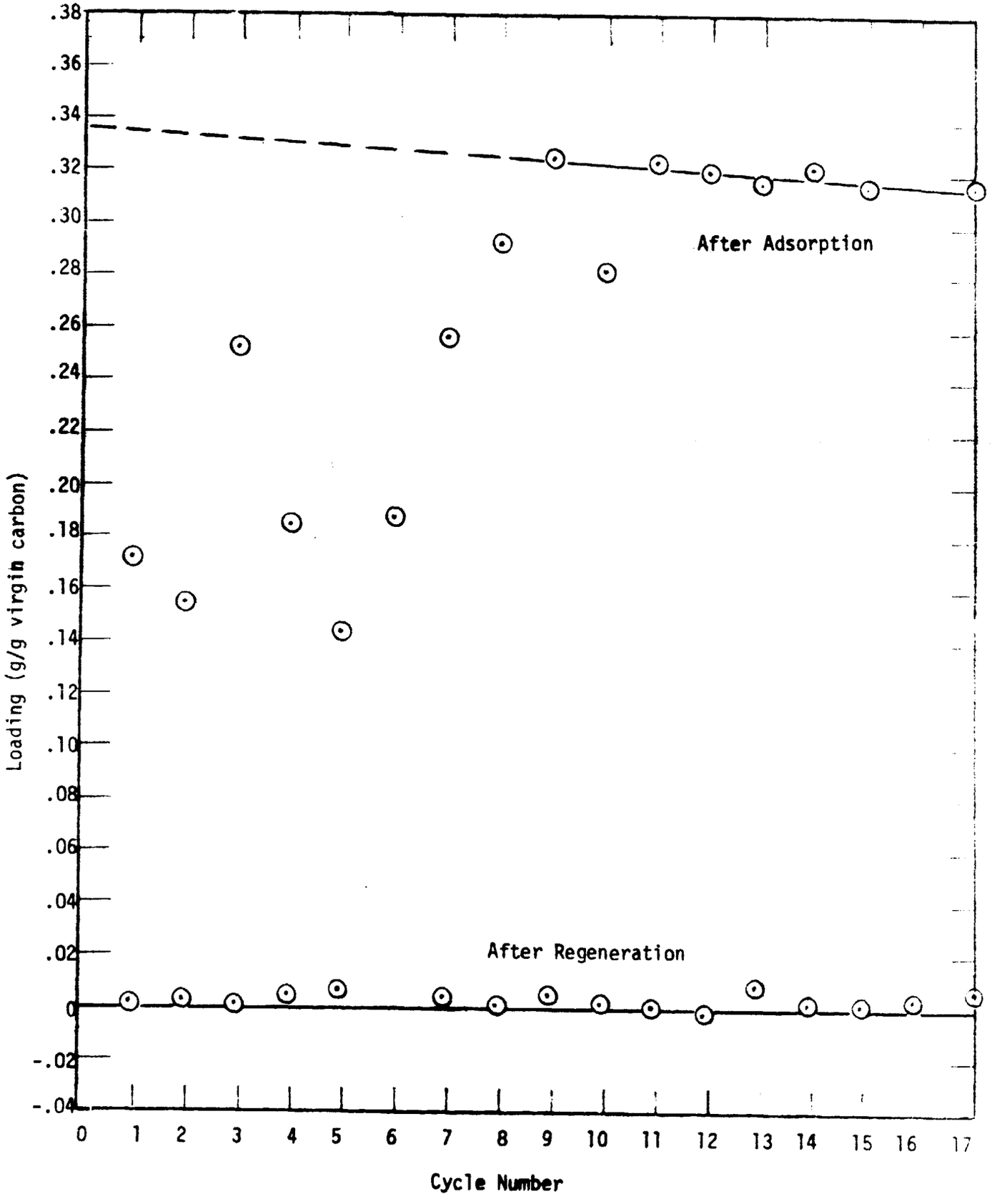

Figure 19: Loading of DIBK vs. cycle number for regeneration by non-catalytic oxidation (Set A)

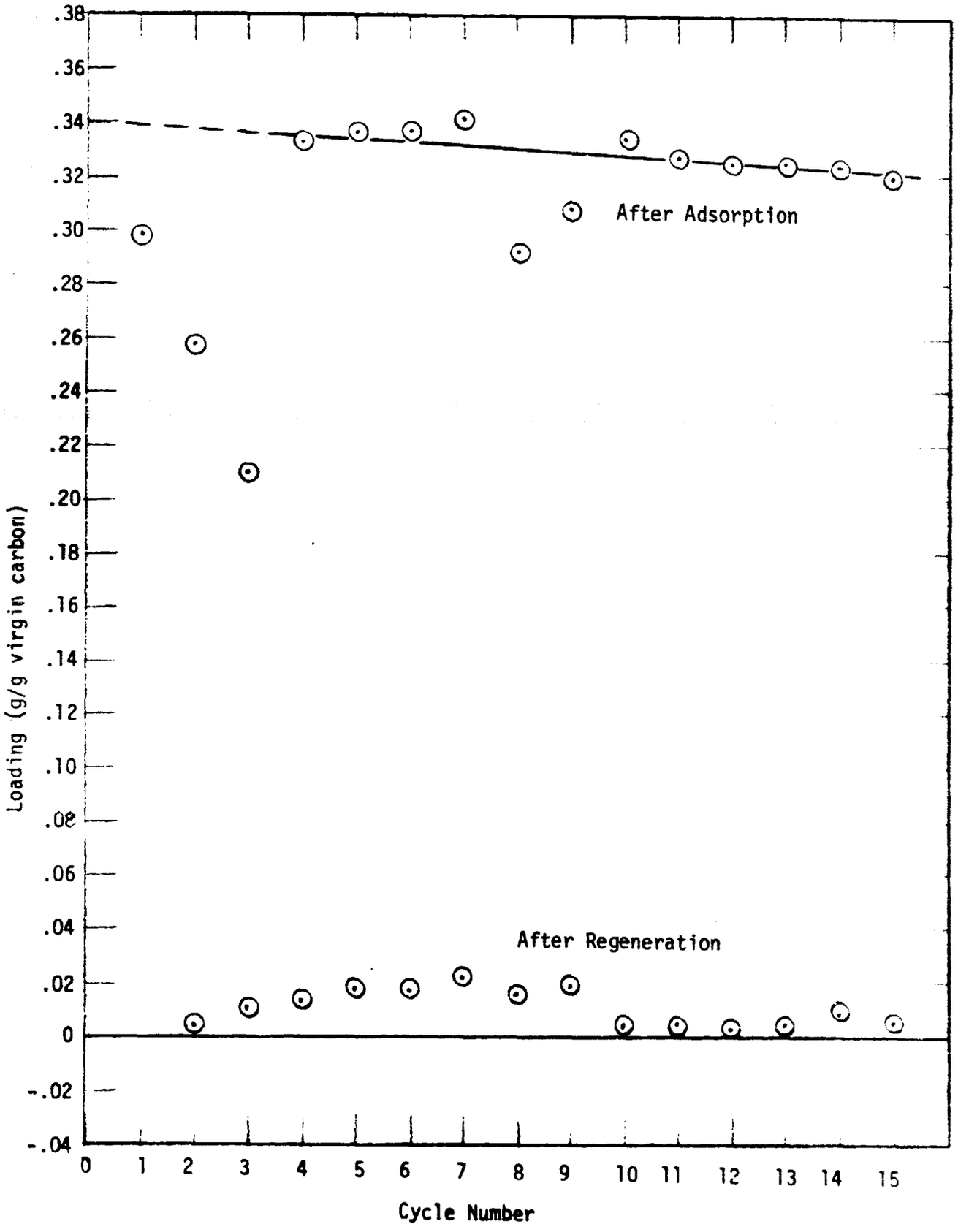

Figure 20. Loading of DIBK vs. cycle number for regeneration by non-catalytic oxidation (Set B).

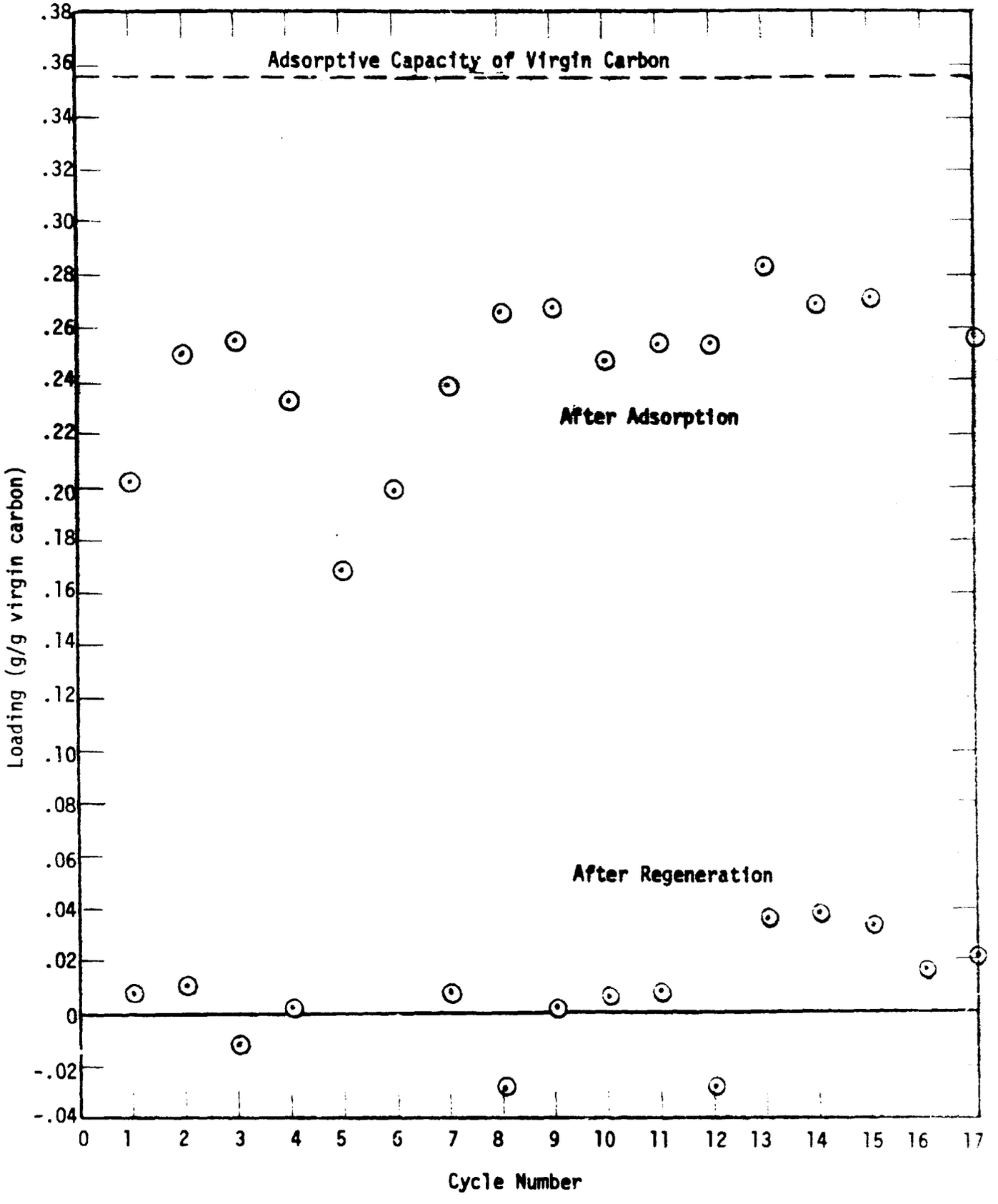

Figure 21: Loading of DIBK vs. cycle number for regeneration by catalytic oxidation with 0.3% catalytic carbon (Set A)

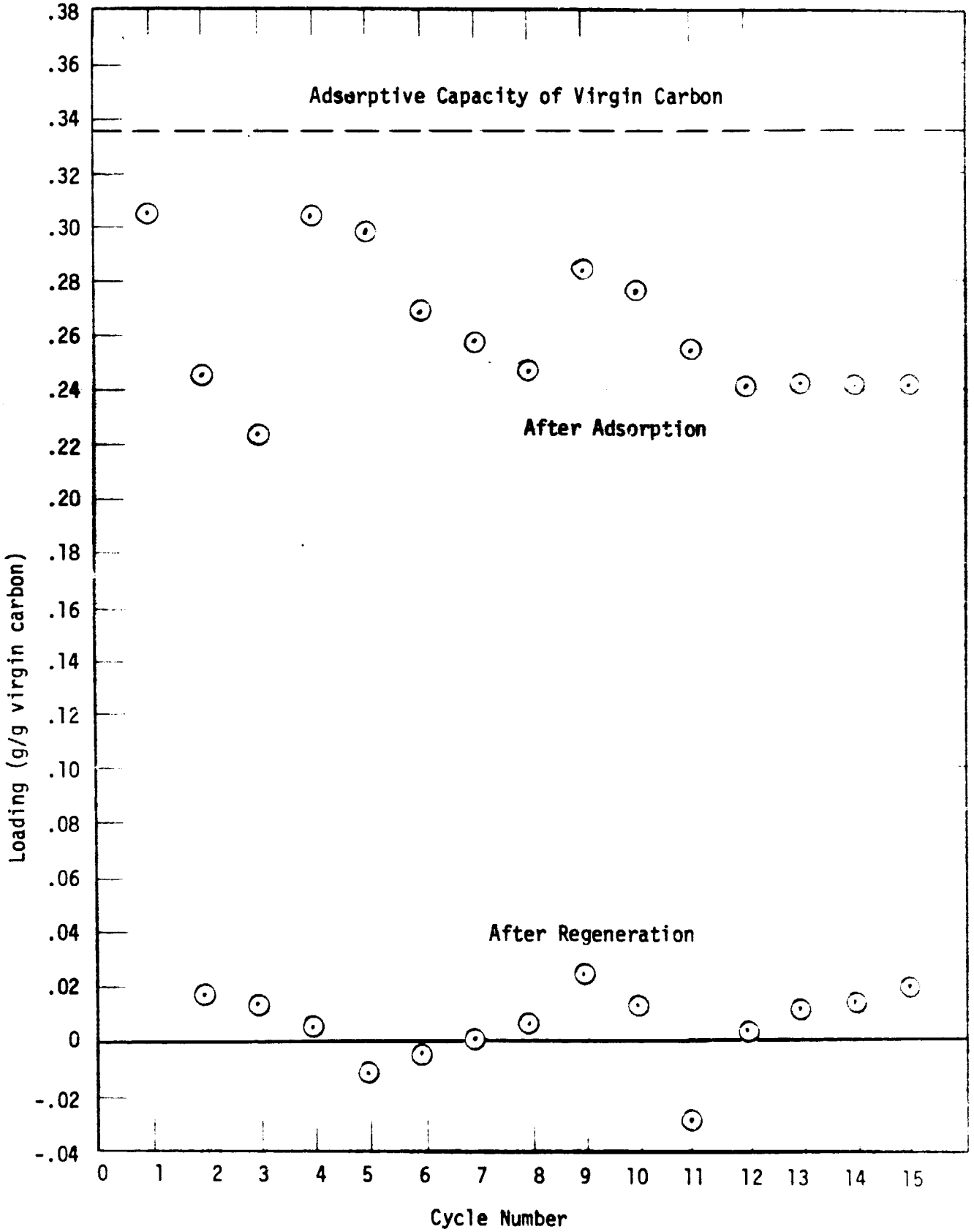

Figure 22. Loading of DIBK vs. cycle number for regeneration by catalytic oxidation with 0.8% catalytic carbon (Set B).

Results for vacuum thermal desorption (Figures 17 and 18) were somewhat more uncertain. After sufficient time was allowed for adsorption, the contaminant loading after adsorption remained constant throughout the tests. This indicates no loss of carbon. The weights recorded for the contaminant heel were erratic but are generally in the range of .02 to .03 g/g carbon. It is not possible to determine from these data whether or not the heel remains constant within this range. The fact that the heel is somewhat higher and the scatter is greater than for nitrogen-purge thermal desorption may be attributed, in part, to the poor heat transfer through the evacuated carbon bed. Carbon close to the axis of the bed may not have been regenerated as completely as the carbon close to the wall.

Ideally the results for nitrogen-purge, and vacuum thermal desorption should be similar. The only difference in these two modes of regeneration is the way in which desorbed contaminants are removed from the carbon bed. Provided the contaminant partial pressure is reduced to the same extent and the temperature-time history of the beds are equivalent, the same heel should remain following desorption. Thus a loss in adsorptive capacity of about 6-9% would be anticipated for vacuum thermal desorption of DIBK.

Results for non-catalytic oxidative regeneration are shown in Figures 19 (Set A) and 20 (Set B). For both Sets of tests, the apparent contaminant heel remaining after the 15th regeneration was less than .01g/g virgin carbon. This is significantly lower than the heel for nitrogen-purge thermal desorption (.02 g/g carbon). However, the total uptake of contaminant at saturation decreased as the number of repetitive cycles increased. The straight line decrease extrapolates to the correct adsorptive capacity for the virgin carbon (0.335 g/g carbon for Set A; 0.340 g/g carbon for Set B). The decrease in total uptake indicates a loss of carbon by oxidation. The fact that positive weights were measured following regeneration indicates that the contaminant heel remaining after regeneration more than compensated for the loss in carbon weight. Based on the amount of contaminant desorbed, the loss in working capacity over 15 cycles is about 7.5%. This is only slightly higher

than the loss in working capacity for nitrogen-purge thermal desorption. However when extrapolated to many cycles, thermal desorption is clearly superior. The working capacity for non-catalytic oxidative regeneration continues to decrease; while, for thermal desorption, it remains constant.

Results for catalytic oxidative regeneration are shown in Figure 21 for Set A (0.3% catalyst) and in Figure 22 for Set B (0.8% catalyst). For both sets significant contaminant residuals and significant losses of carbon were observed. For the 0.3% catalytic carbon the working capacity on the 15th cycle was 29% below the adsorptive capacity of the virgin carbon (0.336 g/g carbon). For the 0.8% catalytic carbon, the working capacity on the 15th cycle was 34% below the adsorptive capacity of the virgin carbon (0.334 g/g carbon). Even though the oxidation temperature for this carbon was reduced from 300°C to 225°C for the ninth and subsequent cycles, loss of carbon and working capacity continued to occur.

D. DISCUSSION OF RESULTS

The repetitive-cycle TGA results and the repetitive-cycle carbon column results appear to be contradictory. Based on the superficial evidence it seems that the TGA results indicate that catalytic oxidation is the preferred mode of regeneration followed by non-catalytic oxidation and finally thermal desorption. The carbon column results indicate just the reverse order of preference.

There are a number of reasons why less reliance is placed on the TGA results. The most important criterion in evaluating regenerability is the working capacity of the carbon. The working capacity was not determined during the TGA tests, only the heel of residual contaminant. The amount of heel remaining on the carbon will equal the loss in working capacity only if the carbon weight remains constant. If carbon is lost by oxidation the heel appears smaller from the weight measurements, but the loss in working capacity is greater.

The TGA curves for uncontaminated carbon (Figures 13 and 14) do not, in general, indicate sufficient carbon oxidation to account for the entire loss

ference in measured residuals between oxidation and desorption. However they do indicate the possibility of carbon oxidation at 350°C and 400°C. Furthermore it is possible that the loss of carbon by oxidation is greater for regeneration of contaminated carbon. The highly exothermic oxidation of contaminant may create a localized temperature excursion at the oxidation site causing oxidation of carbon in the vicinity of that site.

In addition to the lack of working capacity measurements, the TGA tests were conducted with very small amounts (<50 mg) of carbon. Individual carbon particles were spread out on the balance pan of the TGA. The heat transfer characteristics are therefore much different than for a carbon particle in a column.

Finally the TGA tests were carried out at a programmed heating rate of 15°C/min and are less representative of the regeneration conditions expected for spacecraft applications.

The high losses in working capacities for the column tests with the catalytic carbons are the combined result of carbon oxidation and contaminant heel build-up. Substantial losses of carbon occurred even though the temperature during oxidation was maintained below 350°C for 0.3% catalytic carbon and below 250°C for 0.8% catalytic carbon. It is possible that even though the rate of carbon oxidation was slow at these temperatures, the extended oxidation time (5 hours) resulted in a significant loss.

Oxidative regeneration at lower temepratures would certainly decrease the carbon loss, but the amount of heel remaining would probably increase. Even at the temperatures employed in these tests, the amount of actual heel remaining after regeneration (taking into account the loss of carbon) was substantial for both catalytic and non-catalytic oxidation. It is possible to estimate the relative importance of carbon oxidation and contaminant heel build-up in determining the loss in working capacity. The assumption and calculational procedures are given in the Appendix. For non-catalytic carbon after 17 cycles (Figure 19), the loss in working capacity due to carbon oxidation is 1.49%; the loss due to heel build-up is 6.57% for a total loss of 8.06%. For 0.3% catalytic carbon after 17 cycles (Figure 21), the loss in

working capacity due to carbon oxidation is 5.95%; the loss due to heel build-up is 24.11% for a total loss of 30.06%. It is apparent from these numbers that a substantial heel remains after oxidative regeneration. Oxidation at lower temperatures would probably result in a larger heel; while oxidation at higher temperatures would result in greater carbon oxidation. It is concluded that oxidation at a lower or higher temperature would probably not change the relative performance ranking of the various regeneration modes.

In addition to the advantage of better regenerability, thermal desorption is simpler, more reliable, safer, and easier to control than oxidative regeneration. Therefore thermal desorption is selected as the preferred mode of regeneration.

III. CONCLUSIONS

1. Based on the temperature separation between the oxidation of strongly adsorbed DIBK and the oxidation of carbon, the preferred loading of "noble metal" catalyst is 0.8% by weight.

2. The catalytic carbon prepared in the previous program using a solution impregnation procedure to deposit platinum on BPL carbon is very similar in chemical behavior to the commercially prepared catalytic carbon used in this program.

3. Multiple-cycle tests using TGA to measure the weight increase and loss on adsorption and removal of DIBK indicated that the lowest apparent contaminant residuals were obtained with catalytic oxidation; the highest residuals, with thermal desorption. However working capacity was not monitored during these tests, and the low residuals for oxidative regeneration may be due, in part, to oxidation of carbon.

4. Multiple-cycle tests using carbon columns indicated that thermal desorption was the preferred mode of regeneration of carbon contaminated with DIBK. For thermal desorption a heel of undesorbed contaminant built up over ten cycles but remained constant therafter. If extrapolated to 90 cycles (regeneration on alternate days over a 180-day mission) the loss in working capacity would be only 6%.

5. Multiple-cycle column tests showed that oxidation of carbon and heel build-up occurred during non-catalytic oxidative regeneration. Extrapolated over 90 cycles the loss in working capacity for this mode of regeneration would be about 35%.

6. Multiple-cycle column tests indicated that catalytic oxidative regeneration of DIBK-contaminated carbon results in significant oxidation and significant build-up of contaminant heel. The loss in working capacity over 15 cycles was in the range of 30 to 35%.

SECTION 4

PHASE II: DEMONSTRATION OF SELECTED REGENERATION TECHNIQUES

Based on the results and conclusions of Phase I, thermal desorption was selected as the preferred mode of regeneration. Phase II tests were conducted to evaluate both vacuum and nitrogen-purge thermal desorption techniques. Preliminary tests were conducted with single contaminants to determine the effects of various desorption parameters on the rate and extent of desorption. Repetitive adsorption-desorption tests were then conducted with a multi-component contaminant mixture to assess the loss in working capacity over an extended period of operation.

I. EXPERIMENTAL APPARATUS AND PROCEDURES

A. SELECTION OF CARBON

Based on a comparison of potential plots for various carbons, LMSC selected Barneby Cheney BD 6 x 12 activated carbon for the regenerable bed[1]. This same carbon was used for all Phase II experiments. Before use, columns containing fresh carbon were reactivated for a minimum of 16 hours at 105-125°C under 5 cc/min nitrogen purge.

B. SELECTION OF CONTAMINANTS

There are three potential rate-limiting steps in the removal of adsorbed contaminants from activated carbon:

- desorption from the carbon surface,
- pore diffusion to the exterior of the particle, and
- mass transfer from the exterior to the bulk gas phase.

Under typical conditions of adsorption and regeneration, the most likely rate-limiting step is pore diffusion. Therefore, single contaminants should be selected for study which have significantly different pore diffusion coefficients. The pore diffusion coefficient depends on the inverse square root of molecular weight, so different molecular weights should be of importance. Acetone (molecular weight 58) and

Freon 12 (molecular weight 121) were, therefore, chosen as contaminants for use in various single-cycle tests to determine the effect of molecular weight on desorption dynamics.

The repetitive cycle tests were conducted with a mixture of 21 spacecraft contaminants identified[1] as the "primary" contaminants controlled by the regenerable carbon bed. Molecular weights of the 21 contaminants range from 32 (methyl alcohol) to 137 (Freon 11).

C. CARBON COLUMN DESIGN

One of the major modifications made for Phase II tests was the redesign of the carbon adsorption columns. The revised design was based on the dimensions and operating conditions used for the prototype (full-scale) regenerable carbon bed. The relevant prototype specifications are [4]:

Bed Diameter = 19.1 cm (7.5 inches)
Bed Length = 41.9 cm (16.5 inches)
Flow Rate = 120 ℓ/min (4.25 CFM)
Adsorbent = 5.8 kg (12.7 lbs.) 6 x 12 mesh Barneby Cheney BD carbon

The experimental model which is the most closely related to the prototype is one in which the diameter of the prototype carbon bed is reduced to a convenient experimental scale and in which the flow-rate is reduced in direct proportion to the cross-sectional area. The prototype can be viewed as n models operated in parallel, each carrying $1/n^{th}$ of the total volumetric flow. It is apparent, therefore, that the same adsorption dynamics will exist in the model and prototype, i.e., the breakthrough curves will be identical. (This assumes, of course, the absence of wall effects). Furthermore, it is apparent that the same desorption dynamics will exist in the model and prototype regardless of the rate limiting step (desorption, pore diffusion, or bulk mass transfer), provided that diameter-related phenomena such as heat transfer are unimportant. Thus, the data obtained from this model should be directly applicable to the full-scale system.

An outside diameter of 0.5 in. was selected as a convenient scale for the experimental model. The length was kept the same as the prototype to provide the same number of transfer units. The flow rate was decreased in the experimental system to provide the same linear flow rate through the bed as for the prototype. Thus, the dimensions and operating conditions for the experimental model are:

Bed Diameter = 1.09 cm (0.430 in., 0.50 in.)
Bed Length = 41.9 cm (16.5 in.)
Flow Rate = 396 s.cc/min.
Carbon Type = Barneby Cheney BD 6 x 12 mesh

Two columns were fabricated so that adsorption and regeneration could be carried out simultaneously. The columns, 51-cm (20 inch), lengths of 1.27-cm (1/2 inch)- diameter 316 stainless steel tubing, were wrapped into single-turn coils in order to fit them onto the analytical balance for weight measurements. The experimental carbon columns contained 15-16 grams of carbon resulting in a packing density of 0.38-0.41 g/cc. This is somewhat below the packing density calculated for the prototype bed (0.48 g/cc), but no major impact on the program results is anticipated from this difference. The lower packing density for the experimental column may be the result of errors in estimating the actual column length or volume. The above-mentioned coiling of the columns probably caused distortion of the column diameter, making it more difficult to determine actual bed length and volume.

D. SYSTEM DESIGN AND OPERATION

1. Adsorption System: Acetone and Freon 12

The flow-schematic for the adsorption system used in all single-contaminant tests (acetone and Freon 12) is shown in Figure 23. Laboratory compressed air was passed through a pressure regulator (PR) and was purified by passing it in series through a filter/carbon cartridge, an activated carbon column, and a fine-grade filter (Balston Grade AA). The purified air was then split into three streams, A (for

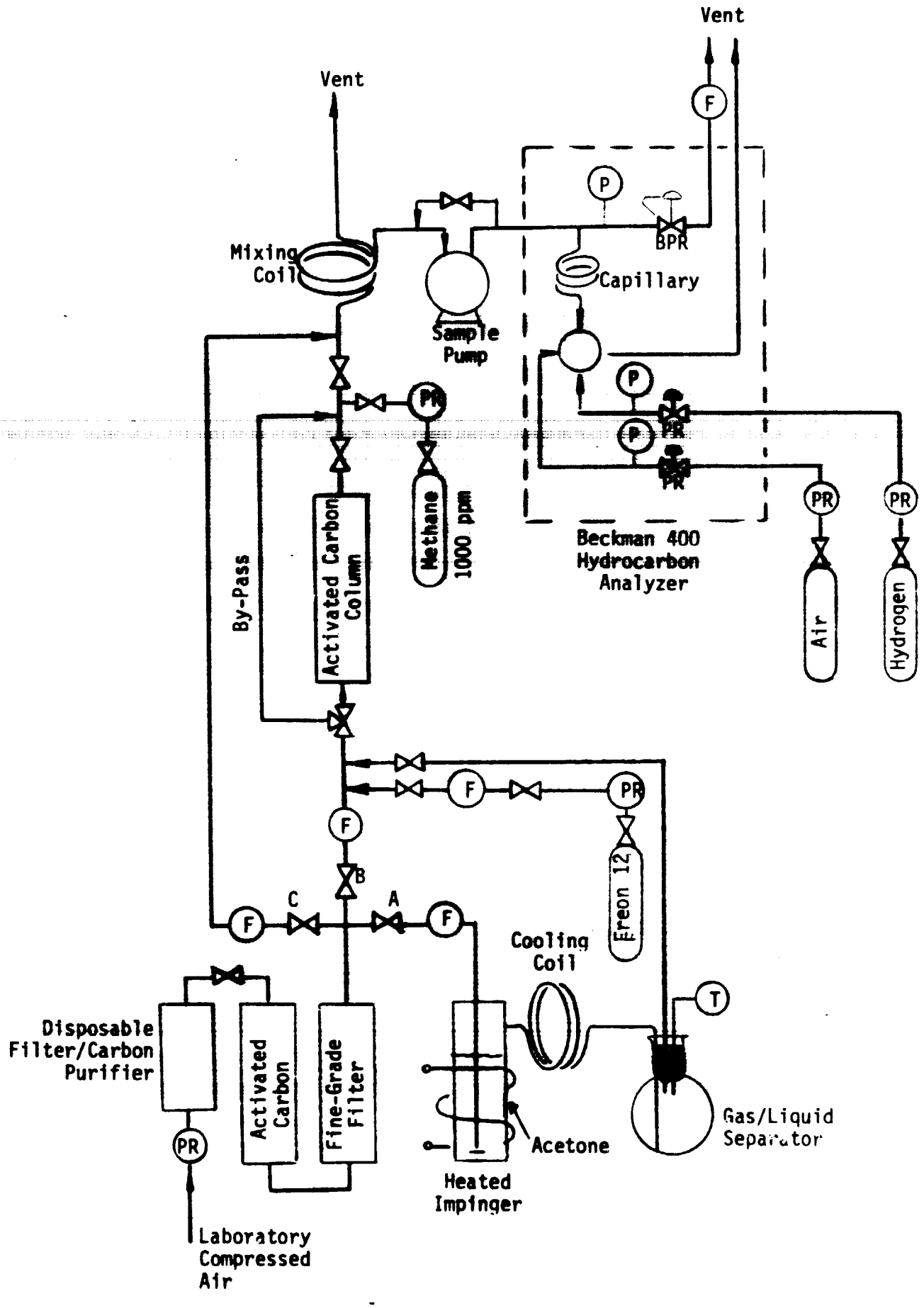

Figure 23 : Flow Schematic for Acetone and Freon 12 Systems

acetone tests only), B, and C; flowmeters (F) were used to measure the flow rate of each stream. For acetone tests, stream A was passed through an impinger filled with the contaminant (reagent-grade acetone, Fisher Scientific Co.). The impinger was wrapped with heating tape and maintained at a temperature of about 35°C. The air stream was then cooled to room temperature and excess contaminant was removed in a gas/liquid separator. The neck of the separation flask was packed with glass wool to remove small particulates by impingement, and the temperature of the acetone-saturated stream leaving the flask was measured with a thermometer (T). This stream was then mixed with diluent stream B, providing a dilution factor of about 10 to 1, and fed to the carbon column.

For Freon 12 tests, stream A was valved off and a low flow of pure Freon 12 (99.0% minimum purity, Matheson Gas Co.) was passed through a pressure regulator (PR), needle valve, and flowmeter, and mixed directly with diluent stream B before entering the carbon column.

The acetone or Freon 12 mixture was then passed through the carbon column and out to vent. Stream C was used to: 1) further dilute the effluent from the carbon column before FID analysis in order to insure that the concentration was within the linear range of the instrument, and 2) zero the analyzer.

A sample pump was used to withdraw a portion of the flow and pass it through an FID hydrocarbon analyzer (Beckman Model 400). The sample flow rate was controlled at about 1 ℓ/min by adjusting the sample-pump bypass. The analyzer had internal pressure regulators (PR) and a back-pressure regulator (BPR) to control the gas flow rates. The concentration of the feed to the carbon column was determined by diverting the feed stream through the column bypass. The analyzer was periodically calibrated using a span gas containing 1000 ppm CH_4 in nitrogen. Operating conditions are listed for the acetone and Freon 12 adsorption systems in Table 5. The flow rate through the column was selected to provide dynamic similarity to the prototype column; the influent concentrations were selected to provide breakthrough at a convenient time (3-5 hours).

TABLE 5

SUMMARY OF OPERATIONAL DATA FOR
ACETONE AND FREON 12 ADSORPTION SYSTEMS

	Flow Rate (s.cc/min)	Acetone/Freon 12 Concentration (ppm)
ACETONE:		
Saturated Stream A	35	220,000 (22%)[b]
Dilution Stream B	335	---
Total Column Influent	370[a]	20,800 (2.08%)
Dilution Stream C	3700	---
Total Analyzer Influent	4070	1891[c]
FREON 12:		
Pure Stream	5	990,000 (99%)
Dilution Stream B	365	---
Total Column Influent	370[a]	13,500 (1.35%)
Dilution Stream C	3330	---
Total Analyzer Influent	3700	1350[c]

GENERAL:

Column Temperature	= 22 - 24°C
Sample Flow	= 1.0 lpm
Analyzer Back-Pressure	= 129 kN/m^2 (4 psig)
Analyzer P_{H_2}	= 274 kN/m^2 (25 psig)
Analyzer P_{AIR}	= 205 kN/m^2 (15 psig)

[a] A flow rate of 370 s.cc/min was calculated on the basis of a reported prototype diameter of 7.75 in. The flow calculated from the final protype design (7.5 in. diameter) is slightly higher (396 s.cc/min).

[b] Calculated value based on a saturated stream temperature of 22 - 24 C.

[c] Calculated value based on actual stream flow rates.

2. Adsorption System: Contaminant Mixture

Repetitive-cycle tests were conducted with a mixture of 21 spacecraft contaminants identified[1] as the "primary" contaminants removed by the regenerable carbon bed. The production rate for these "primary" contaminants is approximately an order of magnitude larger than the production rate for the remaining "secondary" contaminants which were not included in the test mixture. The 21 contaminants were divided into two groups: 9 contaminants which exist as gases at ambient conditions, and 12 contaminants which exist as liquids at ambient conditions. The mixture of gaseous contaminants was prepared by Matheson Gas Products; the mixture of liquid contaminants was prepared in-house.

The acetone and Freon 12 adsorption system was revised, as shown in Figure 24, for multiple-cycle tests using the complex mixture of projected spacecraft contaminants. The following describes only the modifications to the original system.

The hydrocarbon contaminants were contained in two separate gas cylinders, indicated "A" and "B" in Figure 24. The third gas cylinder contained zero-grade nitrogen which was used to zero the FID detector and to dilute the hydrocarbon mixture to the proper feed concentration for the carbon column. The gas from each cylinder passed through pressure regulators (PR), needle valves, and flowmeters before mixing and passing through a back pressure regulator (BPR). The back pressure regulator was used to maintain a constant pressure at the flow meters so that the same calibration curves would apply regardless of the pressure drop through the system. The flowmeters were calibrated at the standard operating pressure using a soap-film flowmeter. The operating conditions are summarized in Table 6

Table 7 gives the physical and adsorptive properties of the 21 contaminants. The nine gaseous contaminants are listed first followed by the 11 liquid contaminants. (Acetaldehyde was refrigerated

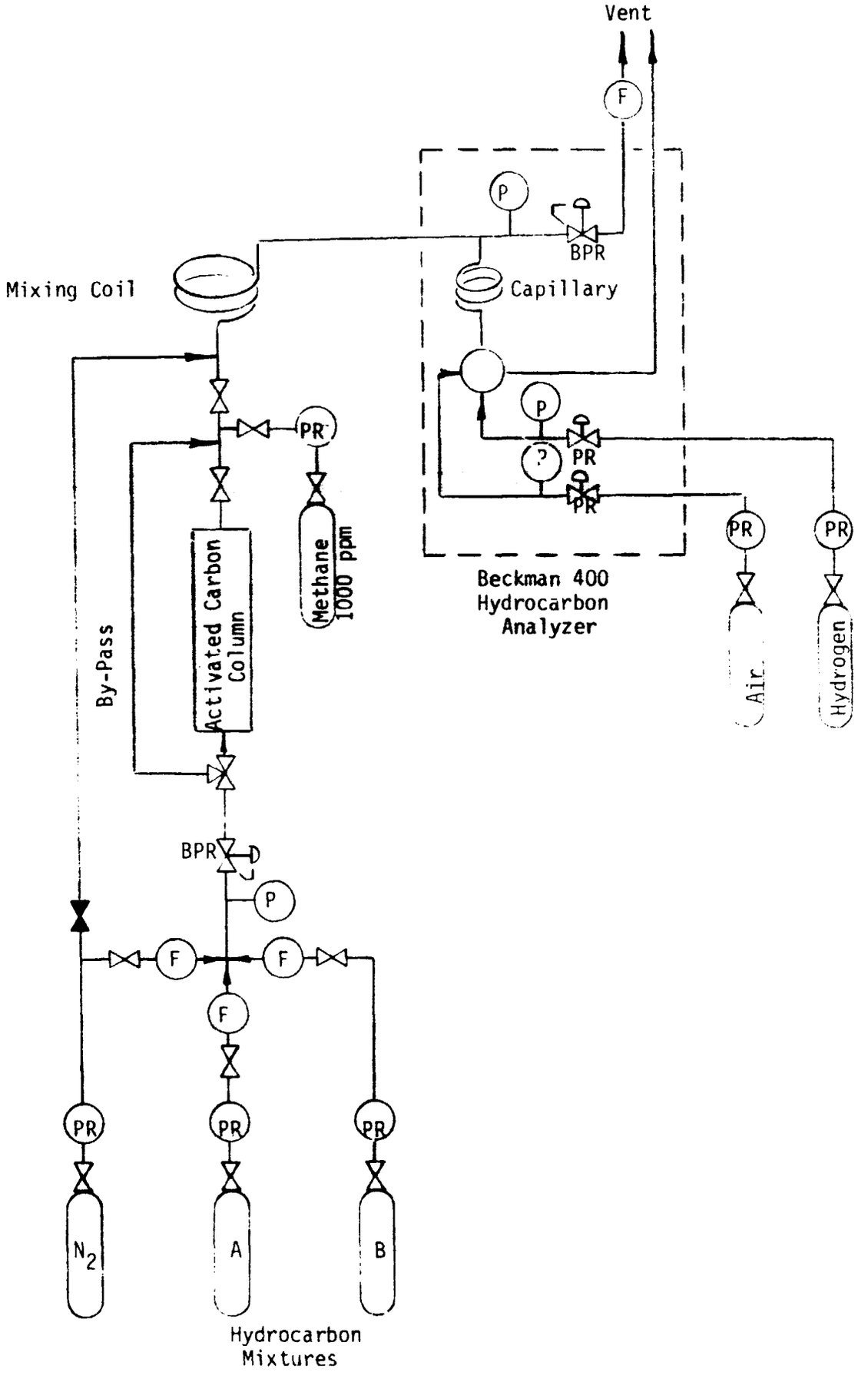

Figure 24: Flow Schematic of Adsorption System for Multiple-cycle Tests

TABLE 6

SUMMARY OF OPERATIONAL DATA FOR COMPLEX MIXTURE ADSORPTION SYSTEM

	Flow Rate (s.cc/min)	Total Hydrocarbons Concentration (ppm)
Hydrocarbon Stream A (Gaseous-Contaminant Mixture)	32	478[a]
Hydrocarbon Stream B (Liquid-Contaminant Mixture)	60 ± 5[c]	614[b]
Nitrogen Dilution Stream	278 ± 5[c]	---
Total Column Influent (= Total Analyzer Influent)	370.0	141[c]

Column Temperature	= 22-24°C
Sample Flow	= 370 scc/min.[d]
Analyzer Back-Pressure = Carbon Column Operating Pressure	= 129 kN/m² (4 psig)[e]
Analyzer P_{H2}	= 274 kN/m² (25 psig)
Analyzer P_{air}	= 239 kN/m² (20 psig)

(a) Concentration based on Matheson analysis of "Cylinder A" contents.
(b) Calculated concentration based on volumetric addition of liquid contaminants and nitrogen to "Cylinder B".
(c) Calculated hydrocarbon concentration = 141 for mixture feed to column. Based on the actual hydrocarbons present and their equivalent FID methane response (provided by Beckman Instruments, Inc.) the equivalent calculated FID response is 308 ppm as CH_4. The carbon column influent was set at 308 ppm as CH_4 by slightly adjusting Stream B and compensating with the nitrogen dilution flow to give a total influent flow of 370 scc/min.
(d) Total flow to column based on prototype diameter of 7.75 in. rather than final selected diameter of 7.5 in.
(e) Column operated at 4 psig to eliminate sample pump to FID.

TABLE 7. PHYSICAL PROPERTIES AND ADSORPTION CHARACTERISTICS OF SELECTED SPACECRAFT CONTAMINANTS

1	2	3	4	5	6	7(a)	8(b)	9	10
Contaminant	MW	P^{o}_{25} (atm)	(g/cc)	Vm (cc/g mole)	Initial Prod. rate (moles/day)	p_i (atm)	A (^{o}C g-mole/cc)	q (cc liq/ g car)	W (g-car/ day)
n-Butane	58.12	2,42		96	0.0430	5.56×10^{-6}	17.50	2.2×10^{-2}	188
1-Butene	56.10	2.95		90	0.0446	5.77×10^{-6}	18.90	1.6×10^{-2}	251
trans-2-Butene	56.10	2.33		89	0.446	5.77×10^{-6}	18.77	1.7×10^{-2}	233
1,3-Butadiene	54.09	2.93		81	0.0462	5.98×10^{-6}	20.93	9.0×10^{-2}	416
Freon 11	137.35	1.04		88	0.0182	2.35×10^{-6}	19.12	1.4×10^{-2}	114
Freon 12	120.91	6.4		75	0.0207	2.68×10^{-6}	25.34	2.7×10^{-2}	578
Propylene	42.08	11.4		67	0.0594	7.68×10^{-6}	27.45	1.5×10^{-2}	2653
Propane	44.09	9.6		74	0.0576	7.45×10^{-6}	24.60	3.2×10^{-2}	1332
Vinyl Chloride	62.50	1.316		80	0.0400	5.17×10^{-6}	20.14	1.2×10^{-2}	267
Acetone	58.05	0.291	0.7908	77	0.1756	22.7×10^{-6}	15.90	3.6×10^{-2}	376
Acetaldehyde	44.05	1.210	0.7834	57	0.0568	7.35×10^{-6}	27.27	1.5×10^{-2}	2158
Chloroform	119.38	0.253	1.4916	83	0.0209	2.70×10^{-6}	17.85	2.1×10^{-2}	93
1,1-Dichloroethane	98.96	0.289	1.1776	88	0.0253	3.27×10^{-6}	16.75	2.9×10^{-2}	77
Ethyl Alcohol	46.07	0.075	0.7893	62	0.0553	7.15×10^{-6}	19.32	1.4×10^{-2}	245
Ethyl Ether	74.12	0.699	0.714	105	0.0337	4.36×10^{-6}	14.77	4.8×10^{-2}	84
Ethyl Formate	74.08	0.325	0.9117	85	0.0337	4.36×10^{-6}	17.08	2.5×10^{-2}	114
Methylene Chloride	84.93	0.549	1.335	65	0.0294	3.89×10^{-6}	23.66	4.1×10^{-2}	466
Methyl Acetate	74.08	0.275	0.9723	85	0.3037	39.3×10^{-6}	13.48	7.0×10^{-2}	369
Methyl Alcohol	32.04	0.160	0.7914	42	0.0786	10.16×10^{-6}	(29.78)	8.0×10^{-2}	4126
Isopropyl Alcohol	60.09	0.057	0.7851	83	0.0416	5.38×10^{-6}	14.45	5.3×10^{-2}	65
Trichloroethylene	131.39	0.100	1.462	78	0.0190	2.46×10^{-6}	17.69	2.1×10^{-2}	70

(a) Col. 5) = (4.25 [illegible])(1 mole/22.4 liters)(1440 min/day)(p_i atm / atm)

(b) Col. 6) $\log_{10}$ (P^{o}_{25} [illegible]

and thereby handled as a liquid). Column 1 gives the contaminant name; column 2, the molecular weight; column 3, the vapor pressure at 25°C; column 4, the liquid density at room temperature; and column 5, the molar volume at the normal boiling point. Column 6 gives the initial production rate[1] of the contaminant from both equipment off-gassing and biological sources. (As the mission continues the production rate decreases because of the decrease in equipment off-gassing rate; however, the initial production rate should be used for the design since the bed must be capable of handling the initial contaminant load as well as the long-term or average contaminant load). Column 7 gives the partial pressure of the contaminant in the feed to the carbon column. This value can be calculated as shown in Table 7 from the known production rate and the flow rate through the regenerable bed (120 ℓ/min=4.25 SCFM). A removal efficiency of 100% and a total pressure of 1 atm was assumed. Column 8 gives the potential parameter, calculated as shown. Column 9 gives the adsorptive capacity of Barneby Cheney BD carbon as determined from the Polanyi potential plot[1]. Column 10 gives the amount of carbon required for the removal of each contaminant based on a cycle time of 24 hours.

The contaminant mixtures were prepared to simulate the feed concentrations given in Column 7 of Table 7. Table 8 gives the concentrations of contaminants in the gaseous-contaminant mixture (stream A) and in the feed to the column. The feed concentrations are about 15 below the projected concentrations given in Column 7 of Table 7. The agreement could be substantially improved by changing the dilution factor. However, the lower concentrations were used because the carbon packing density (grams carbon/cc of bed) in the experimental column was about 15% less than the projected packing density in the full-scale prototype. The low packing density was compensated for by decreasing the feed concentration by about 15 . Thus, the bed service time should be approximately the same for the experimental column and the prototype.

The mixture of liquid contaminants (stream B) was prepared by injecting a quantity of liquid mixture into a 2.38-liter gas sampling

TABLE 8

CONCENTRATIONS OF CONTAMINANTS IN GASEOUS-CONTAMINANT MIXTURE (STREAM A)

Contaminant	Conc. in Mixture[a] (ppm)	Conc. in Feed[b] (ppm)	Projected Feed Conc.[c] (ppm)	Difference (%)
n-Butane	54	4.7	5.56	-15.5
1-Butene	61	5.3	5.77	- 8.1
trans-2-Butene	54	4.7	5.77	-18.5
1,3-Butadiene	58	5.0	5.98	-16.4
Freon 11	27	2.3	2.35	- 2.1
Freon 12	26	2.2	2.68	-17.9
Propylene	68	5.9	7.68	-23.2
Propane	74	6.4	7.45	-14.1
Vinyl Chloride	56	4.8	5.17	- 7.2
Total	478	41.3	48.41	-14.7

(a) Results of gas analysis performed by Matheson Gas Products on the contents of the supplied gas cylinder.

(b) Concentration after dilution. Flow rate from cylinder = 32 scc/min. Total feed flow rate = 370 scc/min.

(c) Expected spacecraft concentration: column 7, Table 7.

cylinder and filling the cylinder to 1000 psig with zero-grade nitrogen. Because of the small volume of the cylinder, a new liquid-contaminant mixture had to be prepared for each adsorption run. Therefore, a concentrated stock solution (100 ml) was prepared in proper volumetric proportion from the pure liquid contaminant, and stored in a septum-sealed refrigerated container. A gas-tight 1.0 ml syringe was then used to inject approximately 0.32 ml of the stored liquid mixture into the cylinder, followed by pressurization to 1000 psig. Sufficient time was allowed for vaporization of the liquid contaminants prior to using the cylinder. Injection error occasionally caused slight initial deviation from the desired total feed concentration of 308 ppm as CH_4 (See Table 6) but was compensated for by adjusting the stream B and dilution-gas flow rates. A total feed concentration of 308 ppm as CH_4 and a total feed flow of 370 s.cc/min were used for each adsorption.

Table 9 gives the concentrations of the contaminants in the liquid-contaminant mixture and in the feed to the column. Again the contaminant feed concentrations were about 15% low in order to compensate for differences in the bed packing density between the experimental model and prototype.

3. Regeneration System: All Tests

The flow schematic for the regeneration systems (used in all tests) is shown in Figure 25. For nitrogen-purge regeneration, prepurified compressed nitrogen was passed through a pressure regulator (PR). The nitrogen flow rate was measured (F) and controlled at a preselected value. The nitrogen was passed through a preheater, through the carbon column and out to vent. The preheater and carbon column were wrapped with heating tape and their temperatures were independently controlled using variable transformers. Thermocouples were used to measure the temperature at the top and bottom of the carbon column; the temperature difference between the two ends of the column was generally less than $10^{o}C$ during desorption.

TABLE 9

CONCENTRATION OF CONTAMINANTS IN LIQUID-CONTAMINANT MIXTURE (STREAM B)

Contaminant	Conc. in Mixture[a] (ppm)	Conc. in Feed[b] (ppm)	Projected Feed Conc.[c] (ppm)	Difference %
Acetone	122	19.8	22.7	-12.8
Acetaldehyde	39	6.3	7.35	-14.3
Chloroform	14	2.3	2.70	-14.8
1,1 Dichloroethane	18	2.9	3.27	-11.3
Ethyl Alcohol	45	7.3	7.15	2.1
Ethyl Ether	23	3.7	4.36	-15.1
Ethyl Formate	23	3.7	4.36	-15.1
Methyl Chloride	20	3.2	3.80	-15.8
Methyl Acetate	210	34.1	39.3	-13.2
Methyl Alcohol	58	9.4	10.16	- 7.5
Isopropyl Alcohol	29	4.7	5.38	-12.6
Trichloroethylene	13	2.1	2.46	-14.6
Total	614	99.5	112.99	-11.9

(a) Mixture not analyzed after preparation. Concentrations based on amounts of contaminant and nitrogen added to gas cylinder.

(b) Concentration after dilution. Flow rate from cylinder = 60 scc/min. Total flow rate = 370 scc/min.

(c) Expected spacecraft concentration: column 7 Table 7.

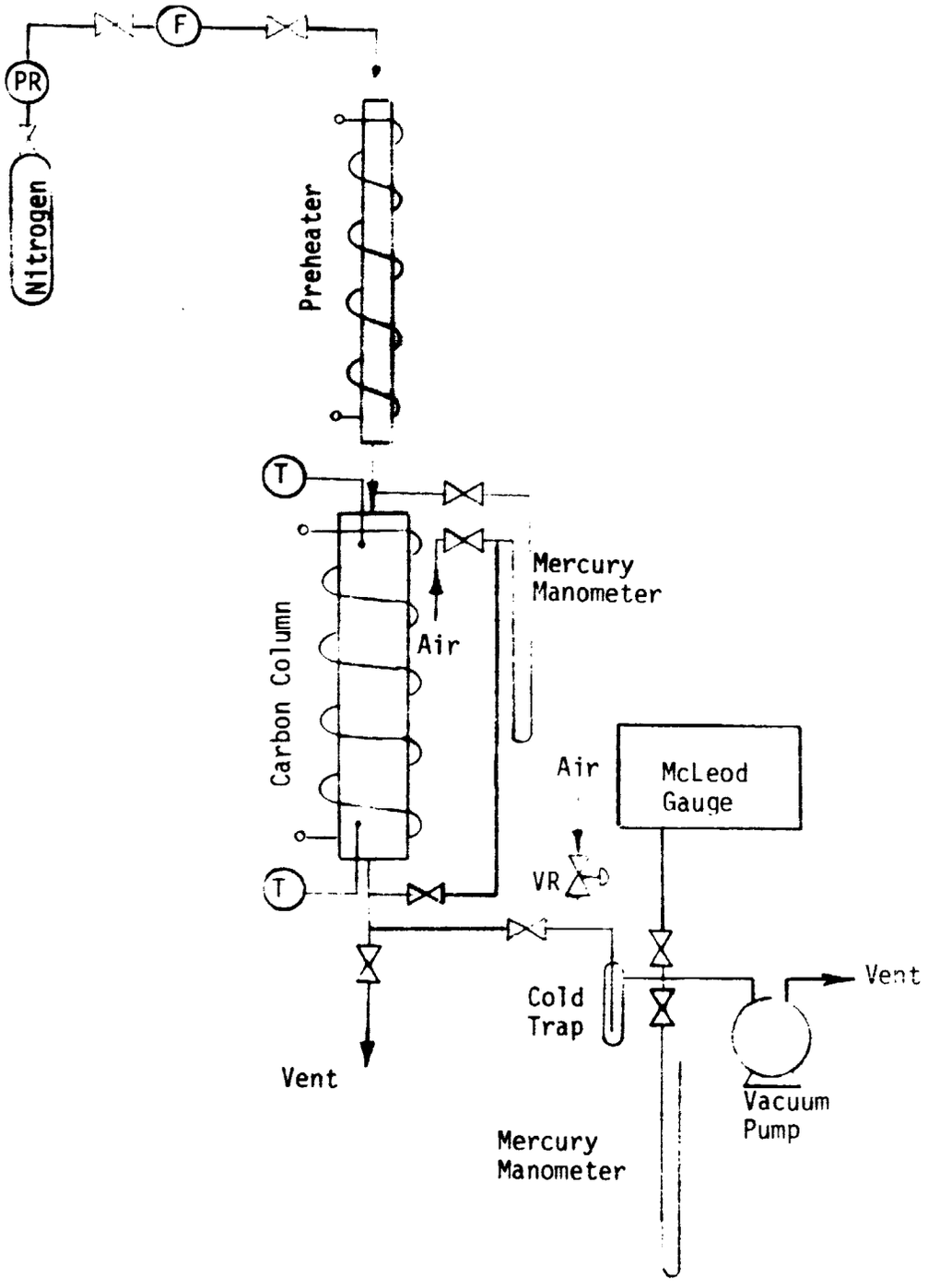

Figure 25: Flow Schematic for Regeneration System

For vacuum regeneration the valve upstream of the preheater was closed and the system was evacuated with a rotary vacuum pump (Welch Scientific Co. Model 1400B). The pressure at the pump suction was measured either with a McLeod gauge or an open-end mercury manometer. The pressure upstream of the carbon column and the pressure drop across the column during desorption were also measured with a mercury manometer. Preselected pressures were maintained by a vacuum regulator (VR).

E. ANALYTICAL METHODS

During adsorption the effluent from the carbon column was monitored with an FID (Beckman Model 400 Hydrocarbon Analyzer). For repetitive-cycle tests the bed service time (time from start of adsorption to breakthrough) was determined for each cycle and was used as an indicator of carbon working capacity.

The uptake of contaminant was also determined by removing the carbon column from the systems and weighing it on an analytical balance (Sartorious Model 2472, maximum sensitivity = 0.1 mg). For each weight determination the column was weighed five separate times, and the weights were averaged. End caps were securely fitted to the column immediately upon removal from the systems to prevent uptake or loss of contaminants during weighing. Following regeneration at elevated temperatures, the column was cooled prior to weighing to reduce weighing errors associated with thermally-induced convection.

II. EXPERIMENTAL RESULTS AND DISCUSSION

Several types of experiments were conducted in order to define the regeneration characteristics of contaminated activated carbon. First, single-cycle tests were conducted using acetone and Freon 12 to determine the rates of desorption. Second, multiple-cycle tests were conducted using acetone to verify the selected regeneration conditions. Third, multiple-cycle tests were conducted using a multi-component contaminant mixture to demonstrate the selected regeneration conditions. These three types of tests are discussed separately below.

A. SINGLE-CYCLE, SINGLE-CONTAMINANT TESTS

1. Acetone

Results for the adsorption and nitrogen-purge thermal desorption of acetone are given in Table 10. The second column gives the weight of carbon following conditioning for 16 hours at 105°C. Fresh carbon was used for each run. The adsorption time prior to breakthrough (defined as 50% removal of the influent concentration), the total adsorption time prior to desorption, and the loading prior to desorption are also given in Table 10. Breakthrough generally occurred in about 4.5 hours.

The equilibrium loading prior to desorption varied from 0.44 to 0.48 g acetone/g carbon. There is some indication that the higher loadings for runs 1 and 3 were the result of the longer adsorption times. For run 3 the loading increased from 0.45 to 0.47 after breakthrough was essentially complete. This slow uptake following complete breakthrough may be the result of a slow migration of adsorbed contaminant into very fine pores in the carbon. In general, the adsorption was terminated about 20 minutes after the 50% breakthrough point, and for these runs the equilibrium loading varied between 0.44 and 0.45 g/g carbon.

Nitrogen purge thermal desorption runs were conducted at the conditions shown in Table 10. The fraction of contaminant desorbed,

TABLE 10

Summary of Adsorption-Desorption Data for Acetone: Nitrogen-Purge Regeneration

Test No	Carbon Weight, grams	Adsorption Time, (a) hours	Breakthrough Time, (b) hours	Equilibrium Loading, g/g Carbon	Regeneration Conditions Temp, ^{o}C	N_2 Flow, scc/min	Time, min	Fraction Desorbed, %
AN-1	14.9809	16.93	3.73	0.477	23	92	3.8	0.24
							7.6	0.67
							15.2	1.63
							38.0	4.45
							76.0	9.07
AN-2	14.5338	5.33	5.02	0.441	75	92	3.8	26.5
							7.6	35.0
							15.2	47.0
							38.0	64.1
							76.0	73.9
AN-3	14.5385	5.10	4.50	0.451	105	92	3.8	54.1
		19.87		0.468			7.6	67.2
							15.2	72.1
							38.0	82.3
							67.4	87.4
							76.0	94.3
AN-4	14.4404	4.58	4.23	0.452	150	92	3.8	69.3
							7.6	81.3
							15.2	91.0
							38.0	91.3
							76.0	92.1
AN-5	14.7418	4.80	4.52	0.451	105	32	3.8	49.3
							7.6	64.0
							15.2	71.3
							38.0	83.4
							76.0	88.9
AN-6	14.9817	4.95	4.60	0.443	105	64	3.8	44.7
							7.6	53.9
							15.2	65.9
							38.0	79.8
							76.0	87.6

(a) Total time that carbon column was exposed to contaminant stream

(b) Time at which effluent conc. reached 50% of influent conc.

as determined by removing and weighing the carbon column at various times, is plotted in Figure 26 as a function of regeneration time. In general the data follow expected trends. As the desorption temperature is increased, the amount desorbed at a given time increases. From the slope of the curves at 76 minutes, it would appear that essentially complete desorption would be achieved at sufficiently long times. This is consistent with the reversible nature of physical adsorption expected for activated carbon.

The rate of desorption of contaminant is greatest at high loadings or short times. For example, at 150°C 90% of the contaminant is removed in the first 15 minutes; removal of an additional 7% requires an additional hour of desorption.

Three different nitrogen-purge flow rates were investigated at 105°C. There is no consistent trend to lower desorption rates as the nitrogen flow rate is decreased. The data at 32 s.cc/min are in very good agreement with the data at 92 s.cc/min. However, at the intermediate flow rate of 64 s.cc/min the rate of desorption at short times is significantly lower than at the other two purge rates. The reason for this is not apparent. At 76 minutes, the data points for all three flow rates nearly coincide. It is concluded that, within the range investigated, the purge-gas flow rate does not significantly affect the rate or extent of desorption.

Vacuum thermal desorption runs were also conducted at various temperatures and pressures. Since vacuum desorption was being evaluated as an alternative to dumping contaminants into space, pressures characteristic of mechanical vacuum pumps (~1 torr and above) were investigated. (Much lower pressures were employed in the LMSC work which simulated evacuation to space). Three pressure levels, 27,000 N/m^2 (200 torr), 270 N/m^2 (20 torr) and <133 N/m^2 (~1 torr), were investigated during this program. Fairly good pressure control was obtained at the two higher pressures by the use of a vacuum regulator. However, at the lowest pressure, there was a significant pressure gradient between the

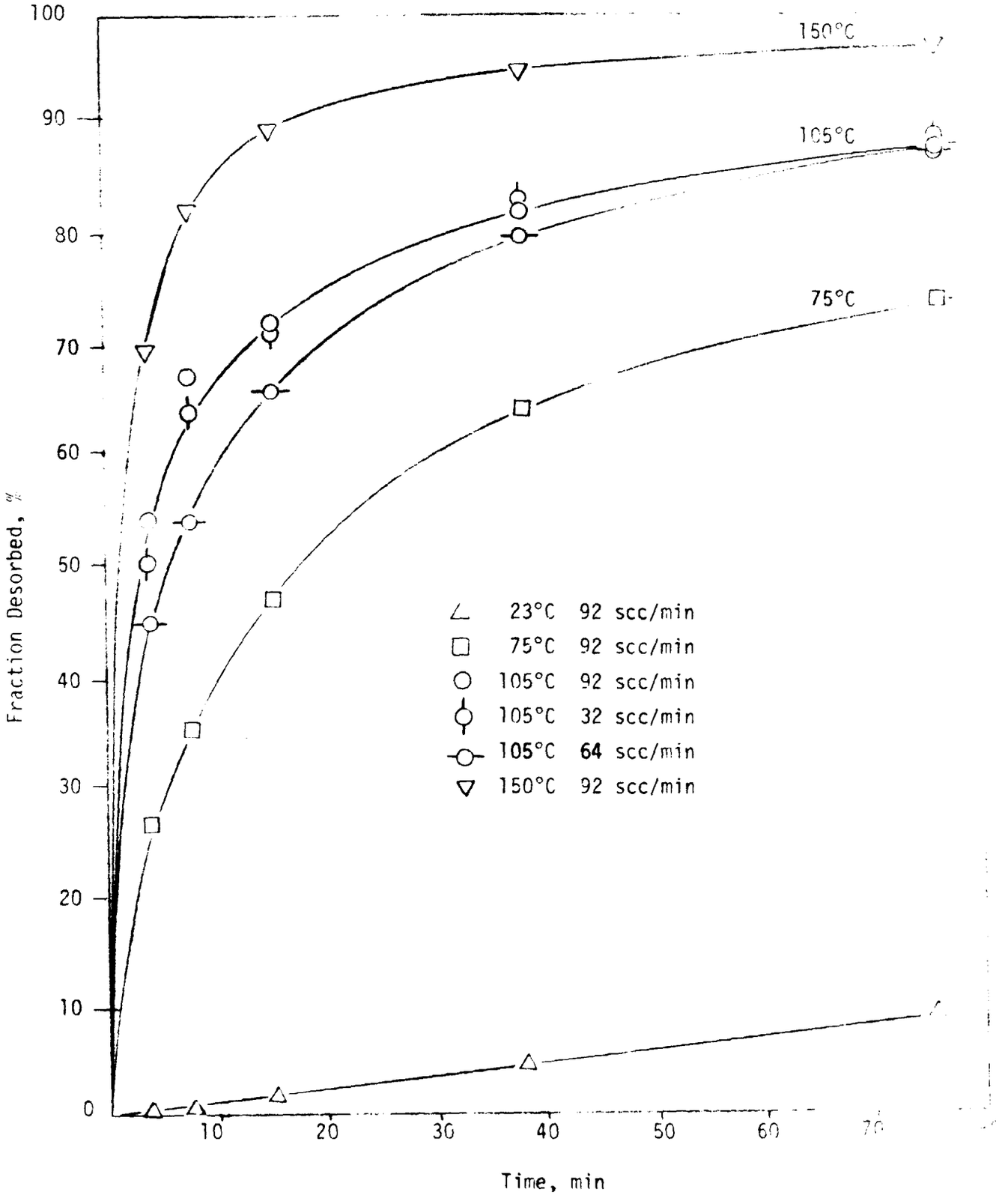

Figure 26: Amount Desorbed vs. Time for Various Temperature and Flow Rates

column and vacuum pump during desorption. This gradient is shown in Figure 27; the mercury manometer was used to measure the pressure upstream of the carbon column and the McLeod gauge was used to measure the pressure at the vacuum pump suction. The high pressure at the column was, no doubt, the result of both acetone desorption from the carbon and the low conductance of the vacuum system. Thus, although the lowest pressure is reported as <1 torr, the pressure at the vacuum pump suction did not fall below 1 torr until after about 50 minutes of desorption.

The results for adsorption and vacuum thermal desorption of acetone are given in Table 11. In general, the breakthrough times and equilibrium loadings are consistent with those given in Table 10. Vacuum thermal desorption runs were conducted at the conditions shown in Table 11. The fraction of contaminant desorbed, as determined by weight loss, is plotted in Figure 28 for various temperatures and a pressure of <133 N/m^2 (<1 torr). As expected, the amount desorbed and the initial rate of desorption both increase with temperature. Comparing these curves to those for nitrogen-purge desorption, the rate and extent of desorption are significantly greater for vacuum desorption at <133 N/m^2 (<1 torr) than for nitrogen-purge desorption at a flow rate of 92 s.cc/min.

The effect of various pressures on the desorption dynamics was also investigated. The results are shown in Figure 29. A significant decrease in the initial rate of desorption is observed as the desorption pressure is increased from <133 N/m^2 (<1 torr) to 27,000 N/m^2 (200 torr). In contrast, the variation in nitrogen flow rate over the range investigated did not significantly affect the rate of desorption.

2. Freon 12

Tests with Freon 12 were conducted in an attempt to define the influence of molecular weight on the desorption dynamics. The data obtained are shown in Table 12. Two runs were conducted using vacuum thermal desorption (75°C <133 N/m^2), and two were conducted using

Figure 27: Pressures during Vacuum Desorption of Acetone at 75°C and < 133 N/m^2 (< 1 Torr)

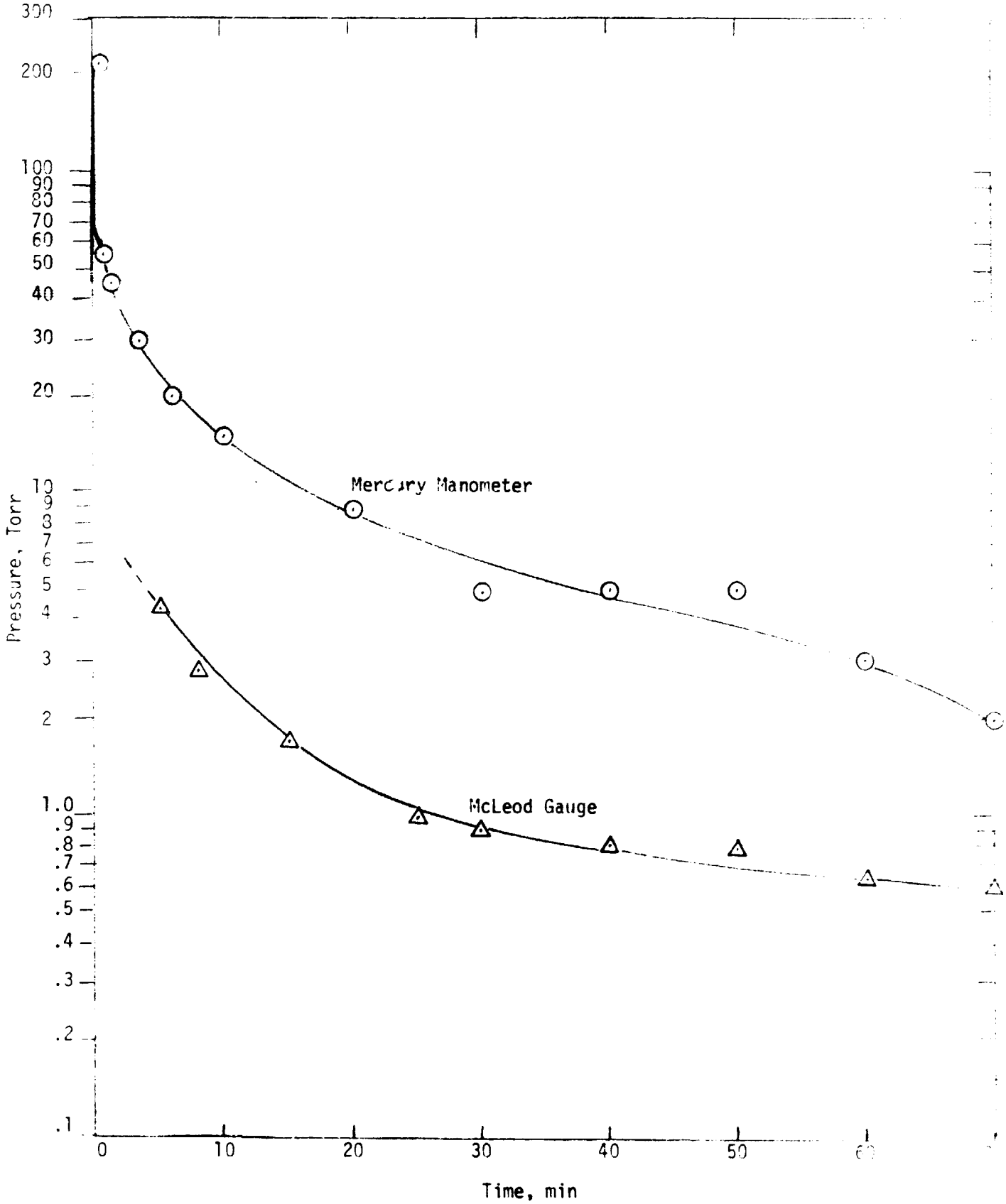

TABLE 11

SUMMARY OF DATA FOR ADSORPTION AND VACUUM THERMAL DESORPTION OF ACETONE

Test No.	Carbon Weight,(a) grams	Adsorption Time,(b) hours	Breakthrough Time,(c) hours	Equilibrium Loading g/g carbon	Regeneration Conditions			Amount [illegible]
					Temp. °C	Abs. Pressure torr	Time, min	
AV-1	14.9555	5.02	4.70	0.443	23	<1	3.8	6.6
							7.6	11.7
							15.2	18.3
							38	27.9
							76	35.8
AV-2	15.0220	4.92	4.55	0.435	75	<1	3.8	59.4
							7.6	74.1
							15.2	82.8
							38	89.4
							76	90.5
AV-3	14.6600	4.67	4.38	0.450	105	<1	3.8	79.3
							7.6	88.0
							15.2	91.7
							38	94.2
							76	95.1
AV-4	14.6320	5.38	5.05	0.431	150	<1	3.8	90.7
							7.6	94.1
							15.2	[illegible]
							38	97.0
							76	97.5
AV-5	14.8600	4.15	3.90	0.444	105	20	3.8	[illegible]
							7.6	[illegible]
							15.2	[illegible]
							38	[illegible]
							76	[illegible]
AV-6	15.3814	4.97	4.73	0.430	105	200	3.8	[illegible]
							7.6	[illegible]
							15.2	[illegible]
							38	[illegible]
							76	[illegible]

a) Fresh carbon used for each run
b) Total time that carbon column was exposed to contaminant stream
c) Time at which effluent concentration reached 50% of influent concentration

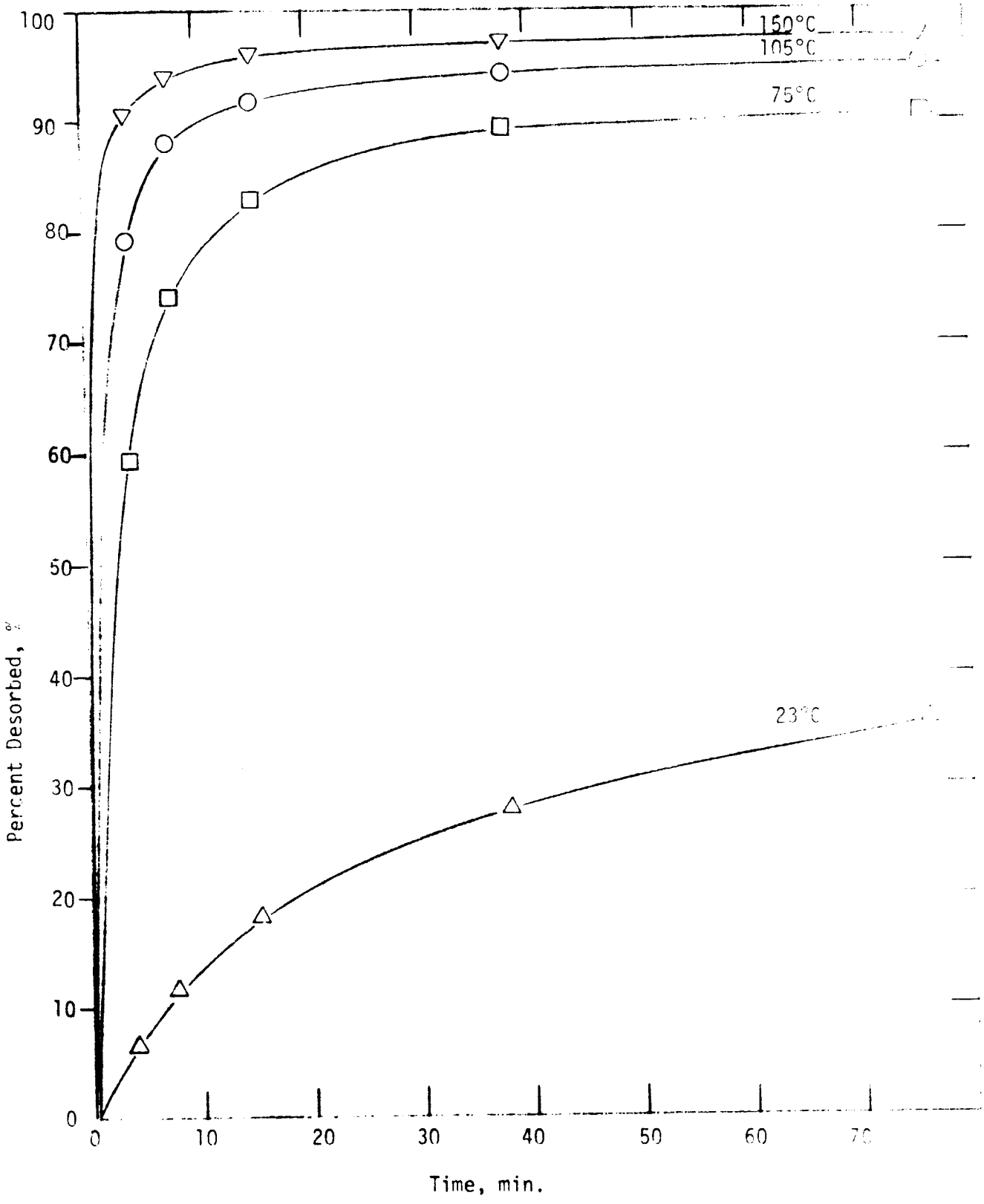

Figure 28: Amount desorbed vs. time for various temperatures and a pressure of < 133 N/m^2 (< 1 torr)

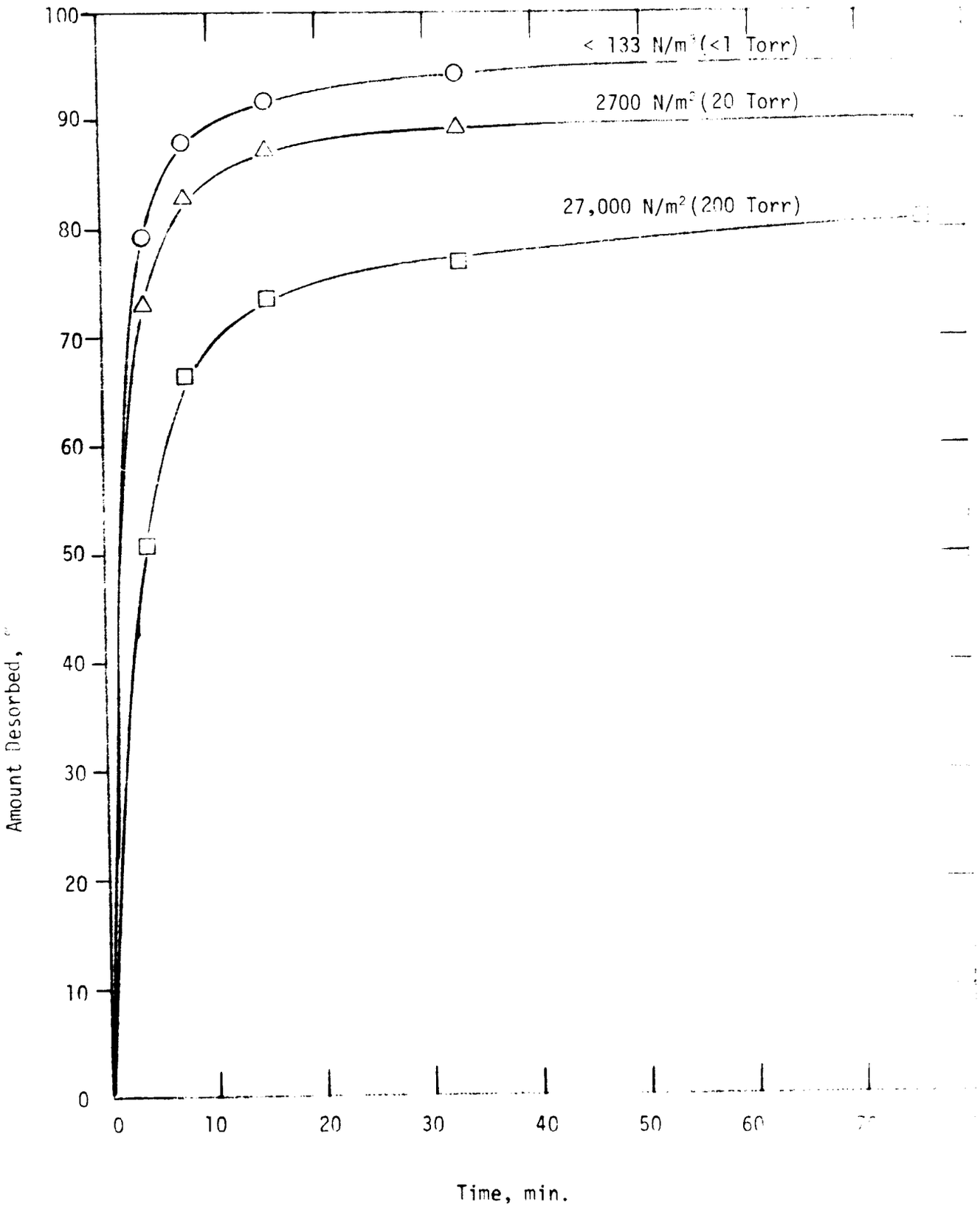

Figure 29: Amount desorbed vs. time for various pressures at a temperature of 105°C

TABLE 12

SUMMARY OF DATA FOR ADSORPTION AND THERMAL DESORPTION OF FREON 12

Test No.	Carbon Weight,[a] grams	Adsorption Time,[b] hours	Breakthrough Time,[c] hours	Equilibrium Loading g/g carbon	REGENERATION CONDITIONS: Temp °C	Pressure or Flow	Time, min	Amount Desorbed %
FV-1	15.0794	2.55	2.28	0.254	75	<133 N/m^2 [d]	76	93.5
FV-2	14.9761	2.50	2.23	0.263	75	<133 N/m^2 [d]	76	94.0
FN-1	14.6160	3.43	2.20	0.262	105	92 scc/min	76	98.6
FN-2	14.8689	2.52	2.25	0.269	105	92 scc/min	76	97.3

a) Fresh carbon used for each run.

b) Total time that carbon column was exposed to contaminant stream.

c) Time at which effluent concentration reached 50 of influent concentration.

d) Measured at pump at end of desorption cycle.

nitrogen-purge thermal desorption (105°C, 92 s.cc/min). At the selected conditions, the nitrogen-purge desorption technique gave more complete regeneration than the vacuum desorption technique. This is in direct contrast to the results for acetone desorption which indicate more complete regeneration for vacuum desorption. This difference is apparently the result of the fact that the potential parameter for Freon 12 is greater than for acetone at the adsorption conditions. This results in the desorption of a greater fraction of the Freon 12 for a given temperature increase. Since the nitrogen-purge runs were conducted at a higher temperature (105°C vs 75°C), they resulted in more complete desorption.

In comparing the results of tests with Freon 12 (Table 12) to results with acetone at similar desorption conditions, it is apparent that the relative rate of desorption, as indicated by the percent desorbed at 76 minutes, is greater for Freon 12. However, the equilibrium loading for acetone was significantly greater than for Freon 12 and, in terms of the absolute rates of desorption, no direct comparisons can be made.

B. MULTIPLE-CYCLE, SINGLE-CONTAMINANT TESTS

Based on the results obtained in the single contaminant tests, regeneration conditions were selected which would give substantial, yet incomplete, regeneration of the carbon. In order to achieve "complete" regeneration of the carbon, the regeneration conditions would have to be particularly severe (high temperature, long times, and high vacuum or nitrogen-purge rate). In selecting conditions that gave incomplete regeneration, it was anticipated that the "heel" of undesorbed contaminant would build up to a constant level during repetitive cycling, as in the Phase I tests. The loss in working capacity due to heel build-up could be compensated for by increasing the size of the carbon bed. Thus, there should be an optimum degree of regeneration which balances the penalty for complete or near-complete regeneration against the excessive weight of carbon for a low degree of regeneration. Al-

though it is difficult to make this optimization without more information on the system design and on the loss of working capacity during repetitive cycling, the following conditions were selected for regeneration:

Nitrogen-Purge	Vacuum
105°C, 76 min, 92 s.cc/min	75°C, 76 min, <133 N/m^2 (<1 torr)

These regeneration conditions were evaluated in multiple-cycle tests using acetone as the contaminant.

A total of six adsorption-desorption cycles were conducted with acetone, using both nitrogen-purge thermal desorption and vacuum thermal desorption. The results are given in Tables 13 and 14, respectively. For both modes of regeneration, the working capacity for the carbon leveled off to a near-steady value after only three cycles. At the selected regeneration conditions, the working capacities are in excess of 80% of the adsorptive capacity of the virgin carbon. Based on these tests, the very slow decrease in working capacity after the third cycle indicates that it would not be necessary to completely regenerate the carbon. A 20% over-design of the carbon bed with regeneration at the selected conditions would appear to be equivalent to a bed designed for near-complete regeneration on each cycle. Therefore, it was concluded that the selected regeneration conditions would be acceptable for tests with the multi-component contaminant mixture.

C. MULTIPLE-CYCLE, MULTIPLE-CONTAMINANT TESTS

In order to demonstrate the two modes of carbon bed regeneration, tests were conducted with a contaminant mixture containing the 21 primary spacecraft contaminants which were to be controlled by the regenerable carbon bed [1]. The feed concentrations of these contaminants were adjusted to simulate the initial contaminant production rate -- a worst case for evaluation of the carbon bed design.

The effluent from the carbon column was continuously monitored during adsorption. A typical breakthrough curve for a fresh carbon

TABLE 13

REPETITIVE CYCLE NITROGEN-PURGE THERMAL DESORPTION OF ACETONE; REGENERATION FOR 76 MIN. AT 105°C AND 92 S.CC/MIN. OF NITROGEN

Cycle No.	Adsorption Time,(a) hours	Breakthrough Time,(b) hours	Equilibrium Loading g/g carbon	Amount Desorbed(c) %
1	4.85	4.43	0.437	84.7
2	3.92	3.50	0.452	85.1
3	3.52	3.00	0.453	80.4
4	3.75	3.17	0.456	81.5
5	3.77	2.93	0.453	81.0
6	2.67	2.23	0.444	81.3

a) Total time that carbon column was exposed to contaminant stream for given cycle

b) Time at which effluent concentration reached 50 % of influent concentration.

c) Based on clean carbon weight before cycle No.1

TABLE 14

REPETITIVE VACUUM THERMAL DESORPTION OF ACETONE;
REGENERATION FOR 76 MIN. AT 75°C AND 133 N/m^2

Cycle No.	Adsorption Time,[a] hours	Breakthrough Time[b] hours	Equilibrium Loading g/g carbon	Amount Desorbed[c]
1	4.72	4.43	0.434	90.9
2	4.17	3.75	0.449	88.7
3	3.72	3.47	0.454	85.6
4	3.73	3.27	0.459	85.9
5	4.05	3.77	0.452	87.1
6	3.37	3.05	0.453	84.2

a) Total time that carbon column was exposed to contaminant stream for given cycle

b) Time at which effluent concentration reached 50 of influent concentration

c) Based on clean carbon weight before cycle No.1

column is shown in Figure 30. The effluent concentration remained close to zero for about 22 hours and then increased in a step-wise manner as various contaminants broke through the bed. As shown in Table 7 (Column 10), methyl alcohol should break through first to give an effluent concentration of 3.8 ppm as CH_4 (equivalent to 9.4 ppm CH_3OH). However, the first plateau in the breakthrough curve occurs at about 44 ppm as CH_4 rather than 3.8 ppm as CH_4. The first plateau is approximately equivalent to the simultaneous breakthrough of the 4 most weakly adsorbed contaminants (methyl alcohol, 3.8 ppm equivalent; propylene, 17.2 ppm equivalent; acetaldehyde, 6.4 ppm equivalent; and propane, 19.4 ppm equivalent; for a total calculated concentration of 46.8 ppm as CH_4 compared to a measured concentration of 44 ppm as CH_4). Similarly, subsequent plateaus in the breakthrough curve can be attributed to breakthrough of the next contaminants in order of adsorptive strength.

For repetitive-cycle tests, the adsorption half-cycle was terminated when the effluent concentration reached 8.6 ppm as CH_4. This value was arbitrarily selected as the point at which the effluent concentration reached approximately 20% of the first plateau.

The results of the repetitive-cycle multi-contaminant tests are given in Tables 15 and 16 for nitrogen-purge thermal desorption and vacuum thermal desorption, respectively. The regeneration conditions were fixed at the levels selected during the single contaminant tests with the exception that the desorption temperature for vacuum thermal desorption was increased from 75°C to 105°C after the third regeneration. The pressure during vacuum desorption showed much less variation than in the single-contaminant loading. The pressure at the carbon column fell to about 133 N/m^2 (1.0 torr) after only four minutes of desorption, and gradually decreased to about 67 N/m^2 (0.5 torr) toward the end of the desorption half-cycle.

Prior to an adsorption half-cycle, the feed concentration to the column was monitored by the FID and adjusted to the proper value. At time zero, the feed was passed through the column and the effluent

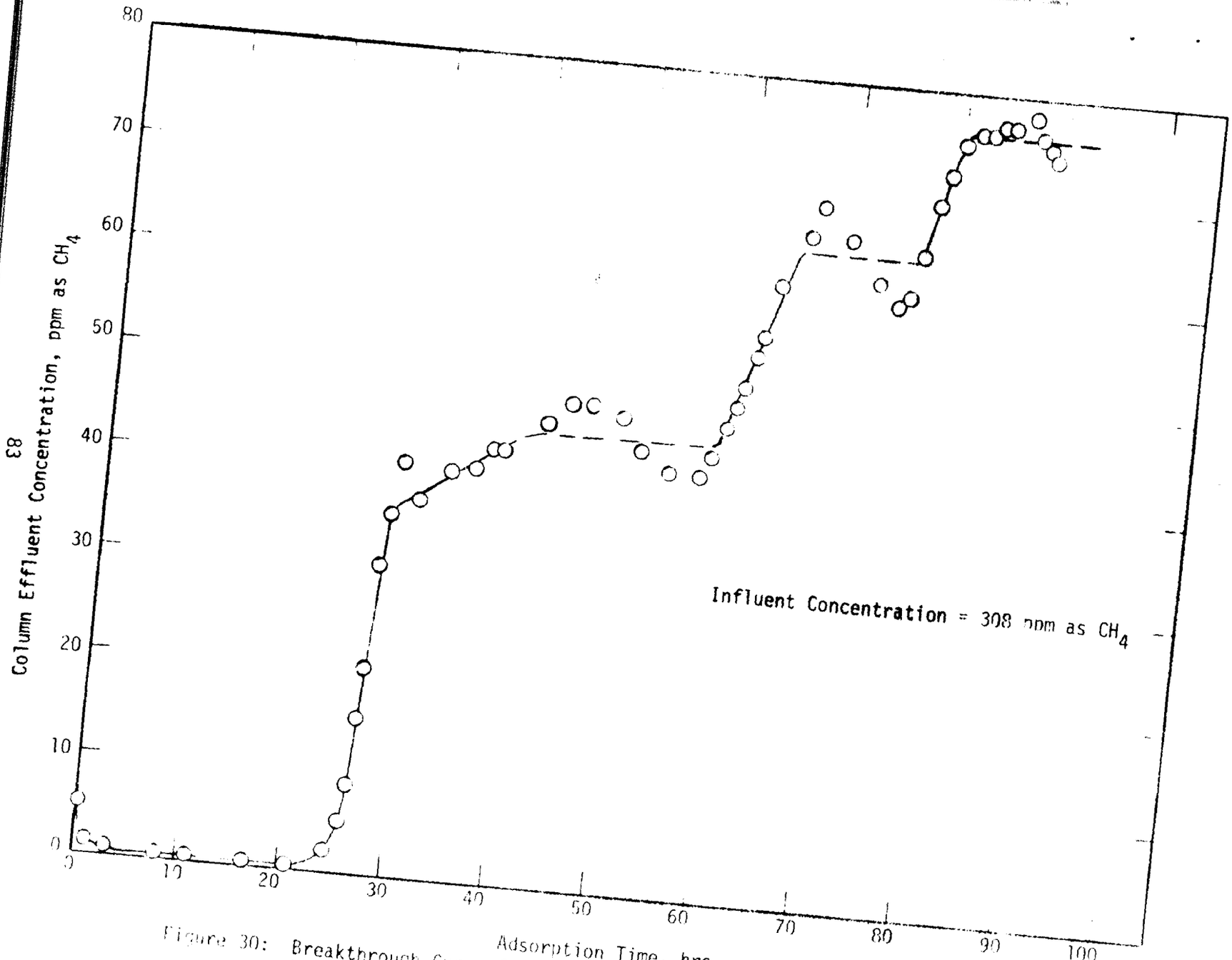

Figure 30: Breakthrough Curve for Adsorption of Multi-component Contaminant Mixture on Virgin Carbon.

TABLE 15

SUMMARY OF REPETITIVE-CYCLE TESTS FOR NITROGEN-PURGE REGENERATION

Cycle Number	Minimum Effluent Concentration (ppm as CH_4)	Loading at Breakthrough (g/g carbon)	Breakthrough Time,[a] (hours)	Service Time,[b] (%)	Amount Desorbed[c] (%)
1	---	0.0221	31.88	100	87.0
2	(0.0)	0.0228	26.13	82.0	84.3
3	(0.0)	0.0269	26.23	86.2	84.5
4	0.2	0.0261	26.22	82.2	82.0
5	0.2	0.0261	26.10	81.9	76.9
6	0.3	0.0271	25.18	79.0	76.6
7	0.3	0.0248	24.87	78.0	81.5
8	0.3	0.0270	26.95	84.5	80.2
9	0.2	0.0272	27.17	85.2	77.0
10	0.3	0.0244	22.93	71.9	68.8
11	0.2	0.0244	23.77	74.6	78.3
12	0.3	0.0250	24.60	77.2	73.2

a) Time to reach 8.6 ppm as CH_4.

b) Determined from breakthrough times.

c) Determined by weight loss during desorption.
Original carbon weight = 15.1750 g.
Regeneration at 105°C.

TABLE 16

SUMMARY OF REPETITIVE-CYCLE TESTS FOR VACUUM REGENERATION

Cycle Number	Minimum Effluent Concentration (ppm as CH_4)	Loading at Breakthrough (g/g carbon)	Breakthrough Time,(a) (hours)	Relative Bed Service Time,(b) (%)	Relative Amount Desorbed(c) (%)
1	(0.2)	0.0176	28.00	100	83.7
2	(4.5)	0.0179	6.80(19.78(d))	24	79.4
3	2.3	0.0220	21.45(22.42(e))	75.6	78.4
4	9.0	0.0235	0 (21.45(f))	0	94.9
5	1.0	0.0218	24.32	86.8	91.8
6	0.3	0.0227	24.83	88.7	85.4
7	0.7	0.0216	23.38	83.5	86.4
8	1.7	0.0232	24.25	86.6	84.9
9	1.1	0.0216	22.77	81.3	84.1
10	1.6	0.0222	21.17	75.6	84.2
11	1.3	0.0199	22.60	80.7	84.5
12	1.1	0.0213	22.02	78.6	84.1
13	1.6	0.0201	21.83	78.0	84.3

a) Time to reach effluent concentration of 8.6 ppm as CH_4.

b) Determined from breakthrough times.

c) Determined by weight loss during desorption. Original carbon weight = 14.6214 g. Regenerated at 75°C (cycles 1-3) or 105°C (cycles 4-12).

d) Total adsorption time; effluent concentration reached 24 ppm as CH_4.

e) Total adsorption time; effluent concentration reached 9.4 ppm as CH_4.

f) Total adsorption time; effluent concentration reached 24 ppm as CH_4.

concentration was monitored. As the column effluent purged the lines to the FID, the recorded concentration reached a minimum after which the concentration increased as breakthrough occurred. The second column of Tables 15 and 16 gives the minimum effluent concentration that was observed during adsorption. For nitrogen-purge desorption, the minimum effluent concentration was 0.3 ppm as CH_4 or less and was acceptably close to "zero" concentration in the effluent. However, for vacuum desorption, the minimum effluent concentration increased over the first four cycles, and on the fourth adsorption cycle, the minimum effluent concentration was 9.0 ppm as CH_4, exceeding the breakthrough value of 8.6 ppm, and resulting in a bed service time of zero. The regeneration temperature was then increased from 75°C to 105°C, and the minimum effluent concentration fell below 2 ppm as CH_4 in all subsequent cycles.

The problems encountered in achieving an acceptably low effluent concentration for the vacuum mode of regeneration are potentially critical in attempting to apply this technique. The results of Table 16 indicate that the minimum effluent concentration is related to the amount desorbed during regeneration: As the "heel" of contaminant built up on the carbon at 75°C, the minimum effluent concentration increased, but when the heel was reduced (by increasing the regeneration temperature), the minimum effluent concentration decreased. To define this trend more clearly, an additional cycle was carried out following the 13th cycle of Table 16. In this additional cycle, the regeneration temperature was lowered to 50°C and only 44% regeneration was obtained. In the subsequent adsorption, the effluent concentration dropped to only 23 ppm as CH_4,

The data for minimum effluent concentration are shown in Figure 31, as a function of percent regeneration for the vacuum and nitrogen-purge desorption. For vacuum desorption, the minimum effluent concentration increases as the percent regeneration drops below 85 . However, for nitrogen-purge desorption, the minimum effluent concentration remains at essentially zero as the percent regeneration drops. The following

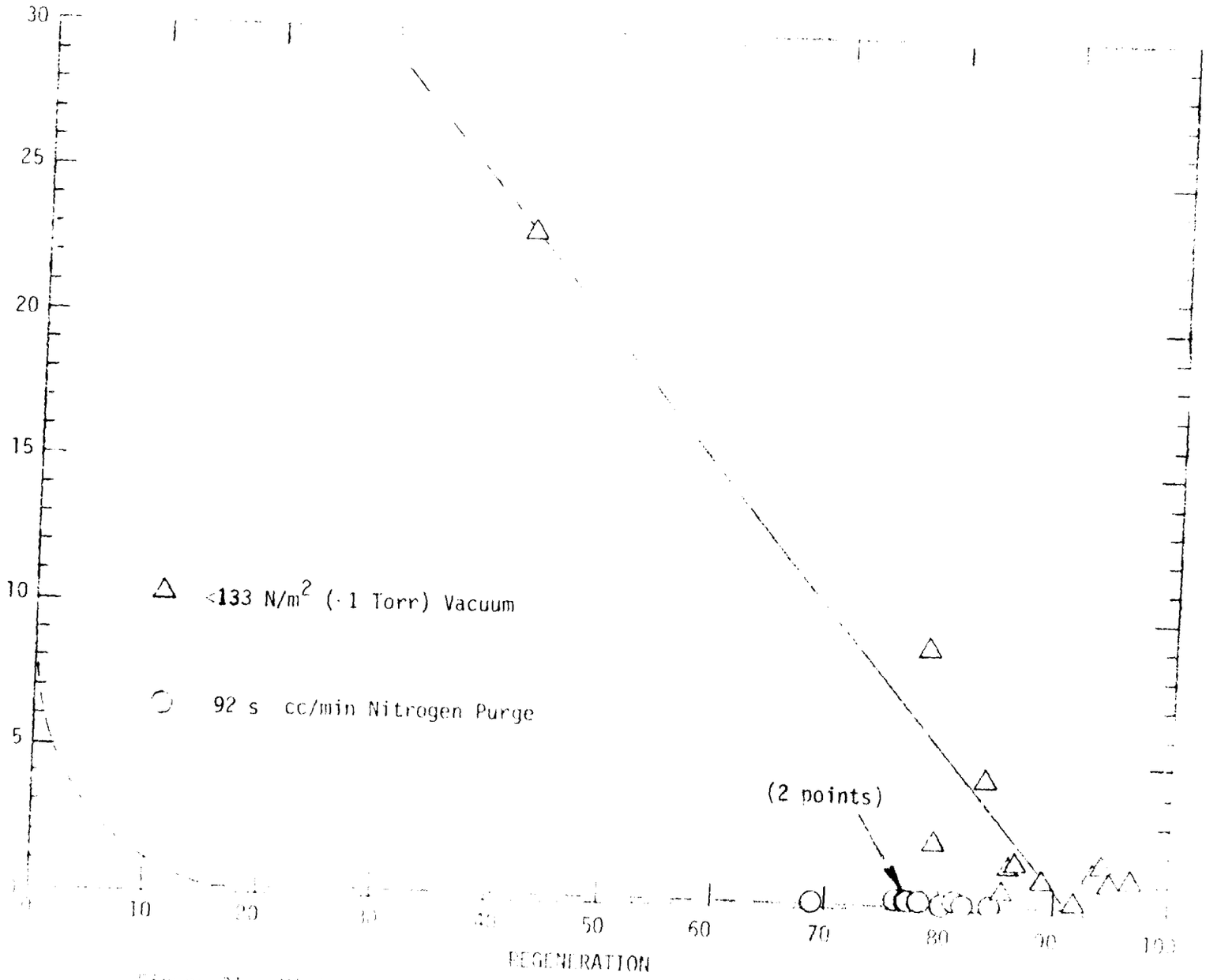

Figure 31: Minimum Column Effluent Concentration vs. % Regeneration

rationale was used in extrapolating the nitrogen-purge curve to zero percent regeneration. If at breakthrough, the column was not regenerated (0% regeneration) the effluent concentration on the next adsorption half-cycle would start at the breakthrough concentration, 8.6 ppm as CH_4, and increase from there.

During adsorption the most strongly adsorbed contaminants are removed from the carrier stream in the first few layers of the bed. When the most weakly adsorbed contaminants break through and the adsorption half-cycle is terminated, a substantial contaminant gradient exists along the length of the bed from a very high loading at the inlet to a very low loading at the outlet. For nitrogen-purge desorption the bed is purged in the reverse direction so that the contaminants are swept from outlet to inlet and out of the column. The most completely regenerated portion of the bed will then be in the region of the outlet (which sees the fresh nitrogen-purge stream), and on the subsequent adsorption half-cycle, the effluent concentration will be zero until the outlet region again becomes saturated with the most weakly adsorbed contaminant. This would explain the low minimum effluent concentrations for nitrogen-purge desorption.

The regeneration process is somewhat different for vacuum desorption. The results of Figure 31 can be explained by postulating that during vacuum desorption there is a redistribution of contaminants on the carbon. At low pressures, a contaminant can move away from the vacuum source by molecular flow. If a strongly adsorbed contaminant is concentrated in the area of the bed inlet, it can be redistributed evenly throughout the bed by molecular flow during regeneration at conditions of high temperature and low pressure. Then, on the subsequent adsorption half-cycle, the weakly adsorbed contaminants will be displaced from the entire bed and will break through immediately.

It is concluded that nitrogen-purge thermal desorption permits higher contaminant removal efficiencies than vacuum thermal desorption and would be the preferred mode of regeneration, particularly if working capacities below 85% are to be used.

The third column of Tables 15 and 16 gives the contaminant loading at breakthrough. The loading is plotted as a function of Cycle No. in Figure 32. After the first two cycles an increase in the loading was observed, but the loading gradually declined over the remaining cycles. This gradual decline in loading for both regeneration techniques could be the result of a slight loss of carbon during regeneration. This would result in an apparent loss in loading. The loading for the vacuum-regenerated column was consistently lower than for the nitrogen-purge-regenerated column. The reason for this difference is not apparent.

The working capacity of the carbon was determined by measuring both the amount desorbed and the amount adsorbed for each cycle. The amount desorbed was determined by weighing the carbon column before and after regeneration. The relative working capacity (or relative amount desorbed) was determined by dividing the desorbed weight by the contaminant weight prior to desorption (loading at breakthrough times original weight of virgin carbon). The amount adsorbed was determined by measuring the time to breakthrough for a fixed feed flow rate and concentration. The relative working capacity (or relative bed service time) was normalized to the breakthrough time for the first cycle. Data on the breakthrough time, relative bed service time, and relative amount desorbed are given in Tables 15 and 16. (The relative amount desorbed for a given cycle corresponds to the relative bed service time for the subsequent cycle).

Figure 33 gives the relative working capacity of the carbon as a function of Cycle No. for nitrogen-purge desorption based on both adsorption (circles) and desorption (triangles) data. The data for cycles 2 through 13 were fit to a straight-line relationship using the method of least squares. The correlation coefficient is -0.71 and the 95 confidence interval for the correlation coefficient is from -0.43 to -0.86. Since this interval does not include a correlation coefficient of zero, it can be concluded that, at the 95 confidence level, the working capacity of the carbon decreases with increasing cycle number.

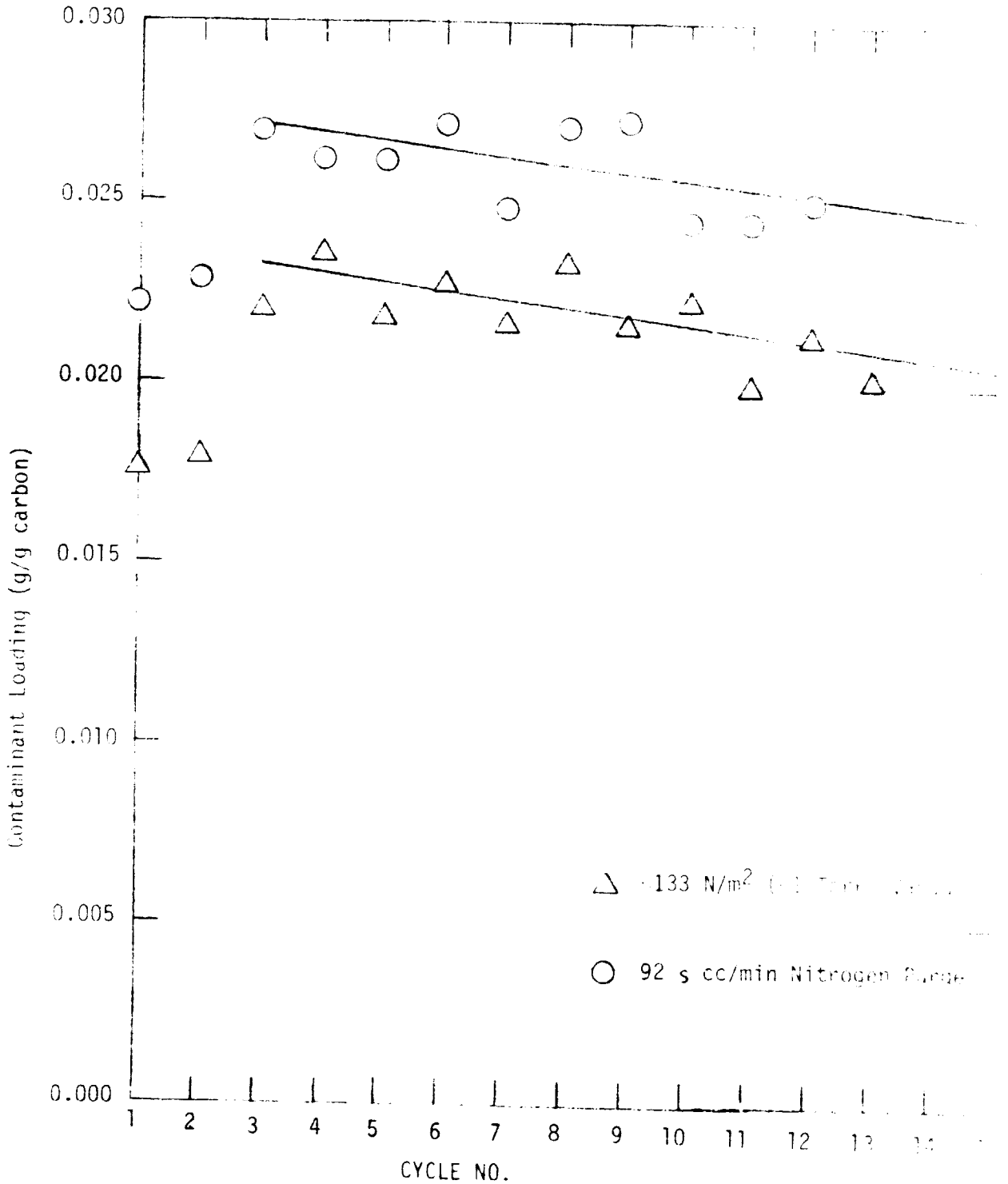

Figure 32: Contaminant Loading vs. Cycle No.

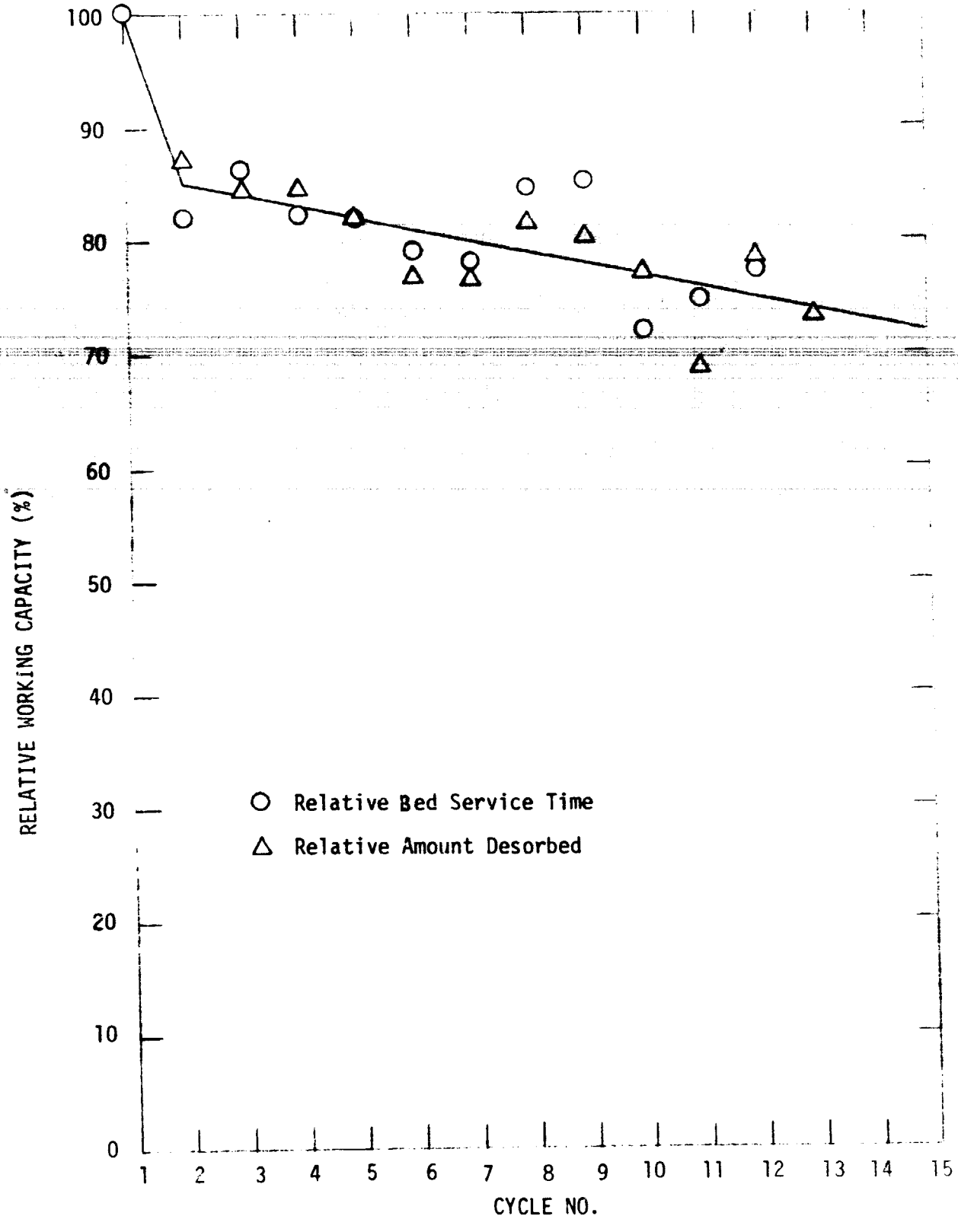

Figure 33: Relative Working Capacity vs. Cycle No. for Carbon Regenerated by Nitrogen - Purge Thermal Desorption

on the fitted regression line, the working capacity would drop to 50% after 36 cycles.

Figure 34 gives the corresponding data on working capacity for vacuum thermal desorption. Over the first four cycles, the regeneration temperature was fixed at 75°C and, as mentioned previously, the relative bed service times were unacceptably low. Data obtained at a regeneration temperature of 105°C were fit by the method of least squares to a straight line relationship shown by the dashed line in Figure 34. The correlation coefficient for this line is only -0.28 and the 95% confidence interval for the correlation coefficient is from -0.65 to 0.27. Since this interval includes a correlation coefficient of zero, it cannot be concluded with 95% confidence that the working capacity decreases with cycle number.

It is apparent from Figure 34 that the working capacity as estimated by bed service time decreases with cycle number while that estimated by amount desorbed tends to increase slightly with cycle number. The divergency of these two indicators is probably the result of a slight loss of carbon from the vacuum-regenerated column. Upon disassembly of the system, traces of carbon were found in the vacuum cold trap. In addition, the apparent decrease in loading with cycle number for the vacuum-regenerated column (Figure 32) is consistent with this hypothesis. A very small loss of carbon could have a substantial effect on the apparent amount desorbed since the contaminant loading is low and any loss in weight would be attributed to desorption of contaminant. On the other hand, a small loss of carbon from the column will have only a minor effect on the bed service time. Therefore, it is concluded that the relative bed service time is the more accurate indicator of relative working capacity.

The data on relative bed service time (circles of Figure 34) were fit to a straight line (solid line of Figure 34) by the method of least squares. The correlation coefficient for this line is -0.83 with a 95% confidence interval of -0.34 to -0.95. Thus, based on the data

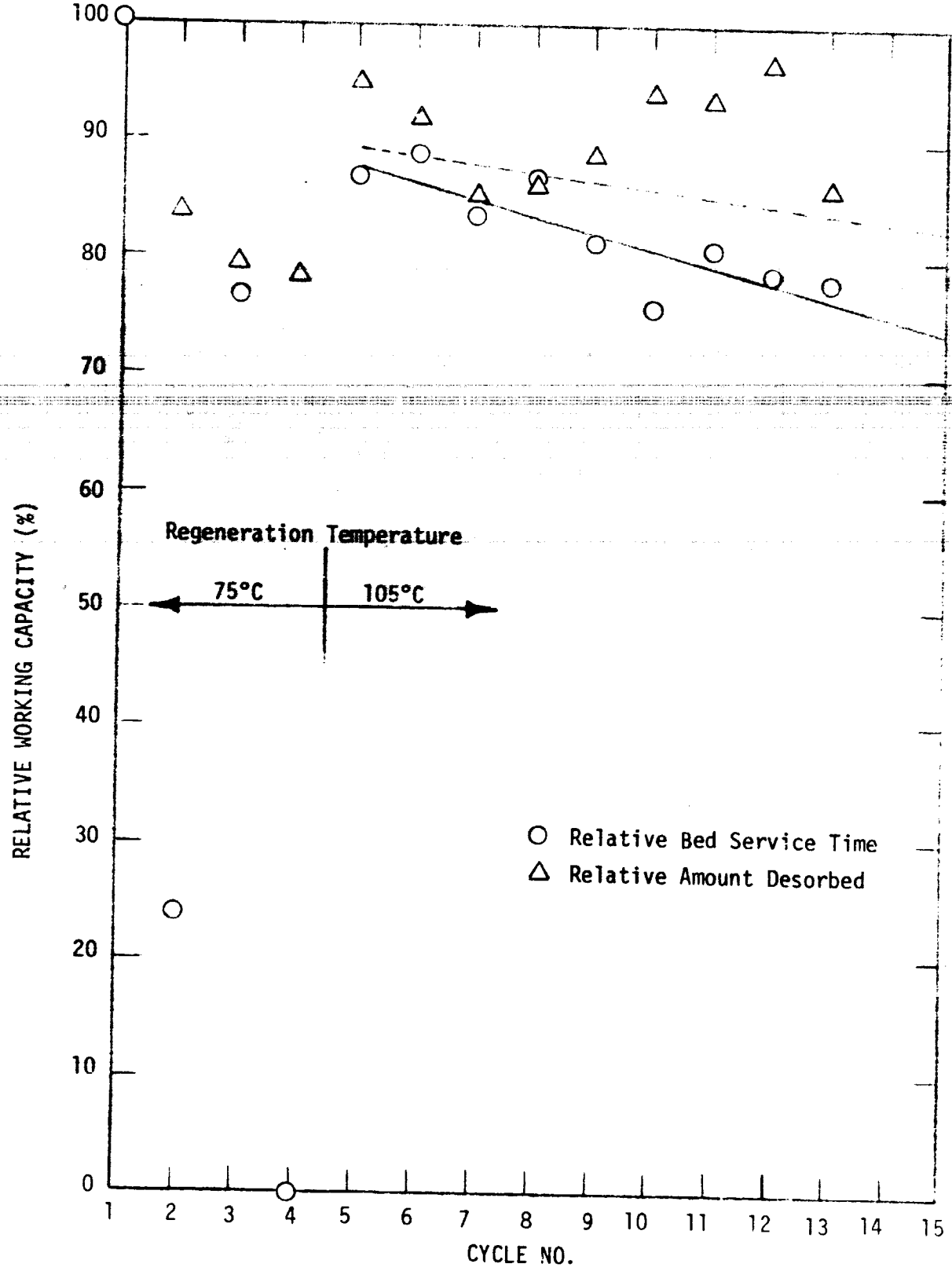

Figure 34: Relative Working Capacity vs. Cycle No. for Carbon Regenerated by Vacuum Thermal Desorption

for relative bed service time, it is concluded with 95% confidence that the working capacity decreases with cycle number. From the fitted regression line the working capacity would drop to 50% after 32 cycles.

It is of interest to note that the working capacity for the multi-contaminant mixture does not level off after a few cycles as it did in the tests with a single contaminant. This may be explained by noting that for the multi-contaminant mixture, the adsorption is terminated long before the bed is saturated with strongly adsorbed contaminant. Since the most strongly adsorbed contaminants are the ones which will most likely contribute to the undesorbed heel, it takes many cycles for the heel to build up to its equilibrium level.

III. CONCLUSIONS

1. Based on desorption tests with single contaminants, the rate and extent of thermal desorption via nitrogen-purge were independent of the nitrogen flow rate over the range investigated. However, for thermal desorption via vacuum, the rate and extent of desorption increased as the desorption pressure decreased.

2. Multiple-cycle tests with a single contaminant (acetone) indicated that the working capacity of the carbon rapidly (3 cycles) reached a steady value. This result is consistent with multiple-cycle single-contaminant results obtained during Phase I.

3. Multi-cycle, multi-contaminant tests, conducted under realistic conditions, indicated a gradual loss in carbon working capacity with increasing number of cycles. The working capacity after 13 cycles decreased to about 75% of the initial working capacity and appeared to be decreasing linearly.

4. In an actual spacecraft system, the working capacity is expected to decrease, as in the multi-cycle, multi-contaminant tests, until the bed is exposed to enough of the most strongly adsorbed contaminants for the heel to reach a steady-state level.

5. Based on the multiple-cycle, multi-contaminant tests, it is concluded that, at the conditions investigated, nitrogen-purge thermal desorption is preferred to vacuum thermal desorption. The desorption temperatures (105^{o}C) and times (76 minutes) were the same for both modes of regeneration. The vacuum-regeneration mode exhibited the disadvantage of poor removal efficiencies for weakly adsorbed contaminants at working capacities below 85%. In addition, the decrease in working capacity with cycle number was somewhat greater for the

vacuum-regenerated column. Furthermore, it is anticipated that the implementation of a nitrogen-purge system (or an air-purge system) will involve fewer development problems than the implementation of a self-contained vacuum system for regeneration without the dumping of contaminants into space.

SECTION 5
REFERENCES

1. Olcott, T.M., "Development of a Sorber Trace Contaminant Control System Including Pre- and Post-Sorbers for a Catalytic Oxidizer". NASA Report No. CR-2027, May 1972.

2. Olcott, T.M., "Design of a Spacecraft Contaminant Control System". Presented at the SAE/ASME/AIAA Life Support and Environmental Control Conference, San Francisco, California, July 12-14, 1971.

3. Olcott, T.M., "Design, Fabrication, and Evaluation of a Trace Contaminant Control System". ASME Publication No. 75-ENA2-23. Presented at the Inter-society Conference on Environmental Systems, San Francisco, California, July 21-24, 1975.

4. "Design, Fabrication, and Test of a Trace Contaminant Control System", Final Report, NASA Contract No. NAS-1-11526, Crew Systems Div., JSC; Prepared by Lockheed Missiles and Space Company, Inc., 28 November, 1975.

5. Goldsmith, R.L., McNulty, K.J., Freedland, G.M., Turk, A., and Nwankwo, J., "Contaminant Removal from Enclosed Atmospheres by Regenerable Adsorbents". Final Report Contract No. NAS2-7896, May, 1974.

SECTION 6

APPENDIX

BREAKDOWN OF LOSSES IN WORKING CAPACITY

Losses in working capacity can occur both by carbon oxidation and by the build-up of a contaminant heel. The purpose of this appendix is to estimate the relative importance of each of these mechanisms in determining the overall loss in working capacity.

In the case of thermal desorption the situation is simple. The total uptake at saturation remained constant throughout the test. This indicates no loss of carbon by oxidation as would be expected for thermal desorption in an inert atmosphere. The entire loss in working capacity is then due to the build-up of a contaminant heel.

For oxidative regeneration, the total uptake at saturation decreases. If it is assumed that the intrinsic adsorptive capacity of the carbon (grams adsorbed per gram of active carbon) does not decline, the only means by which the total uptake can decrease is by carbon oxidation. The assumption of a constant intrinsic adsorptive capacity for the active portion of the carbon appears to be justified by the fact that the intrinsic adsorptive capacity remained constant for thermal desorption.

The following calculation illustrates the break-down in the loss of working capacity for non-catalytic regeneration of DIBK - contaminated carbon after 17 cycles (Data Set A).

Adsorptive Capacity (Initial Working Capacity) = 0.335 g/g carbon
Saturation Loading after 17 cycles = 0.316 g/g virgin carbon
Residual Loading after 17 cycles = 0.008 g/g virgin carbon
Working capacity after 17 cycles = 0.316 - 0.008 = 0.308 g/g virgin carbon
Overall Loss in Working Capacity = $\frac{0.335 - 0.308}{0.335} \times 100\% = 8.06\%$
Weight of Virgin Carbon = 33.2385 g
Total Saturated Weight Loss = (0.335 - 0.316)(33.2385) = 0.6315 g

This weight loss results from oxidation of carbon and from the loss in the weight of contaminant that this carbon could adsorb (i.e. 0.335 g/g carbon).

If X is the weight of carbon lost by oxidation,

$$X + 0.335X = 0.6315 \text{ g}$$

Weight of Carbon Lost by Oxidation (X) = 0.4730 g
Apparent Weight of Heel = (0.008)(33.2385) = 0.2659 g
Actual Weight of Heel = 0.2659 + 0.4730 = 0.7389 g
Working Capacity Considering Carbon Loss Only

$$= \frac{0.335 \text{ g}}{\text{g active carbon}} \times \frac{(33.2385 - 0.4730)\text{g active carbon}}{33.2385 \text{ g virgin carbon}} = 0.330 \text{ g/g carbon}$$

Working Capacity Considering Heel Build-up Only

$$= \frac{0.335 \text{ g}}{\text{g virgin carbon}} - \frac{0.7389 \text{ g}}{33.2385 \text{ g virgin carbon}} = 0.313$$

Working Capacity Loss Due To Carbon Oxidation

$$= \frac{0.335 - 0.330}{0.335} \times 100\% = 1.49\%$$

Working Capacity Loss Due To Contaminant Heel

$$= \frac{0.335 - 0.313}{0.335} \times 100\% = 6.57\%$$

Total Loss = 1.49% + 6.57% = 8.06%

Thus the contaminant heel is about four times as important as the carbon loss in determining the loss of working capacity.

Similar calculations for the catalytic carbon of Set A show that after 17 cycles the following losses apply.

Working Capacity Loss Due to Carbon Oxidation

$$= \frac{0.336 - 0.316}{0.336} \times 100\% = 5.95\%$$

Working Capacity Loss Due to Contaminant Heel

$$= \frac{0.336 - 0.255}{0.336} \times 100\% = 24.11\%$$

Total Loss = 5.95% - 24.11% = 30.06%

As for non-catalytic oxidation the contaminant heel contributes about four times as much to the loss in working capacity as carbon oxidation.

END

DATE

FILMED

10-1077